Netrin1:DCC signalling in the development of somatotopic order in the somatosensory system

By Shima Rastegar-Pouyani

Integrated Program in Neurosciences (IPN)

McGill University, Montréal, QC, Canada

August 2022

A thesis submitted to McGill University in partial fulfilment of the requirements of the degree of Doctor of Philosophy

To my parents, who taught me to follow my dreams

Table of Contents

Abstract:

The ability to localize noxious stimuli, also known as nociceptive topognosis, is critical for animal survival. Anterolateral system neurons (AS), many of which are commissural, transmit nociceptive information from the periphery to different brain regions. Indeed, mice with spinal cord-specific loss of the netrin-1 receptor *Dcc* are unable to accurately localize noxious stimuli, similar to *DCC* mutant humans, but the identity of the ASs whose miswiring causes the topognostic deficits is unknown. A recently characterized transgenic mouse, $Phox2a^{Cre}$, labels a distinct population of spinal AS neurons in spinal laminae I and V, with many of them expressing *Dcc*. To see if Phox2a AS neurons contribute to noxious stimulus localization, I created Dcc^{Phox2a} mice with a *Dcc* deletion in Phox2a AS neurons.

Anatomical tracing experiments in Dcc^{Phox2a} mice demonstrate an increase in the number of cervical AS neurons innervating the ipsilateral thalamus, a brain centre involved in somatosensory stimulus localization. Furthermore, the cervical and lumbar innervating axons within the ventroposterolateral thalamus (VPL) region are miswired, as there is an expansion of cervical innervating axons and a reduction of lumbar axons in the VPL, while there is an increased overlap between the lumbar and cervical innervation territory in Dcc^{Phox2a} mice. These anatomical defects in Dcc^{Phox2a} mice suggest a netrin-1:DCC signalling function in AS neuron axon guidance at the spinal commissure and/or somatotopic ordering once they arrive in nociceptive brain centres.

To test whether *Dcc* loss in Phox2a neurons affects nociceptive topognosis, I injected capsaicin, a noxious stimulus, into one of the hindlimbs of Dcc^{Phox2a} or control mice. The accuracy with which Dcc^{Phox2a} mice direct their licking to the injection site was significantly reduced compared to control, while spinal level nocifensive reflexes, duration of nocifensive responses and conditioned place aversion were normal. These findings imply a disorganized somatotopic order within VPL

in Dcc^{Phox2a} mice, as well as altered laterality of Phox2a-expressing AS neurons. It can be linked to a reduced discriminatory component of pain and suggests the *Dcc* function in dissociating the discriminative and affective dimensions of pain.

Investigation of Phox2a AS neuron innervation of their targets reveals that at E15.5, spinal Phox2a AS neurons innervate the developing thalamus and continue to express *Dcc*, whereas netrin-1, its ligand, is also present in the thalamus. This synchrony raised the possibility that guiding the somatotopic map formation is a novel function of netrin1:DCC signalling, classically associated with commissural axon guidance and neuronal migration.

Résumé:

La capacité à localiser les stimuli nocifs, un processus connu sous le nom de topognosie nociceptive, est essentielle à la survie des animaux. Les neurones du système antérolatéral (SA), dont plusieurs sont commissuraux, transmettent des informations nociceptives de la périphérie aux différentes régions du cerveau. En effet, les souris présentant une perte du récepteur de la nétrine-1, *Dcc*, au niveau de la moelle épinière sont incapables de localiser avec précision les stimuli nocifs, tout comme les humains ayant une mutation *DCC*. Toutefois, l'identité des neurones AS dont les erreurs de circuit provoquent les déficits topognostiques est inconnue. Chez la souris transgénique *Phox2a*^{Cre}, récemment caractérisée, une population distincte de neurones AS des lames spinales I et V de la moelle épinière, dont plusieurs expriment *Dcc*, est marquée. Pour déterminer si les neurones AS *Phox2a* AS contribuent à la localisation des stimuli nocifs, j'ai créé des souris avec une délétion *Dcc* au niveau de ces neurones (*Dcc*^{Phox2a}).

Des expériences de traçage anatomique chez des souris *Dcc*^{Phox2a} démontrent une augmentation du nombre de neurones AS cervicaux innervant le thalamus ipsilatéral, un centre du cerveau impliqué dans la localisation des stimuli somatosensoriels. De plus, on observe des erreurs de circuits entre les axones innervant les zones cervicales et lombaires et situés dans la région du thalamus ventropostérolatéral (VPL), en raison d'une expansion des axones cervicaux et d'une réduction des axones lombaires dans le VPL, alors qu'il y a un chevauchement accru des trajectoires d'innervation lombaire et cervicale chez les souris *Dcc*^{Phox2a}. Ces défauts anatomiques chez les souris *Dcc*^{Phox2a} suggèrent que le complexe nétrine-1:DCC exerce une fonction de signalisation dans le guidage axonal des neurones AS au niveau de la commissure vertébrale et/ou dans l'ordre somatotopique suivant leur entrée dans les centres nociceptifs du cerveau.

Pour vérifier si la perte de *Dcc* dans les neurones *Phox2a* affecte la topognosie nociceptive, j'ai injecté de la capsaïcine, un stimulus nocif, dans l'un des membres postérieurs des souris Dcc^{Phox2a} ou témoins. La précision avec laquelle les souris Dcc^{Phox2a} dirigent leur léchage vers le site d'injection a été considérablement réduite par rapport au témoin, tandis que les réflexes nocifensifs au niveau de la colonne vertébrale, la durée des réponses nocifensives et l'aversion conditionnée à un endroit donné étaient normaux. Ces résultats indiquent une désorganisation de l'ordre somatotopique au sein du VPL chez les souris Dcc^{Phox2a}, ainsi qu'une altération de la latéralité des neurones AS exprimant *Phox2a*. Ces observations peuvent être liées à une réduction d'une composante discriminatoire de la douleur et suggèrent un rôle pour *Dcc* dans la dissociation des dimensions discriminatoires et affectives de la douleur.

L'étude de l'innervation par les neurones AS *Phox2a* des zones-cibles révèle qu'à E15.5, les neurones AS *Phox2a* de la moelle épinière innervent le thalamus en développement et continuent d'exprimer *Dcc*, tandis que la nétrine-1, son ligand, est également présente dans le thalamus. Cette synchronisation a soulevé la possibilité que le guidage de la formation de la carte somatotopique soit une nouvelle fonction de la signalisation nétrine1:DCC, classiquement associée au guidage axonal commissural et à la migration neuronale.

Acknowledgements:

This thesis is dedicated to my parents, Jahanshah and Nasrin, whose love and support have always inspired me. I can't thank my incredible little brother, Saleh, enough. Even though we are 10000 kilometres apart, your energy, support, and passion have always given me the energy to overcome obstacles. I'd like to express my gratitude to my wonderful Montrealer friends, who have become like a second family to me here. You've brought me joy on both happy and sad days over the last five years. I'd like to thank Parham in particular because I couldn't have completed this work without his support.

I must thank my supervisor, Dr. Artur Kania for granting me the freedom to explore and teaching so many invaluable lessons. Thanks for all the support and help you provided for this work during all these years. I would also like to thank my senior colleagues in Kania Lab, Dr. Brian Roome and Dr. Farin Bourojeni for their mentorship and comments on this project. All my colleagues, Chao Chang, Dr. Sara Banerji, Kevin Sangster, Xinying Zhang and Sung Soon Park, Thanks for being supportive and kind. Thanks, Chao, for all the beautiful singing that makes the lab environment enjoyable. Thanks, Sara, for your positive energy and I wish we met earlier. Thanks, Kevin, for all your feedback and helps.

I would like to extend my gratitude to Meiring Liang, for her years of hard effort and dedication in genotyping, and for the friendly chat, we had in the mornings. Thanks to all IRCM staff, Manon Laprise for her amazing effort on the AAV labelling experiment, Dominic Fillion for technical assistance with confocal microscopy and Dimitar Dimitrov for keeping the mouse colony well organized.

A big thank you to Dr. Tim Kennedy and his student Melissa Pestemalcyan, for generously sharing the transgenic mice and technical assistance. I would like to thank my committee

members, Dr. Reza Sharif-Naeini, Dr. Jeffrey Mogil and Dr. Dusica Maysinger. Your guidance, enthusiasm and expertise were truly instrumental.

Finally, I am very grateful for financial support from McGill University's Healthy Brains, Healthy lives (HBHL) and IRCM foundation whose help gave me more freedom to expand this work.

Contribution to original knowledge:

This thesis contributes significantly to our understanding of the development of the somatosensory system. In it, I describe how the absence of DCC in Phox2a-expressing anterolateral system neurons results in an aberrant connection between the spinal cord and the ventroposterolateral (VPL) thalamus, as evidenced by increased cervical axon innervation to the VPL and decreased lumbar innervation to the VPL. Such mice with aberrant wiring of the anterolateral system neurons have an impaired ability to localise painful stimuli. Thus, my experiments demonstrate genetically the contribution of the anterolateral system neurons to localisation of noxious stimuli.

Although, mice with *Dcc* deletion in Phox2a neurons have a reduced ability to locate noxious stimuli on their body's surface they have a normal perception of the aversive component of the pain. Thus, my experiments provide a genetic means of separating the discriminatory and aversive components of pain.

Axon guidance molecules such as DCC are known to be involved in midline crossing in the developing spinal cord. Here I showed that the expression of DCC protein in anterolateral system axons is not restricted to the midline crossing stage, but it persists several days after crossing and can be detected as first axons of the anterolateral tract arrive in the embryonic thalamus.

Furthermore, labelling Phox2a anterolateral system neurons revealed the exact date and pattern of anterolateral system innervation to several pain-related brain targets. The earliest spinal cord-thalamus connection occurred at embryonic day 15.5, with the innervation pattern shifting from

the lateral to the medial side of the dorsal thalamus in later embryonic stages. This is contrary to the previous assumption on the timeline of projection neurons' arrival at the supraspinal targets.

Contribution of Authors:

Compilation of the work presented here: Shima Rastegarpouyani

The conception of project and experiments: Shima Rastegarpouyani & Artur Kania

Procurement and development of materials, experimental work, data collection and analysis: Shima Rastegarpouyani, unless noted otherwise below (by results section)

Section 3.1.1:

Dr. R. Brian Roome: generating *Phox2a*^{Cre} transgenic mouse line.

Dr. Tim Kennedy and Melissa Pestemalciyan: provision of the *Bgeo* mouse line.

Kevin Sangster: Harvesting *Bgeo* embryos.

IRCM animal facility: Maintenance

Section 3.1.2:

Martyn Goulding (Salk Institute, San Diego, CA – collaboration): provision of the *Cdx2FlpO* mouse line.

Section 3.1.3 and 3.2.3:

Manon Laprise: intraspinal AAV injection.

Chapter 1: Introduction

1.1 Pain as a complex phenomenon:

Interpreting pain has remained a challenge in the history of medicine. The dualistic approach to pain is one of the several attempts to understand pain which suggests discriminative and motivational components of pain as two main characteristics of the pain perception (Hodge and Apkarian, 1990). Sensory-discriminative components of pain include different qualities such as intensity, temperature, and location of the noxious stimuli. The motivational component of pain is another important characteristic of pain that leads to an unpleasant perception of pain (Mercer Lindsay et al., 2021). Pain is defined by the international association for the study of pain (IASP) as: "An unpleasant sensory and emotional experience associated with, or resembling that associated with, actual or potential tissue damage" (Pain terms: a list with definitions and notes on usage. Recommended by the IASP Subcommittee on Taxonomy, 1979). This definition emphasizes the cooperation of sensory and emotional components of pain in response to a painful experience.

Although the discriminatory and motivational components of the pain usually work together during disease or physical damage as a warning system, in some cases this communication is impaired. Patients with thalamic pain syndrome often report unpleasant pain sensations in the body without being able to accurately localize it. Speigel et al showed that lesion of the ventrobasal (VB) complex of the thalamus results in excessive response to feeling burning pain while this sensation is poorly localized in VB damaged patient (Kenshalo and Willis, 1991).

Current pain therapeutic strategies are focused on using opioids (e.g., morphine) which act as agonists to opioid receptors in the nociceptive circuits of the nervous system (Corder et al., 2018). While opioids are widely used in pain treatment, there are shortcomings associated with

the opioid therapeutic approach because of the risk of addiction and increased tolerance in patients (Vowles et al., 2015). Therefore, understanding the mechanism behind pain-related circuits is important to introduce alternative therapies.

1.2 Somatosensory system organization:

The somatosensory system is consisting of interoceptive and exteroceptive receptors that enable animals to perceive their internal and external environment. The interoceptive system with visceral and proprioceptive receptors relay proprioceptive information about body position and muscle tension which is necessary for the sense of self. The Exteroceptive system gathers information on the body's interaction with the external environment. Stimulations with different characteristics including touch, pruritic, temperature and noxious stimuli are relayed by exteroceptive cutaneous receptors. Many of the interneurons within the spinal cord work as connectors between proprioceptors and cutaneous afferents. Therefore, external and internal information integrate to adjust the body posture and movement based on the external environment signals (Koch et al., 2018).

The exteroceptive somatosensory system relay sensory modalities that are generally classified as noxious, innocuous and pruriceptive. These sensory modalities are conveyed by primary afferents with different conduction velocities and myelination properties. Highly myelinated Aβ fibres transmit innocuous stimuli such as light touch and C fibres with no myelin coating carry nociceptive information (Abraira and Ginty, 2013). Despite this general classification, there are many subgroups that add complexity to the general categorization. For example, C low threshold mechanoreceptors(C-LTMRs) transmit touch stimuli, unlike other nociceptive C fibers.

Two known groups of nociceptive primary afferents, C-fibres and myelinated Aδ fibres, transmit different types of noxious stimuli to the spinal cord. Aδ fibres are relaying fast chemical, mechanical and thermal noxious stimuli while the unmyelinated C-fibres are involved in relaying slow mechanical and thermal nociception. Multiple subclasses of nociceptors have been identified based on their molecular expression profile. Transient receptor potential (TRP) channel family receptor induces a wide range of modality sensitivities in both C and Aδ fibres nociceptors. Trpa1 is a cation channel activated by formalin and Trpm8 is a cold sensor (Gentry et al., 2010). Trpv1 is another member of the TRP family which is responsive to noxious thermal stimuli and its expression induces sensitivity to Capsaicin.

Primary afferent's input is processed within the dorsal horn spinal cord and relayed to the long ascending projection neurons in the anterolateral system for further transmission to the supraspinal targets (Fig I.). Spinal neurons are not homogeneous. They are classified based on different properties such as morphology, electrophysiological properties, protein expression and their location within the spinal cord (Abraira et al., 2017). Rexed lamina organization classifies neurons in 10 clusters called lamina I-X which start with lamina I as the first layer of neurons in the dorsal horn spinal cord. It has been shown that most of the pain-relaying anterolateral system neurons are located in lamina I and V (Basbaum et al., 2009). These two regions appear to be in charge of relaying polymodal pain information. Before the anterolateral system transmits nociceptive information to the supraspinal site, inhibitory and excitatory interneurons gate afferent nociceptive inputs. Also, incoming nociceptive information is relayed to the ventral horn spinal cord for a quick protective response to damaging or potentially damaging situations triggered by spinal cord neurons. This spinally mediated response is called nocifensive reflexes (Sivilotti and Woolf, 1994).

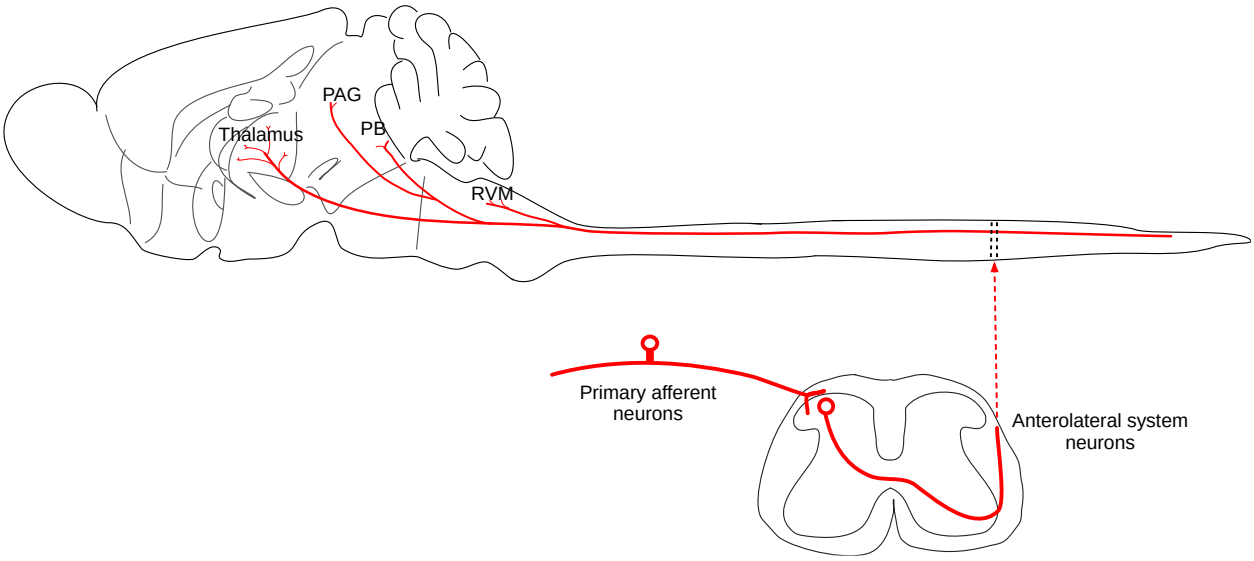

Figure I. **The anterolateral system's connection to central pain processing**

Primary afferent nociceptors transmit noxious information to anterolateral system neurons in the spinal cord's dorsal horn. Anterolateral system neurons send signals to pain-processing brain centres such as the thalamus, parabrachial nucleus (PB), Periaqueductal grey (PAG), and rostroventral medulla (RVM).

1.2.1 Anterolateral system:

Anterolateral system (AS) neurons are concentrated in lamina I and V and scattered through lamina III to IV. Among these, Lamina I AS neurons are well studied. One major feature of lamina I AS neurons is that their axons cross the spinal cord midline during development and travel in the contralateral white matter to reach the brainstem and thalamic nuclei. Anterograde tracing experiment demonstrated several brain targets for lamina I neurons including the parabrachial nucleus (PB), thalamus, periaqueductal gray (PAG), caudal ventrolateral medulla (CVLM) and nucleus of solitary tract (NTS) (Gauriau and Bernard, 2004). Quantification of lamina I AS neurons in rat lumbar cord shows that approximately 95% of their project to lateral PB, a third to PAG, and a small portion, less than 5 %, to the thalamus. However, at the cervical

level higher number of lamina I projection neurons are spinothalamic (~15 cells vs ~90 cells per side in L4 and C7, respectively) (Al-Khater et al., 2008; Spike et al., 2003). According to Polgar et al quantitative study on cervical spinothalamic neurons, approximately 42 percent of lamina I projection neurons are spinothalamic, which differs greatly from the lumbar spinothalamic population estimate. (Polgar et al., 2010). The difference between the number of lumbar and cervical spinothalamic neurons seems to be species-specific since monkeys' spinothalamic neurons have less difference in the number of spinothalamic neurons located in lumbar and cervical spinal cord (Zhang and Craig, 1997). Overall, the difference in the number of lumbar and cervical neurons suggests that the forelimb has a greater representation in the somatosensory cortex than the hindlimb, allowing animals to perform fine tasks with their upper limbs that are normally missed in lower limbs. (Kaas, 1983; Remple et al., 2003). Few numbers of ventroposterolateral (VPL) projecting cervical lamina I neurons could cover several digits of dermatome due to their large receptive fields. If lumbar projections follow the same rule, it could explain how a small number of lumbar spinothalamic neurons are enough to relay the entire dermatome input to the somatosensory cortex (Zhang et al., 2006). Compare to the lumbar spinal cord, the number of spinoparabrachial projection neurons at the cervical cord is lower but the number of PAG projections is unchanged between spinal levels (Al-Khater and Todd, 2009). A proportion of anterolateral system neurons send collaterals to multiple brain regions. A significant proportion of lamina I spinothalamic neurons send collateral branches to both PAG and PB. More than 80% of lamina I spinothalamic neurons also project to lateral PB and 30-35% of spinoparabrachial projection neurons are spinothalamic. These emphasize the multiple functions of individual anterolateral system neurons and the possibility that each neuron could

contribute to discriminatory properties such as localization and intensity as well as the affective component of pain by sending input to different brain nuclei (Al-Khater and Todd, 2009).

Although the anterolateral system has been extensively studied in the superficial dorsal horn, the impact of deep dorsal horn has been neglected in contemporary pain research (Wercberger and Basbaum, 2019). Lamina III-V neurons with long dendrites are receiving inputs from primary afferents and many anterolateral system neurons located in the lamina V and lateral spinal nucleus (LSN) area. LSN neurons are located in the white matter of the rodent dorsal horn and project to the brainstem, hypothalamus and thalamus (Todd, 2010).

Recent advances in biology tools provide an opportunity to study and categorize the heterogenous projection neurons at the molecular level. The neurokinin 1 receptor (Nk1r) is one of the first molecular markers identified in lamina I projection neurons. Ablating Nk1r expressing neurons decreases the hyperalgesia in the neuropathic model of the pain (Mantyh et al., 1997). Although introducing Nk1r raised a lot of hope as a new alternative therapeutic approach for hyperalgesia but the major caveat of the Nk1r marker is the fact that not only projection neurons but also a considerable number of interneurons in lamina I are expressing Nk1r and it does not label the long ascending projection neurons specifically.

The *preprotachykinin* 1(*Tac1*) gene is encodes the neuropeptide substance P which is expressed in response to noxious stimuli (Gutierrez-Mecinas et al., 2017). *Tac1* expressing neurons in the spinal cord located in both superficial and deep dorsal horn areas and projects external lateral PB as well as medial thalamus. Recently, *Tac1* has been introduced as a marker for a proportion of AS neurons that are involved in the motivational component of pain. Ablation of *Tac1* neurons results in loss of conditioned aversion triggered by a noxious stimulus (Huang et al., 2019).

Another recent study introduces *Tacr1*(expressing Nk1r) and *Gpr83* expressing neurons as two parallel ascending circuits within the anterolateral tract. Tacr1 and Gpr83 neurons make up to 88% of the total spinoparabrachial neurons in the superficial dorsal horn. Tac1 neurons also partially overlap with *Tacr1* and *Gpr83* expressing neurons. Although *Tacr1* and *Gpr83* positive AS neurons are highly innervating the PB, no innervation has been observed within VPL thalamus. Nonetheless, labelling the commissural spinal projection neurons by using *Robo3,* encodes roundabout guidance receptor 3, demonstrates that many of the commissural anterolateral system neurons project to VPL (Barik et al., 2021; Choi et al., 2020). These findings show that Tacr1 and Gpr83 neurons are absent in VPL commissural axons and lack laterality specification as the first level of somatotopy, implying that these neurons focus on the aversive component of pain, which is consistent with behavioural phenotype.

Despite the fact that most research on finding a molecular handle to classify anterolateral system neurons has focused on adult markers, Phox2a is a newly identified developmental marker to label anterolateral system neurons. Phox2a specifically labels long ascending projection neurons without labelling interneurons within the spinal cord. They are located at lamina I as well as the deep dorsal horn, Lamina V and LSN. Phox2a projection neurons are not overlapping with Tac1 spinal neurons but there is a possible partial overlap between Phox2a lineage projection neurons and Tacr1/ Gpr83 neurons (no data to prove this yet). Unlike Tacr1/ Gpr83 neurons, Phox2a expressing neurons are all commissural and innervate both VPL and PB nucleus (Roome et al., 2020a). This raises the possibility of Phox2a anterolateral system neurons being involved in not only the aversive but also discriminatory components of pain.

1.3 Brain targets of the nociceptive circuit:

The anterolateral system relays sensory information such as pain, touch, and thermosensation to various supraspinal targets such as the Thalamus, PB, and PAG. In this section, I will discuss the thalamus, PB, and PAG as the three main recipients of nociceptive inputs in the brain.

1.3.1 Thalamus:

Spinothalamic neurons relay nociceptive information to different thalamic subnuclei. Posterior nucleus (PO), ventral posterior inferior nucleus(VPI) and ventral posterior lateral(VPL) are the main recipients of spinothalamic fibres (Kuner and Kuner, 2021).

Multiple studies show the VPL response to noxious stimuli (Abdul Aziz et al., 2005; Bordi and Quartaroli, 2000; Guilbaud et al., 1980; Peschanski et al., 1980). Noxious stimuli in the rat hind paw induce glutamate release in the VPL (Silva et al., 2001). Also, electrophysiological recording in rats demonstrates that VPL neurons with smaller receptive fields are encodes the discriminatory component of the pain (Willis and Westlund, 1997). Moreover, VPL neurons are responsive to innocuous mechanical stimuli and thermal nociception, but this response is not as strong as their response to the noxious stimulus (Bordi and Quartaroli, 2000).

Different thalamic nuclei relay the received sensory inputs to the cortex via thalamocortical axons. VPL and VPI thalamocortical axons target the S1 and S2 cortex respectively, to convey sensory-discriminatory aspect of nociception but VPI-S2 connection seems to be involved in higher order- cognitive functions (Kuner and Kuner, 2021). PO with widespread cortical

projection, connect the spinothalamic input recipient neurons to the posterior insular cortex (Dum et al., 2009).

Thalamus lesion in stroke patients often induces central pain syndrome which is described by allodynia (evoking pain by cold or tactile stimuli which is normally not supposed to be painful) and spontaneous ongoing pain in the body (DAVISON and SCHICK, 1935). Studies suggest that patients with post-stroke thalamic syndrome mostly have lesions in thalamic subnuclei associated with spinothalamic neurons (Kim et al., 2007). MRI analysis in two groups of patients with post-stroke thalamic syndrome shows that in patients who develop central pain after stroke, thalamic lesion happens at the lateral and posterior side of the thalamus. Particularly, Pulvinar and VP nuclei are affected in post-stroke thalamic syndrome patients with central pain (Sprenger et al., 2012). 94% of patients with post-stroke thalamic syndrome reported having a decreased temperature, pain and touch sensation (Andersen et al., 1995). The affected somatosensorial intensity in the VB-associated thalamic lesion suggests the crucial role of this subnucleus in the discriminatory component of pain. Furthermore, a clinical case with a stroke lesion in the somatosensory cortex provided an intriguing model for comparing the lateral pain system, which includes the lateral thalamic nuclei and the somatosensory cortex, to the medial pain system, which includes the medial thalamic nuclei and the anterior cingulate cortex. This patient provides a rare opportunity to show the dissociation of discriminatory and motivational components of pain as lesion in the lateral pain system results in loss of pain sensation without affecting the motivational aspect of pain (Ploner et al., 1999).

Although post-stroke thalamic lesion is solid evidence of the role of the thalamus (mostly VB) in the discriminatory component of pain, this association needs to be evaluated in the rodent models as well. Gritsch et al performed unilaterally lesion of the VPL to generate a post-stroke thalamic

syndrome mouse model. Consistent with human results, post-stroke thalamic syndrome mice showed a comparable sensory deficit. Interestingly, inhibition of spinal and peripheral inputs had no effect to control the evoked hypersensitivity in post-stroke thalamic syndrome model while injection of an anesthetic drug, Lidocaine, in the thalamus alleviates the symptoms (Gritsch et al., 2016). These results link the ongoing neuronal activity in the VPL to hypersensitivity induced by post-stroke thalamic syndrome.

VPL in the rodent model could be subdivided into three subregions based on the received inputs. Rostral VPL contains proprioceptive information and is responsive to both proprioceptive and cutaneous stimulation. The medial VPL poses the focal cutaneous receptive fields with a somatotopically organized forelimb/ hindlimb inputs but does not receive much proprioceptive information. The caudal VPL is a major recipient of superficial dorsal horn spinothalamic neurons and is related to cutaneous information such as nociception and visceral stimuli (Berkley et al., 1993; Gauriau and Bernard, 2004; Guilbaud et al., 1993)

VPL provides a fine topographic map of the forelimb and hindlimb. Anterolateral system projection neurons innervating from the rostral spinal cord to the VPL end up on the medial side while caudal innervations locate more laterally within VPL (Francis et al., 2008). Other than VPL, PO provides a somatotopic representation which could be considered another potential center in processing discriminatory components of pain in the thalamus.

1.3.2 Parabrachial nucleus:

Parabrachial nucleus is a hindbrain structure involved in processing of various behavioural and physiological responses. This evolutionarily conserved nucleus has been studied in different species as a pivotal hub for processing pain and aversion (Fulwiler and Saper, 1984). PB can be divided into different subnuclei based on connectivity, neurochemistry and cytoarchitectural properties. Neurons in the medial PB are more heterogenous in morphology and size, while lateral PB encompasses multiple homogenous groups.

Several lines of evidence including electrophysiological data, neuron activity markers and calcium imaging data show the lateral PB response to t nociception (Bernard et al., 1994; Uddin et al., 2018). External lateral PB with concentrated nociresponsive neuron population is projected to other brain nuclei such as central amygdala and makes connection to thalamus-insular circuit which implies the role of the lateral PB in motivational qualities of pain (Jasmin et al., 1997). Furthermore, PB projection to descending modulators of pain such as rostral ventromedial medulla (RVM) and midbrain preaquaductal grey (PAG) suggests the role of PB in modulating the pain inhibitory circuit. (Roeder et al., 2016). Lateral PB inputs to the reticular formation construct another descending brain stem circuit that controls escape behaviour in response to noxious stimuli. *Tac1* expressing neurons in the PB and reticular formation are involved in modulating the aversive nocifensive response in this circuit (Barik et al., 2018).

PB contributes to the motivational components of pain by sending inputs to the other nociceptive nucleus in the brain such as central amygdala. Calcitonin gene related peptide (CGRP) expressing inputs from lateral PB to central amygdala induce hyperalgesia and ultrasonic vocalisation in rodents (Han et al., 2010). On the other hand, reciprocal connection from central

amygdala to the lateral PB prevent PB hyperexcitability (Chiang et al., 2019). Also, lateral PB is activated by nociceptive sensory axons which results in stress vocalization and conditional avoidance (Rodriguez et al., 2017).

Lateral PB nucleus is a major recipient of nociceptive inputs which are conveyed through spinoparabrachial (SPB) tract from the trigeminal and spinal dorsal horn (Craig, 1995; Gauriau and Bernard, 2002). spinoparabrachial neurons relay various sensations including nociception, temperature, and touch from the spinal cord to the PB through the anterolateral pathway. Recently, two populations of SPB neurons with Tacr1 and Gpr83 expression have been identified. Tacr1 and Gpr83 neurons label two distinct subdivisions of SPB neurons which have different anatomical, physiological, and functional characteristics. Tacr1 and Gpr83 SPB neurons are involved in the affective components of pain but studying their axonal organization within PB do not show a somatotopic organization, therefore, these neurons do not seem to be involved in the discriminatory aspect of the pain (Choi *et al.*, 2020).

1.3.3 PAG:

Periaqueductal gray in the midbrain is best known for its role in defensive responses. Classic studies back in the 1980s demonstrate that lesions in the dorsal PAG cause an impaired defensive behaviour in response to danger (Blanchard et al., 1981). Neuronal activity in PAG neurons increases during a defensive response and stimulation of the PAG by electrical and pharmacological stimuli or optogenetic activation produces defensive behaviour in rodents (Bittencourt et al., 2005; Chen et al., 2015).

PAG receives direct nociceptive inputs from the spinal cord as well as relaying descending inputs to RVM which project to the spinal cord. The involvement of PAG in both ascending and descending circuit of nociception exhibit its critical role in processing nociceptive information which is associated with the aversive component of the pain (Mercer Lindsay *et al.*, 2021). Inhibition of dorsal PAG neurons during an aversive incident decreases memory formation in mice. This effect could be due to the connection of PAG to the forebrain structures that control memory formation and learning (Yeh et al., 2021).

1.4 Development of the nervous system associated with somatosensation:

During embryonic development, neural circuits are constructed with amazing precision, and the selectivity inherent in their construction helps to define the mature organism's behavioural repertoire. This developmental program in the vertebrate central nervous system starts with the differentiation of discrete types of neurons from progenitor cells situated at specific locations within the neural tube. The mechanisms that determine the identity of neural cells have been studied in many different parts of the nervous system, and they demonstrate a high degree of conservation in how essential signalling molecules determine cell fate. Here, I summarise the major findings on the development of the thalamus, one of the major nuclei in the central nervous system that plays an important role in somatosensation. In addition, our understanding of the development of the spinal cord and neurons in the anterolateral system will be reviewed.

1.4.1 Development of the thalamus:

Thalamus is one of the main nuclei in the brain that receives sensory inputs from various body areas and sends rectified sensory information in coded topographic order to the somatosensory cortex. Studies on the organization of the thalamus and its anatomical feature in animal models suggest two models for the developing thalamus. The first model suggests by Herrick and Kuhlenbeck in 1973 is called the columnar model (Kuhlenbeck, 1973). In this model, the diencephalon is divided into four domains in the dorsal-ventral axis: epithalamus, dorsal thalamus (dTH), ventral thalamus (vTH) and hypothalamus. The dorsal thalamus is the domain that gives rise to the VP area further during development and contains cortex-projecting excitatory neurons. In contrast to the columnar model, the prosomeric model suggests that the dorsal thalamus is not in the same rostral-caudal axis as the ventral thalamus. The prosomeric model proposes that the thalamus, known as the dorsal thalamus in the columnar model, is located caudal to the ventral thalamus (prethalamus in the prosomeric model) based on molecular expression, neurogenesis patterns, and morphology. The mechanism behind the formation of each thalamic subnuclei has been extensively studied in the last two decades and demonstrated distinct progenitor domains within the thalamus with a specific molecular expression profile that gives rise to different subnuclei in the thalamus. Shh is one of the key signalling pathways that define the progenitor domains along the rostrocaudal axis of the thalamus. (Jeong et al., 2011; Nakagawa and Shimogori, 2012; Vue et al., 2009). This contrasts with the role of Shh signalling in the ventral spinal cord development along the dorsoventral axis (Dessaud et al., 2007; Jessell, 2000).

1.4.2 Neurogenesis in the thalamus:

Birth-dating studies in the 1970s and 1980s proposed a gradient of neurogenesis along different axes within the thalamus. The thalamus begins neurogenesis at E10, and while the peak of neurogenesis in the ventral nuclei occurs at E10-E11.5, the dorsal thalamic nuclei show heavy labelling by tritiated thymidine (birth-date marker) one day later at E11.5-E12.5 (Vue et al., 2007). This delayed neurogenesis is also observed in the dorsoventral axis in the ventroposterior complex (VP). Furthermore, Medially located nuclei were born later than the lateral ones explaining earlier neurogenesis in the lateral posterior than in the posterior nucleus (PO) and parafascicular (Pf) (Nakagawa, 2019).

Although neurogenesis starts as early as E10.5, a distinct regional pattern of gene expression is more evident around E14.5 (Gezelius and Lopez-Bendito, 2017; Nakagawa and O'Leary, 2001; Suzuki-Hirano et al., 2011) And differential gene expression at late embryogenesis and early postnatal stages could identify most of the thalamic nuclei (Horng et al., 2009; Jones and Rubenstein, 2004; Yuge et al., 2011).

1.4.3 Roles of the afferent inputs on thalamic development:

The cortical and subcortical areas send information to the thalamus during development. As early as E16, trigeminal and retinal ganglion cells innervate the VP and dLG nuclei in mice (Godement et al., 1984; Mirza et al., 2013). Layer 5,6 and subplate corticothalamic projection neurons reach the thalamus during the first week after birth (Grant et al., 2012). Also, spinal cord

relays the somatosensory information to the thalamus via spinothalamic neurons during development. Davidson et al. demonstrated that spinothalamic axons reach the thalamus by E18 in mice, but this study does not show when this innervation begins. Distinguishing the time of afferent arrival is crucial in understanding the impact of spinothalamic neurons on post-mitotic migration or sensory-driven refinement of thalamic neurons (Molnar et al., 2012). Given the development of the thalamus between E10 and E16, the observed thalamic reorganisation during this period could be due to the potential role of spinal inputs.

1.4.4 Development of the spinal cord:

Spinal cord neurons are organized into two functional systems that are anatomically separated. The dorsal horn contains a system that relays sensory information to supraspinal targets, and the ventral spinal cord contains neurons and circuits that integrate proprioceptive inputs and motor outputs. (Jessell, 2000).

The location of the progenitors in the neural tube is one of the main determinants of the assigned identity. Expression of the combination of the transcription factors (TFs) along the anterior-posterior and dorsal-ventral axis of the neural tube determines the fate of neurons during development. Along the anterior-posterior axis of the spinal cord, Hox family's differential expression provides a patterning signal, and a combination of TFs expression divides the spinal cord into 4 major units including cervical, thoracic, lumbar and sacral spinal cord with several segments. Neurogenesis at different segments of the spinal cord happened at different time points. Studies in rats showed that neurogenesis in the caudal spinal cord happens with one day delay compared to rostral spinal cord (Nornes and Das, 1974).

Dorsal-ventral patterning of the spinal cord is influenced by two sets of organizer cells in the roof and floor plate of the neural tube. Morphogenic cues secreted by floor plate and roof plate cells act antagonistically and provide a concentration gradient in which progenitor cells are responding to them in a dose-dependent manner. Sonic hedgehog (Shh) secretion by floor plate and Wnt protein secretion by roof plate are the main morphogenic cues in determining the fate of the neighbouring progenitor cells (Liem et al., 1997; Roelink et al., 1995). *Shh* is inducing the ventral cell type identity of the neurons by activating or suppressing the HD TFs based on their proximity to the floor plate secreted Shh (Briscoe et al., 2000). Bmps and Wnts, on the other hand, are the major signalling pathways that arrange the TFs that determine the dorsal cell-type identity (Chesnutt et al., 2004).

The identification of 11 early borns (embryonic day (E)10-E12.5) neuronal groups was based on the combinatorial expression of numerous families of TFs, primarily homeodomain (HD) and basic helix-loop-helix (bHLH) factors. These 11 neuronal populations are called dorsal interneurons (dI) 1 to 6 located in the dorsal horn in addition to V0-3 and MN populations in the ventral spinal cord (Fig II.). Besides early-born neurons, there are dIL_A and dIL_B late-born domains in the dorsal horn that emerge between E11 to E13. TFs expression is dynamic in these populations and although they are used as lineage markers but do not necessarily express throughout the development of the lineage. For example, bHLH factors including Atoh1, Neurog1and Ascl1 are present in a subset of proliferating progenitors but immediately downregulated in postmitotic neurons. Contrary to the bHLH factors, some HD TFs including Pax2 and Tlx3 are expressed only post-mitotically.

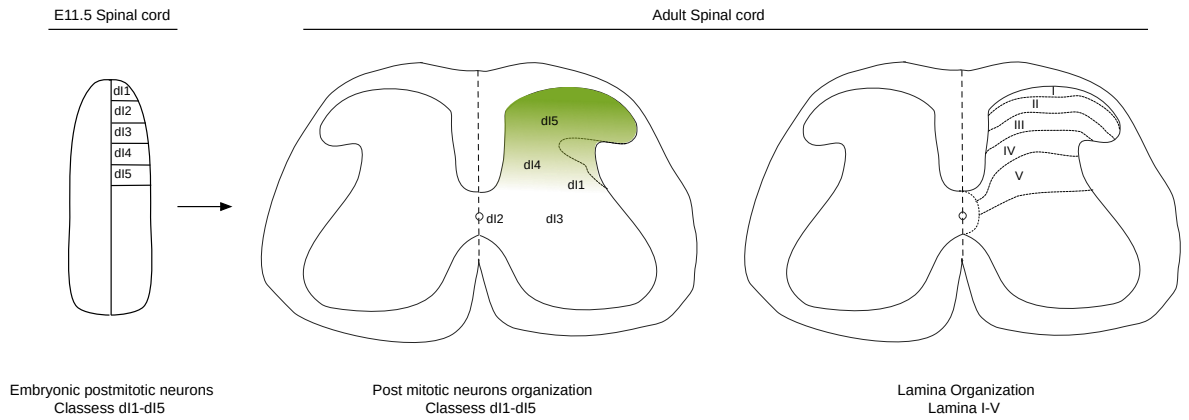

Figure II. **The neuronal migration during spinal cord development.**

Five early postmitotic neuron classes (dI1-dI5) are present within distinct domains along the dorsoventral axis of the dorsal horn at E11.5 (left) and these later migrate to their positions within the adult spinal cord (right). The adult spinal cord is also classified into lamina layers based on the number and size of the neurons as well as the fibres that come into contact with them. For example, dI5 post mitotic neurons are found in lamina I to Lmina V in the adult spinal cord.

Cross-repression between TFs is directing neurons to the appropriate cell fate by repressing all alternative fates. For example, Nkx2.2, Nkx6.1 and Olig2 are three ventral neural tube TFs that repress dorsal fate programs in the ventral horn neurons (Kutejova et al., 2016; Nishi et al., 2015). Cross-repression is not only defining the progenitor domain boundaries but also works as a switch to regulate post-mitotic populations. One example is repressing the inhibitory neuronal program in dI4 and dI6 inhibitory neurons that are regulated by dI5 population. DI5 excitatory neurons express Tlx3 that inhibits Lbx1. Since Lbx1 is a regulator of Pax2 expression in inhibitory neurons, inhibition of Lbx1 by dI5 neurons leads to repressing inhibitory programs in dI4 and dI6 post-mitotic neurons (Cheng et al., 2004).

While the interplay between different TFs and signalling pathways is investigating the developmental mechanism behind cell specification in the spinal cord, one unanswered question is how these neurons' development is related to their function.

Many of the developmental TFs are working upstream of the terminal differentiation processes such as neuropeptide or axon guidance fate (Avraham et al., 2009). *Robo3* is an axon guidance receptor found in commissural neurons and is regulated by Lhx2 and Lhx9 TFs (Wilson et al., 2008). Also, two other HD TFs, Isl1 and Lhx3, regulate the cholinergic pathway genes in the ventral horn (Cho et al., 2014). Current classifications of spinal neurons based on their molecular profile, anatomy, and electrophysiological properties suggest that the developmental lineage is only marginally useful in identifying a specific sensory function. Neurons with similar anatomical properties may arise from multiple developmental lineages. Furthermore, proprioceptive neurons are derived from the dI1, V1, V2, and V3 developmental populations, implying that the relationship between a particular developmental population and a set of neurons with a specific function requires further investigation. (Lai et al., 2016; Pivetta et al., 2014).

One main function of the spinal cord neurons is processing and relaying sensory information. Local processing of the sensory inputs is done by excitatory and inhibitory interneurons in the dorsal horn. The excitatory interneurons originated mostly from the dI5 or dIL_B lineages (Szabo et al., 2015). The role of the dI5/ dIL_B has been shown in various nociceptive modalities. As impaired dI5/ dIL_B lineage results in defected thermal, chemical and mechanical nociception while having no effect on the motor control (Xu et al., 2013). Lmx1b+ neurons in the dI5 lineage that comprise a portion of anterolateral system neurons located in the adult lamina I spinal cord, appear to be involved in the noxious thermosensation (Szabo *et al.*, 2015).

1.4.5 Phox2a as a marker of dI5 domain in the developing spinal cord:

Other than Lmx1b, Paired-like homeobox 2a (Phox2a) is a more refined marker of dI5 domain. Phox2a is a developmental marker expressed transiently in anterolateral system neurons but not interneurons. Anterolateral system neurons are mainly located in lamina I, superficial dorsal horn, and Lamina V/LSN domain which is called the deep dorsal horn. About 60% of the superficial dorsal horn AS neurons are Phox2a expressing neurons while only 30% of the deep ASs are Phox2a positive. Although Phox2a expression is absent in adults, the location of neurons from the Phox2a domain could be traced by using a *Phox2*^{Cre} mouse model crossed to a tdT reporter mouse line. The characterization of the *Phox2*^{Cre} mouse line by Roome et al revealed that, while this mouse line is a good proxy to lamina I Phox2a neurons (83% of Phox2a cells express tdT), only 33% of deep dorsal horn Phox2a neurons are represented in the *Phox2*^{Cre} model, implying that the *Phox2*^{Cre} driver is biased for superficial lamina ASs. (Roome *et al.*, 2020a).

Phox2a expression starts as early as E9.5 in the mouse embryo and in Lmx1b/Phox2a expressing neurons appear at E10.5. Most of the Phox2a neurons express axon guidance receptors, DCC and Robo3, suggesting that the Phox2a AS neurons are commissural neurons. Retrograde tracing studies demonstrated that almost all of the Phox2a spinal neurons are innervating brain targets including PB, Thalamus and PAG (Roome *et al.*, 2020a).

Although Phox2a has been used as a marker to identify the dI5 domain, its role as a transcription factor seems to be essential in the nociceptive properties of dI5-originated neurons. Phox2a express in noradrenergic neurons with dopamine beta-hydroxylase and tyrosine hydroxylase expression (Guo et al., 1999). Phox2a neurons are present in a range of autonomic circuits

including sympathetic and para-sympathetic ganglia implying its potential role in regulating homeostasis and autonomic functions. The spinal cord Phox2a knockout model revealed the remarkable decrease of AS innervation to the lateral PB. Further investigation by retrograde tracing shows that this decrease is due to less innervation in the deep dorsal horn at the lumbar level while normal innervation was observed in the cervical spinal cord. Besides Phox2a TF effect on the connectivity of AS neurons, Phox2a knockout in the caudal spinal cord results in a decreased nocifensive response in mice. Phox2a^{cKO} mice demonstrate less sensitivity to noxious thermal stimulus as well as mechanical nociception which shows the role of Phox2a AS neurons in transmitting nociceptive information from the spinal cord to the brain (Roome *et al.*, 2020a).

1.4.6 The migration of spinal cord neurons during development:

Lineage-tracing studies have demonstrated that developing spinal cord neurons travel considerable distances alongside the dorsal-ventral axis from their progenitor locations in the ventricular zone. The processes that control this migration are mostly unknown. DI1 lineage neurons express *Atoh1* and are born in the dorsal progenitor domain but migrate ventrally and located in lamina V-VII in the adult spinal cord (Miesegaes et al., 2009). V3 lineage neurons, expressing *Sim1,* are mostly located at lamina VIII but can migrate as far as Lamina IV(Borowska et al., 2013). A recent study on the migration of the Phox2a AS neurons demonstrated that these dI5-originated neurons rely on netrin-1 and reelin signalling to migrate into their final position in the lamina I and deep lamina (lamina V) in the spinal cord (Roome et al., 2022). Phox2a AS neurons could be divided into two main subgroups based on their migratory pathways/final position, proximity to primary afferent presynaptic neurons and birth

time. Superficial dorsal horn Phox2a neurons are mostly located at lamina I and migrate tangentially during development to reach their final position in lamina I. Superficial dorsal horn Phox2a neurons are adjacent to TrkA expressing sensory afferents and in TrkA null model, Phox2a lamina I neurons are significantly reduced (Roome *et al.*, 2020a). Another population of Phox2a neurons are migrating radially into the deep dorsal horn, lamina V and lateral spinal nucleus (LSN), and are born later than lamina I phox2a neurons (Roome *et al.*, 2022). Radial migration of deep lamina Phox2a neurons is regulated by reelin signalling which is modulated by disabled-1 (Dab1) protein, a crucial protein in intracellular transduction which controls the neuronal motility in the central nervous system (Akopians et al., 2008; Trommsdorff et al., 1999; Villeda et al., 2006). On the other hand, Phox2a neurons in superficial lamina are mostly affected by axon guidance signalling, *Ntn1*, during migration. *Ntn1* is controlling both afferent axons arrival and lamina I Phox2a neurons positioning in the superficial dorsal horn. It's possible that the developmental reason for this is to ensure that primary afferent axons enter the dorsal horn after their postsynaptic targets have settled in a specific location within the superficial lamina. The role of the netrin-1:DCC signalling is not limited to neuronal cell body positioning in the spinal cord; as this signalling is well known for its role in guiding axons through the spinal cord midline crossing.

1.5 axon guidance pathways and their role in wiring the nociceptive circuit:

Bilateria refers to a taxon in animal kingdom that poses bilateral symmetry as embryos or adults. The central nervous system (CNS) in bilateral animals contains subgroups of axons called commissures that project across the CNS midline and connect the ipsilateral and contralateral

sides of the CNS (Chedotal, 2014; Denes et al., 2007). Commissural circuits are preserved in different parts of the nervous system such as retinal ganglionic cell (RGC) axons project contralaterally to visual centers (Petros et al., 2008) and hearing system and sound localization relies on the commissures (Borst and Soria van Hoeve, 2012). In the spinal cord, commissural interneurons integrate relayed sensory inputs from the periphery and play a key role in controlling locomotion and rhythmic movements (Goulding, 2009; Kiehn, 2011). Also, many of long ascending projection neurons are commissures and cross the spinal cord midline to reach their supraspinal targets on the contralateral side. The mechanism that controls the midline crossing is heavily studied and several signalling pathways are introduced as the main principles controlling the midline crossing and axon guidance.

Axon guidance pathways are classified into four major groups of ligands and their corresponding receptors. Netrin, Slit, Ephrin and Semaphorin are the main ligands directing axons to the proper target by providing a series of attractive and repulsive cues guidance molecules family that regulate several switch points in the central nervous system (Lin et al., 2009).

The Netrin family with five members, netrin1 to netrin5, are well-studied extracellular molecules involved in axon guidance. Netrin poses different receptors such as DCC, Unc5/6 and Neogenin and based on the interacting receptor could induce either attractive or repulsive effects. For example, netrin/DCC interaction promotes axonal attraction which is crucial for axonal decussation while netrin binding to Unc5 receptor or netrin interaction with DCC/Unc5 complex is triggering the repulsive activity (Moore et al., 2007).

DCC is a receptor of the immunoglobulin superfamily which is composed of a single transmembrane protein with four immunoglobulin-like domains (Ig) and six fibronectin type III (Finci et al., 2015).

The role of *Dcc* in the central nervous system is not limited to lateralization and midline crossing but the adult expression of the *Dcc* has been shown in dendritic spines (Liang et al., 2014). Dcc heterozygote mice have smaller spines and lower spine density and length, and Dcc function in synapse formation has been demonstrated in mice. (Horn et al., 2013). *Dcc* mutation in humans causes congenital mirror movement disorder (CMM) in which unilateral stimulation induced bilateral sensation. A recent study in the Kania lab showed that *Dcc* is required for commissural PN development and the topognosis function (da Silva et al., 2018a). Deletion of *Dcc* in the lumbar-thoracic spinal cord causes nociceptive topognosis deficits in mice. Mice with *Dcc* deletion in the spinal cord lick the non-painful hind paw more than controls. This could be explained by ipsilateral spinothalamic tract axons whereas, in normal control mice, these neurons should innervate the contralateral VPL thalamus. Contralateral projection to the thalamus is the first level of the somatotopic organization of ST neurons. More complex somatotopic maps will be found in the VPL where studies showed discrete maps of forelimbs and hindlimbs as separate areas in the VPL (Francis *et al.*, 2008). It is still unknown which ST neurons define this map and which subpopulations require DCC to perform their functions.

As early as E9-E10, newborn spinal cord neurons begin extending their axons, and the first challenge for them is determining which direction the axons should travel. Many of the early born spinal projection neurons prefer ventral midline crossing in the floor plate, but midline crossing still occurs above the central canal at dorsal spinal cord after E13-E14 (Chedotal, 2019; Orlino et al., 2000). The spinal cord's first commissures are kept in the CNS by repulsive mechanisms such as repellent molecule secretion from meningeal cells, but growth-promoting molecules such as netrin-1 are also required to confine commissural axons to the spinal cord. (Laumonnerie et al., 2014; Moreno-Bravo et al., 2018; Suter et al., 2017). It has been shown that

in the lack of netrin-1 or its receptor DCC, commissural axons are misrouted through the dorsal root entry zone (DREZ) or extend toward the ventral motor roots (Moreno-Bravo *et al.*, 2018; Suter *et al.*, 2017). Moreover, midline crossing is highly reduced in both netrin-1 and DCC knockout models (da Silva *et al.*, 2018a; Fazeli et al., 1997; Serafini et al., 1996).

For many years floor plate secreted netrin-1 was known as a long-range chemoattractant providing a gradient to attract commissures to the ventral midline. Findings on ventricular zone netrrin1 secretion are questioning the classic model. Beside the floorplate, netrin-1 protein and mRNA are accumulated in the pial surface. Mice with selective deletion of floor plate netrin-1 but not the VZ netrin-1 still manage to extend commissural axons toward the ventral midline. These results show that, unlike the previous netrin-1 gradient attraction model, commissural are responsive to VZ netrin 1 in the pial surface adjacent to their extension path and axon outgrowth happens through the haptotaxis (Varadarajan et al., 2017).

Commissural axons do not stay in the ventral midline for a long time. Immediately after reaching the floor plate, commissural axons tend to leave there by extending on the contralateral side of the spinal cord. Despite years of research, it is still unclear how this change in responsiveness is coordinated (Chedotal, 2011; Ducuing et al., 2019). One explanation is that commissural axons stop responding to floor plate attractants and instead being responsive to other guidance cues such as Slit and Sema3b (Stein and Tessier-Lavigne, 2001; Zou et al., 2000). Lack of Sema3b or Slit (triple knockout of Slit1, Slit2 and Slit3) induces axon midline crossing impairment in mice and both in-vivo/in vitro data show the Sema3b and Slit function in the midline repulsion (Jaworski et al., 2010; Long et al., 2004). Given that netrin-1, Slit and Sema3b are all present at the floor plate prior to commissural axon crossing, the modulation of commissural axons response most likely takes place at the level of their receptors or downstream signalling partners.

One model suggests that floor plate cells express Neuropilin 2 transiently to trap Sema3b and prevent early repulsion of pre-crossing commissural axons (Hernandez-Enriquez et al., 2015).

Robo3 receptor is another effector of axon midline crossing in the spinal cord. Two different splice isoforms of Robo3, Robo3.1 and Robo3.2 have been identified in mice which are differentially expressed in pre and post-crossing axons (Chen et al., 2008). Gain of function experiment in *Robo3* knockout mice shows that re-expression of the Robo 3.1 but not the Robo3.2 could restore midline crossing. Robo.1 seems to be involved in suppressing the Robo1 and Robo2 repulsive effect in pre-crossing axons, while in post Crossing commissures, Robo3.2 isoform cooperates with repulsive Robo1 and Robo2 to lead axons toward the outside of the midline (Jaworski *et al.*, 2010). Although, Robo3 model of the midline switch is interesting but there are shortcomings regarding this model. First, this model is based on the ROBO3 interaction with Robo1 and Robo2, while there is no evidence of heterodimerization of these receptors. Also, Robo1 and Robo2 expression in pre-crossing axons is still not clear (Jaworski *et al.*, 2010; Sabatier et al., 2004). Robo3.1 interaction with DCC receptor in mammals proposes another potential mechanism of regulating axon midline crossing through the interaction of Robo3 with DCC that triggers netrin-1 function. Because of the high divergence of Robo3 receptor, proposed regulatory mechanisms could be specific to the species under study (Friocourt and Chedotal, 2017).

Post-crossing commissural axons need to proceed to the next step when they complete the midline crossing. The majority of these axons choose to grow longitudinally in an anterior direction however there are some caudal extensions as well (Kadison and Kaprielian, 2004; Kadison et al., 2006; Sakai and Kaprielian, 2012). The mechanism behind anterior turning is not well understood. Though, some insights have been provided by studying the role of Wnt and Shh

proteins in regulating longitudinal outgrowth of the commissural axons. Shh expression in the mouse floor plate changes based on the spinal cord level. Higher Shh expression in the caudal spinal cord compared to the rostral side creates a gradient that repels commissural axons from the caudal cord and provokes them to extend toward the rostral side. (Yam et al., 2012).

Other than Shh protein, Wnt family is involved in longitudinal axon guidance. Five Wnt proteins have been identified in the ventricular zone and floorplate progenitors and provide a gradient in the rostral-Caudal axis of the spinal cord. Wnt activity is regulated by non-canonical planar cell polarity (PCP) pathway which is essential for the rostral turning (Lyuksyutova et al., 2003; Wolf et al., 2008). Regulation of Wnt protein by PCP pathway is mediated by a protein called Fzd3 that itself is regulated by Shisa2 which is indirectly regulated by Shh. These findings imply that Shh regulates midline crossing and rostral turning of commissural axons via two different routes. It is still unclear how the post-crossing growth cone integrates attractive and repulsive Shh signals (Onishi and Zou, 2017).

1.5.1 Axon guidance-associated neurological disorder:

The balance of commissural and non-commissural axons ratio in the CNS is essential for proper function and lack of this balance lead to various neurological disorder. One example of impaired commissures ratio is albinism. In albino patients, defected ipsilateral/contralateral ratio of retino-thalamic innervation leads to changes in binocular vision and depth perception (Lund, 1965; Petros *et al.*, 2008).

A rare neurological disorder called horizontal gaze palsy with progressive scoliosis (HGPPS) is associated with an autosomal recessive mutation in the *Robo3* axon guidance receptor (Engle, 2010; Jen et al., 2004). Lateral eye movement is impaired in HGPPS patients. Furthermore, they develop severe scoliosis during childhood, but the mirror movement is not observed in HGPPS patients. *Robo3* mutant mice fail to cross the CNS midline results in increased ipsilateral innervation of ascending sensory axons as well as CST axons (Abu-Amero et al., 2009; Jen *et al.*, 2004). Although midline innervation is affected in *Robo3* mutant model, ascending axons manage to reach their designated targets however on the wrong side of the CNS. Electrophysiological recordings show that although *Robo3* knockout axons manage to reach their brain target, ipsilateral innervating axons seem to have different synaptic properties compared to normal contralateral innervation. The medial nucleus of the trapezoid body (MNTB) is normally synapsed by a unique contralateral VCN but in *Robo3* mutants, several ipsilateral VCN axons are connected to MNTB neurons and produce a smaller presynaptic current with an impaired neurotransmitter release (Michalski et al., 2013).

Mirror movement disorder (MMD) is another neurological disorder caused by the miswiring of commissural axons. Intended unilateral movements lead to unintended symmetrical movement on another side of the body in humans with MMD (Gallea et al., 2011). Studies on the mechanism behind MMD introduce an autosomal dominant mutation in *DCC* gene as a causal gene inducing MMD. Deleted in colorectal cancer (*DCC*) is an axon guidance receptor (Djarmati-Westenberger et al., 2011; Srour et al., 2010). Impaired expression of *DCC* in developing corticospinal tract (CST) changes the ratio of commissures and induces the movement deficit in MMD patients (Finger et al., 2002).

1.6 Hypothesis and aims:

Given the suggested role of Phox2a AS neurons in conveying nociceptive information and evidence on *Dcc* function in wiring the nociceptive circuit, I hypothesize that Phox2a AS neurons are a critical population in relaying information regarding the discriminatory component of pain. Selective knockout of *Dcc* in Phox2a neurons is going to impair the axonal arrangement of the nociceptive circuit in the spinal cord and brain. Three principal aims were sought:

Given the demonstrated role of *Dcc* in changing the laterality of somatosensory circuit and inducing impaired nociceptive topognosis, I hypothesize that in Dcc^{Phox2a} mice, the ipsilateral AS axons compete for brain target (e.g.: thalamus) connectivity with the appropriate contralateral PN axons and through developmental plasticity and pruning of connections, the somatotopic order of these connection becomes disrupted.

Chapter 2: Materials and Methods

Mouse Colony Management and Maintenance

Mice of either sex were used in this study. All animal handling protocols were reviewed and approved by the Animal Care Committee of the Institut de recherches cliniques de Montréal (IRCM). Adult mice were 11-17 weeks old at the start of the experiments and were maintained on a 12 h light/dark cycle in cages with a maximum cage capacity of five mice, and chow available ad libitum.

Generation of mice and embryos

The following transgene combinations were generated: *Phox2a*^{Cre}*; Dcc*$^{f/f}$*, Phox2a*^{Cre}*, Dcc*$^{f/+}$*, Dcc*$^{f/f}$, *Ntn1*^{Bgeo} and *Phox2a*^{Cre}*; Cdx2*^{FlpO}*; R26*$^{FSF\text{-}LSL}$*-tdT* by breeding mice carrying one or more of the required alleles/transgenes. Detailed transgenic line information is in Table 1. Resources table. Genotyping of mouse tail DNA samples was done by PCR with primers for *Dcc*^{f} and *Dcc*$^{+}$ alleles, as well as *Cre, FlpO, R26*$^{LSL\text{-}tdT/+}$ and *lacZ* (*Bgeo*) as previously described (Abraira *et al.*, 2017; Krimpenfort et al., 2012; Madisen et al., 2010; Roome et al., 2020b; Skarnes et al., 1995). To generate embryos of specific developmental ages, the presence of a vaginal plug at 6:00 am defined the embryonic day 0.5 (E0.5).

Tissue preparation

Embryos were harvested after anesthetizing their mother with 0.4 mL ketamine/xylazine (10 mg/mL Ketamine (DIN 02374994, 100mg/mL, Vetoquinol), 1 mg/mL Xylazine (DIN 02450240, 100 mg/mL, Dechra Veterinary Products Inc.) in 0.9% saline followed by cervical dislocation and dissected in 1X phosphate-buffered saline (PBS; Fisher BioReagents, cat. #: BP399) at 4°C, transferred to 4% paraformaldehyde (PFA) solution and left to fix for two hours while shaking at 4°C. After fixation, embryos were rinsed in 1X PBS, kept in cryo-protection solution (30% sucrose in 1X PBS) in 4°C until they sank and trimmed for mounting in Tissue-Tek O.C.T. Compound (VWR, cat. #: 4583) before cryo-sectioning.

Adult mice were transcardially perfused with 15 mL of 0.9% saline (9 g of NaCl in 1000 mL H_2O filtered by an Ultrapure Milli-Q system (Milli-Q water)) followed with 15 mL of 4% PFA. Dissected brain and spinal cord were rinsed with 1X PBS and kept in PFA fixative for one hour at 4°C while shaking. These were washed again with 1X cold PBS and equilibrated in 30% sucrose solution at 4°C. Tissues were cut into 25 μm sections for all experiments using a cryostat (NX70 Thermo Fisher).

Immunostaining and *in situ* mRNA detection

Sections were washed 3 times for 5 minutes with 1X PBS at room temperature. Then, a blocking solution containing 5% heat-inactivated normal horse serum (MilliporeSigma, cat. #: 119K0364) in 1X PBS containing 0.1% Triton X-100 (PBS-T; Fisher BioReagents, cat. #: 9002-93-1) was

gently applied to the sections and incubated for 30 minutes at room temperature. Next, slides were incubated with primary antibodies (Table 1. Resources table) overnight at 4°C. On the next day, slides were rinsed 3 times with PBS and incubated with fluorophore-conjugated secondary antibodies for 2 hours at room temperature. After incubation, slides were washed and coverslipped with 10% Mowiol (MilliporeSigma, cat. #: 81381) and 25% glycerol (MilliporeSigma, cat. #: 56-81-5) in MilliQ water. Slides were kept at room temperature until dry, and then at 4°C until imaging. To detect netrin-1 protein, antigen retrieval was performed prior to immunostaining: slides were post-fixed with 4% PFA for 10 minutes and rinsed with PBS 3 times for 5 minutes each. Sodium Citrate buffer containing 0.05% Tween 20 (MilliporeSigma, cat. #: 9005-64-5), pH 6.0 was brought to a boil on a bench-top heater and the slides were incubated in the boiling buffer for 2.5 minutes. Slides were allowed to cool in the buffer solution for 20 minutes at room temperature, rinsed 3 times for 5 minutes each and processed for immunohistochemistry as above.

In situ mRNA hybridization: *Ntn1* amplification primers (FORWARD: CTTCCTCACCGACCTCAATAAC and REVERSE: GGTAATACGACTCACTATAGGGTAGAGCTCCATGTTGAATCTGC) were designed using Primer3 V. 0.4.0 software (Rozen and Skaletsky, 2000), with the Reverse primer containing the T7 polymerase promoter. One-step RT-PCR (Eppendorf, Mastercycler Nexus GX2) was performed using T7 polymerase (Invitrogen) to make cDNA template from E11.5 mouse pooled brain RNA. The PCR product was purified by gel electrophoresis in 1% agarose gel and extracted from the gel using QIAquick extraction kit (Qiagen, cat. #: 28706X4). The purified DNA was then reamplified by PCR. The yield of DNA was estimated by the Low DNA Mass Ladder (Invitrogen) after gel electrophoresis. DIG-labeled RNA probes were synthesized by *in vitro* transcription with

T7 RNA polymerase using DIG RNA labeling kit (Roche, cat. #: 11175025910). The *Ntn1* probe was verified by sequencing.

Stereotaxic injection of retrograde tracers

Three to four hours before the surgery, mice received 1 mg/kg buprenorphine for analgesia. A mixture of 5% isoflurane (Fresenius Kabi, cat. #: CP0406V2) in oxygen was used to anesthetize the mice and the isoflurane level was set at 2.5 % in oxygen during the operation. Eye ointment was applied to the eyes to keep them moist. Top of the head was shaved with a razor blade and an incision was made longitudinally along the scalp to access the bregma, defined as the crossing point of two straight and perpendicular lines running along the sagittal and the coronal sutures (Geiger et al., 2008). Mouse head was stabilized in the stereotaxic frame with a digital coordinate display (David Kopf Instruments, cat. #: 940, 960, 1770, 900C, 922 and 933-B). Coordinates adapted from the Allen Institute for Brain Science reference atlas (Lein et al., 2007) were used to target the thalamus: 1.700 mm caudal and 2.000 mm lateral from bregma, at a depth of 3.400 mm. A solution of retrograde tracer, 1% Cholera Toxin Subunit B conjugated to Alexa Fluor™ 488 (CTB-488; Thermo Fisher, cat. #: C22841) in 1X PBS, was injected into the thalamus using the above stereotaxic apparatus via a 5 μL syringe (Hamilton company) attached to an UltraMicroPump3 infuser with a Micro4 controller (World Precision Instruments). 500 nL of the tracer was loaded into a pulled glass capillary needle attached to the syringe and injected at a rate of 100 nL/min. Following surgery, mice were monitored for infection and signs of pain for one week prior to collection of the brain and spinal cords. No animals died as a direct result of this manipulation.

Tracing and quantification of retrogradely labelled cells

Following perfusion of fixative, cryoprotection and cryosectioning, CTB-488-labelled neurons were counted in one of every four sections of the spinal cord, at C5-7 and L3-4 levels. A total number of 10 cervical and 10 lumbar sections of 25 μm thickness were analyzed per animal. Images were captured by confocal microscope (Leica SP8) through a 20x objective and CTB-labelled neurons were counted using the semi-manual cell counter plugin, Image J v. 2.0.0 software. The Allen Institute for Brain Science's adult mouse spinal cord atlas and the Rexed system were used to define the location of labelled neurons (Lein *et al.*, 2007; Rexed, 1952).

Anterograde tracing of PNs from spinal cord

Three to four hours prior to surgery, mice received 1 mg/kg buprenorphine for analgesia (Slow-release buprenorphine HCl 0.6 mg/mL, RxN698382, Chiron). To anesthetize the mice, we used a mixture of 5% isoflurane in oxygen, which was reduced to 2.5% during surgery. The anesthetized mouse was placed in the stereotaxic frame (David Kopf Instruments, cat. #: 940, 960, 1770, 900C, 922 and 933-B). Back skin was disinfected by povidone-iodine and cut to access the spinal cord with the spine held in place via ear bars. The injection was performed as in the reference protocol (Kohro et al., 2015). 300 nL solution of AAV2/8-Syn-SYP1-mSOG-citrine, (titer: $2.2x10^{13}$ genome copies (GC) /mL; lot 1385) and AAV2/8-Syn-SYP1-mSOG-mCherry, (titer: $2.0x10^{13}$ GC/mL; lot 1410, The Neurophotonics Centre, CERVO), were injected unilaterally at lumbar and cervical levels, respectively (ML 0.45 mm; AP 0 ± 0.5 mm; DV 0.35 mm from the dorsal spinal

midline). Two injections with 0.5 mm distance along the anterior-posterior axis were performed at each level of the spinal cord. After four weeks, mice were perfused with fixative and brains harvested as above and cut in the coronal plane into 25 μm sections to access ventral posterolateral thalamus (VPL), parabrachial nucleus (PB) and other brain areas. Axonal citrine and mCherry signals were amplified with anti- GFP and anti-RFP antibodies and localised with respect to standard anatomical features (Kohro *et al.*, 2015). Signal quantification and overlap were assessed using Image J v. 2.0.0 software (Schneider et al., 2012).

Mouse behavior

Capsaicin Test: To assess the localization of thermal noxious stimuli, the capsaicin test was performed on eight $Phox2a^{Cre}$; $Dcc^{f/f}$ ($Dcc^{Phox2a:CreKO}$) and eight control littermates which were either $Phox2a^{Cre}$, $Dcc^{f/+}$ or $Dcc^{f/f}$ mice. Mice were habituated for 30-45 minutes in the test chamber, which was a 10x10 cm plexiglass box resting on a 25 cm-high glass platform. The mice were restrained with a towel and a volume of 15-20 μL of a 1.5 μg/20 μL capsaicin (TOCRIS, cat. #: 0462) in DMSO solution was subcutaneously injected into the hindpaw plantar surface using a 26G3/8 needle as in the standard protocol (Sakurada et al., 1992). The mice were immediately returned to the chamber and their behaviour recorded for 15 minutes using the video rate camera of a Galaxy A7 phone (Samsung Inc.). Raw videos were processed using Gnome software (Linux OS) to calculate the total licking time and time spent licking a specific paw. The output as a Srt file was processed using a Python script. Data were subjected to Student's t-test statistical analysis using Microsoft Excel and plotted using Prism 9 (GraphPad).

Hargreaves Test: Seven Dcc^{Phox2a} and six control littermate mice were placed inside 5x10 cm

Plexiglass boxes (IITC Life Science) on top of a transparent glass platform (5 mm thick) and habituated for 30-45 minutes. The plantar surface of the hindpaw was stimulated by an infrared light source (IITC Life Science, cat. #: PE34) at 192 W/cm^2 and withdrawal latency was recorded. To prevent tissue damage caused by radiant heat, 40 seconds of exposure was set as the cut-off time. The withdrawal latency was measured for each animal as the average of eight trials with a 5-minutes minimum interval to avoid overexposure (Hargreaves et al., 1988).

Von Frey Test: Mice were placed individually inside 5x10 cm Plexiglass boxes (IITC Life Science) set on top of a mesh surface table and habituated for 45 minutes. A mesh surface table was used, an easy-to-clean metal platform, with laser-cut perforations producing an open grid of 5x5 mm square holes allowing access to the mice's hind paw. Nylon filaments (Touch Test Sensory Evaluators, North Coast Medical, Inc. Kit #2 to #9), calibrated using a microbalance, to exert respectively, 0.015, 0.04, 0.07, 0.15, 0.44, 0.55, 1.0 and 1.3 g of force, were firmly applied to the plantar surface of the hind paw (alternating the side of the body being tested) until they bowed for 5 s. Only withdrawal responses, evoked in an obvious manner in response to the applied stimulus, were scored (Mogil et al., 2010). The series started with filament #5 (0.15g) and continued with increasingly thicker filaments until the first withdrawal response. Each series consisted of 4 trials after the first withdrawal, using a lighter filament if there was no withdrawal and using a higher filament if there was withdrawal, as per the up-down protocol (Chaplan et al., 1994).

Conditioned place avoidance (CPA) test: A CPA box with two 25.5x20x20 cm conditioning chambers and a neutral central room of 15x20x20 cm, connected via 5x5.5 cm openings was used (Cunningham et al., 2006; Tzschentke, 2014). On the first day of testing, mice were restricted to the central room for 1 minute and then allowed to freely explore the apparatus for 30 min to visit

the two lateral chambers with different visual cues. On the second day, mice were allowed to freely explore the chambers for 30 min. Their movements throughout the CPA box were recorded by a top-view camera (Galaxy A7 phone, Samsung Inc.), and the recordings were processed using Gnome software (Linux OS) to calculate the time spent in each chamber. The chamber that the mouse spent most time in was chosen as the conditioning chamber. In the next two days, mice were placed in one of the conditioning chambers, and a volume of 15-20 μL of 5 μg/20 μL capsaicin (TOCRIS, cat. #: 0462) in DMSO was subcutaneously injected into the hindpaw plantar surface. On the fifth day, mice were restricted in the central room for 1 min and allowed to freely roam the CPA box for 30 min. Times spent in chambers before and after the injection phases (second day versus the fifth day) were compared.

c-Fos detection

c-Fos expression was assessed as an indicator of neuronal activity in response to nociceptive stimuli: 15-20 μL of 1.5 μg/20 μL capsaicin (TOCRIS, cat. #: 0462) in DMSO solution was subcutaneously injected into the hind paw plantar surface. Mice were kept in their cages for 90 minutes after capsaicin injection, perfused, and spinal cord tissue and the whole brain were harvested. Spinal cord segments L3-4 and brains from -4.95 mm to -5.55 mm with respect to bregma were cut into 25 μm coronal sections to assess c-Fos immunoreactivity in the spinal cord and the PB, respectively (Hunt et al., 1987; Pilyavskii et al., 2005).

X-gal staining

X-gal solution consisting of 40 mg/mL X-gal powder (MilliporeSigma, cat. #: 7240-90-6) in DMSO was freshly prepared and mixed with solution A: 1M $MgCl_2$, 2% NP40, 2% Na-deoxycholate in 1X PBS (pH=7.2), potassium hexacyanoferrate (II) and potassium hexacyanoferrate (III) mixed at a volume ratio of 1:47:1:1, respectively). This buffer was poured gently to cover all the slides in a slide holder in a glass receptacle. Slide holders were wrapped in aluminium foil and incubated in a 37°C water bath. Slides were periodically examined to monitor enzymatic reaction over 3-4 hours. Slides were rinsed with Mili-Q water and coverslipped with the Mowiol solution.

Microscopy and image processing

Confocal laser scanning microscope (Leica SP8) was used to capture the images. Image processing and cell count analysis was performed by Image J v.2.0.0 software, cell count plugin. In Fig. 4E, the innervation area of cervical and lumbar AS axons was first normalized by pixel size in ImageJ; then the innervated area was selected using the freehand selection tool in each of the 10 sections (5 caudal and 5 rostral) per animal. The average cervical/lumbar AS axons area for each bregma level was measured in 3 control and 3 Dcc^{Phox2a} mice by ImageJ ROI measure. The average innervation area in each bregma is shown as an outline and these are stacked on top of each other in the caudal and rostral VPL.

Statistics

Quantification and statistical analysis were prepared using either Microsoft Excel or GraphPad prism 9. All experiments were performed by a blinded researcher. Data were analyzed using paired

and unpaired Student's t-tests as well as between subjects and Mixed ANOVA, one within and one between-subject factor test. Bonferroni pot-hoc analysis was performed for data with a significant ANOVA effect. Significance is presented as $p < 0.05$ is significant and ns: non-significant. The detailed statistic test performed on each data set and exact p-values are listed in the figure legends.

Chapter 3: Results

3.1 Decreased accuracy of topognosis in mice with selective deletion of DCC from Phox2a-expressing neurons

Although DCC's role in mediating the nociceptive topognosis has been demonstrated, the primary population that requires DCC for normal nocifensive behaviour has remained unknown

(Da Silva et al., 2018b). To selectively manipulate DCC expression in anterolateral system (AS) neurons of the nociceptive circuit, *Phox2a*^{Cre} driver was used as a proxy of Phox2a AS neurons that represent ~80% of the superficial dorsal horn (AS^{Sup}) and ~30% of the deep dorsal horn (AS^{Deep}) Phox2a neurons. Given the expression of Phox2a in ~60% of AS^{Sup} neurons and ~30% of AS^{Deep} neurons, *Phox2a*^{Cre} driver is allowing access to ~50% of AS^{Sup} in contrast to only ~10% of AS^{Deep} neurons (Alsulaiman et al., 2021; Roome *et al.*, 2020b). I generated the *Phox2a*^{Cre}-specific *Dcc* knock-out mice by crossing the *Phox2a*^{Cre} driver to the Cre-excisable alleles of *Dcc* (*Dcc*^{f}; (Krimpenfort *et al.*, 2012)) or null *Dcc* allele (*Dcc*^{Ko}). *Phox2a*^{Cre}; *Dcc*$^{f/f}$ mutants are called *Dcc*^{Phox2a} and I used *Phox2a*^{Cre}, *Dcc*$^{f/+}$ and *Dcc*$^{f/f}$ as control littermates. Also, alternative *Dcc* knockout mice were generated by using one *Dcc* null allele and one *Dcc*^{f} (*Dcc f/Ko* ^{Phox2a}) to compare the efficiency of *flox* excision by Cre driver in a model with one or two *flox* alleles. Also, I produced a heterozygote control group with one wildtype *Dcc* and one null *Dcc* allele (heterozygote control or het control) to check the potential *Dcc* haploinsufficiency.

At embryonic day E10.5, Phox2a AS neurons, which are all commissural, express DCC. Assessing *Phox2a*^{Cre} embryonic spinal cord at E10.5 demonstrated that *Phox2a*^{Cre} is able to delete DCC expression sufficiently in spinal Phox2a neurons (Fig 1A). To evaluate the effect of *Dcc* deletion on neuronal survival, I bred *Dcc*^{Phox2a} mice with those carrying the Cre-tdTomato reporter (*R26* $^{LSL\text{-}tdT)}$ and counted the number of the *Phox2a*^{Cre} expressing neurons in the adult spinal cord (Madisen *et al.*, 2010). TdTomato labelled Phox2a+ neurons at lamina I (AS^{Sup}) and lamina V/LSN (AS^{Deep}) of the adult spinal cord have been counted separately. The absence of *Dcc* in Phox2a neurons does not appear to influence the survival rate of these neurons, since the quantity and general position of the tdTomato-expressing Phox2a AS^{Sup} and AS^{Deep} neurons did not differ between control and *Dcc*^{Phox2a} mice (Fig 1B and 1B').

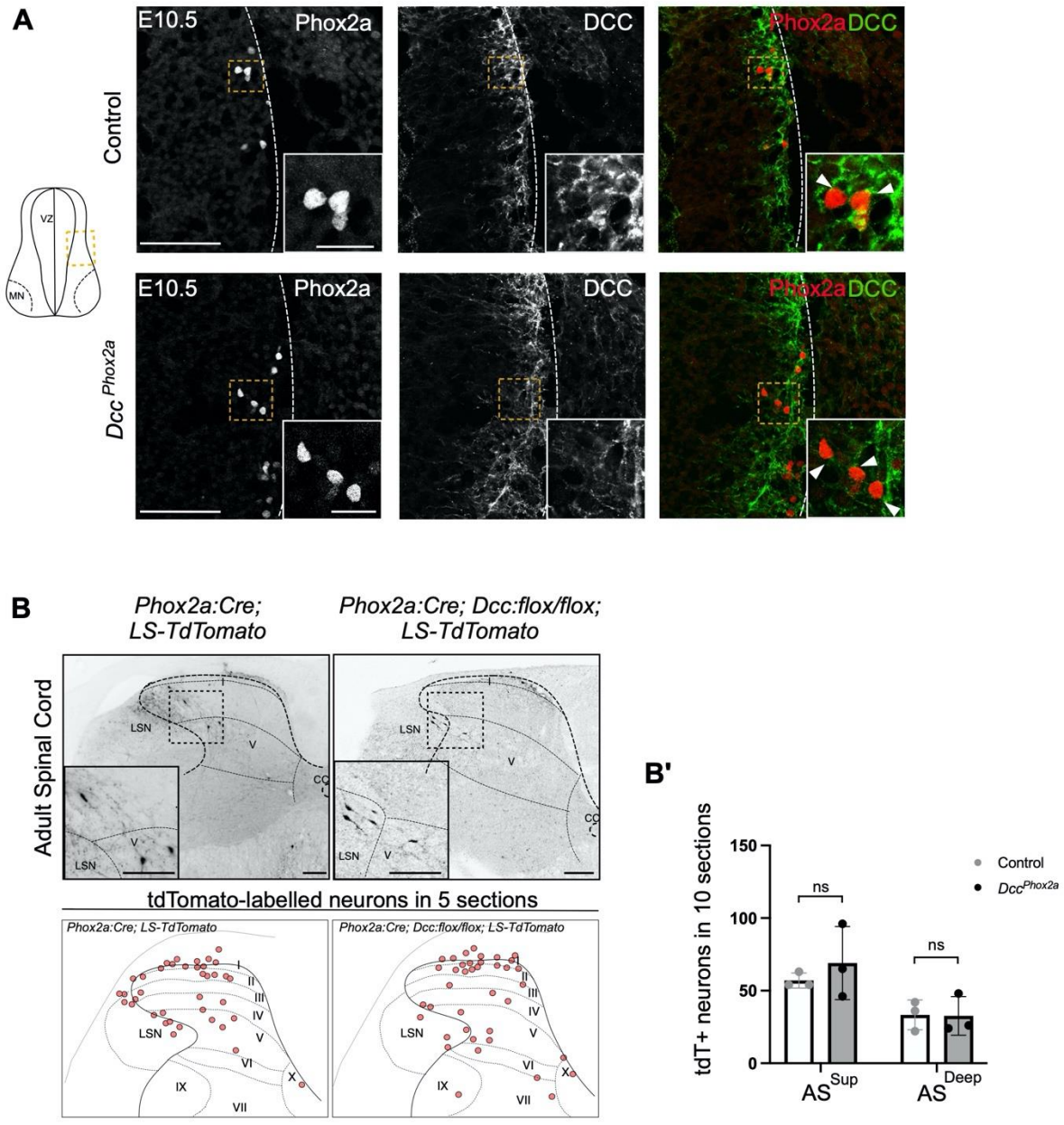

Figure 1. Decreased topognosis accuracy in mice with DCC deleted from Phox2a-expressing neurons

A- Phox2a immunofluorescence in E10.5 embryonic spinal cord. Arrowheads: Phox2a in the nucleus of commissural neurons with and without DCC cell body immunoreactivity in control and *Dcc*^{Phox2a}, respectively. n = 3 control and n = 3 *Dcc*^{Phox2a} mice. Scale bars: 100 μm in (A) and 25 μm in (inset).

B and B'- Phox2a neuron viability in adult *Dcc*^{Phox2a} model. The total number (summation) of tdT + neurons in 10 sections of cervical spinal cord in 25 μm thick sections (control AS^{Sup}, 57% ± 5.19%; control AS^{Deep}, 33.3% ± 10.26%; *Dcc*^{Phox2a} AS^{Sup}, 69% ± 25.23%; *Dcc*^{Phox2a} AS^{Deep}, 32.66% ± 13.31%). n = 3 control and n = 3 *Dcc*^{Phox2a} mice. Unpaired student's t-test in (B'); ns, non-significant. Data are represented as mean ± SD. Scale bars: 100 μm.

I then tested how *Dcc* ablation in Phox2a neurons might change the spinal nociceptive circuits. Hargreaves and von Frey tests have been performed to evaluate the quick reflexive response of the mice to thermal and mechanical nociception, respectively (Chaplan *et al.*, 1994; Hargreaves *et al.*, 1988). Comparing Dcc^{Phox2a} (n=7) spinal thermal reflex latency with control mice (n=6) showed there is not a notable difference between control and Dcc^{Phox2a} response to radiant heat in Hargreaves test (p= 0.15) (Fig 1C). Also, in von Frey test the change of response threshold in Dcc^{Phox2a} is not significantly different from control groups (p=0.42; Fig 1D). Overall, comparing knockout and controls in this experiment showed that the heat and mechanical spinal reflexes are unaffected in Dcc^{Phox2a} mice.

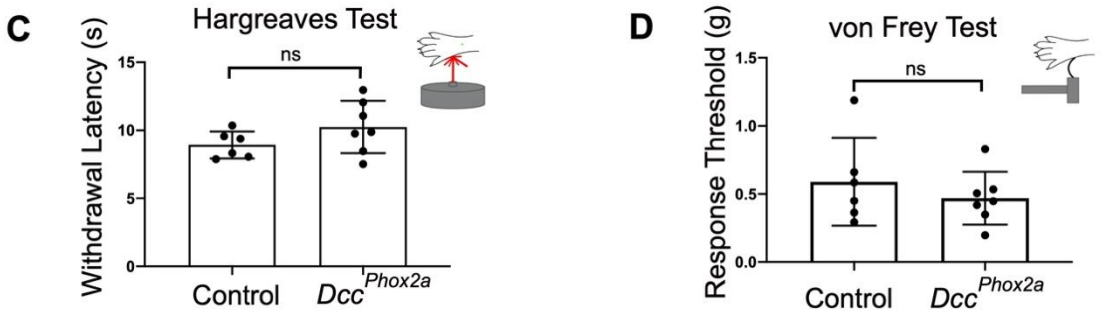

Figure 1.

C- Withdrawal latency response to radiant heat in Hargreaves test. (Control, 8.92s ± 0.99s; Dcc^{Phox2a}, 10.24s ± 1.92s). n = 6 control and n = 7 Dcc^{Phox2a} mice. Unpaired Student's t-test; ns, non-significant. Data are represented as mean ± SD.

D- Mechanical response threshold in von Frey test. (Control, 0.59g ± 0.32g; *Dcc*^{Phox2a}, 0.46g ± 0.19g). n = 6 control and n = 7 *Dcc*^{Phox2a} mice. Unpaired Student's t-test; ns, non-significant. Data are represented as mean ± SD.

Local neuronal activity in the spinal cord has been measured by counting the neurons expressing the activity-induced protein, c-Fos, 90 minutes after inducing thermal noxious stimuli. Capsaicin, a noxious stimulus that evokes thermal nociception has been injected and spinal c-Fos expression level did not show a significant difference between control and *Dcc*^{Phox2a} mice which suggests the normal function of the spinal nociceptive circuit (p= 0.13; n=3; Fig 1E and 1E').

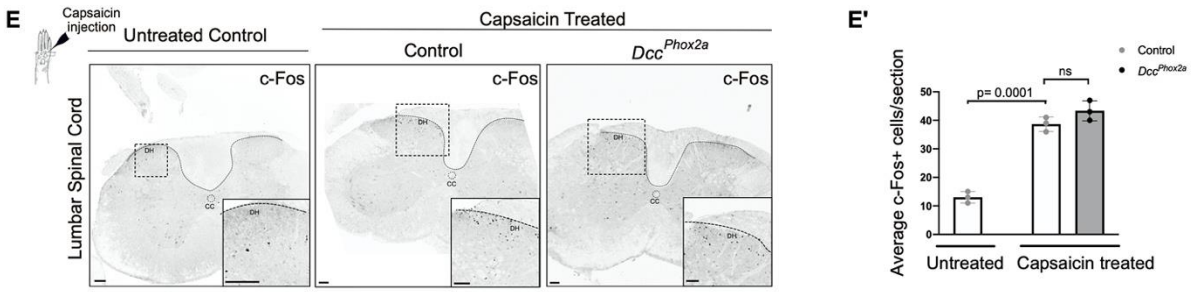

Figure 1.

E and E'- c-Fos expression in the dorsal horn of lumbar spinal cord after 1.5µg/20µL capsaicin injection in the plantar hind paw. The average number of c-Fos+ cells in a 25 µm section of lumbar spinal cord. n = 3 mice per group (untreated control, 13 ± 2; capsaicin treated control, 38.66 ± 2.51; capsaicin treated *Dcc*^{Phox2a}, 43.33 ± 3.51). Unpaired Student's t-test in (E'); P = 0.0001, significant; ns, non-significant. Data are represented as mean ± SD. Scale bars: 100 µm.

Having examined the normal function of the local spinal nociceptive circuit, I next asked how the function of supraspinal-related nociception changes. To examine whether *Dcc* knockout in Phox2a neurons affects the nocifensive response in mice, Capsaicin was injected as a thermal noxious stimulus into one of the hind paws and recorded the licking response as an indicator of pain in rodents (Fig 1F). The total licking time over the recorded period did not differ between Dcc^{Phox2a} and control mice, suggesting a comparable perceived stimulus intensity in mutants (Fig 1G). However, measuring the amount of time spent licking each paw shows that control mice spent 94.55 % ± 7.71% of this time licking the injected limb, 2.67% ± 3.62% of this time licking the contralateral forelimb, 0.26% ± 0.74% of this time licking the contralateral hindlimb, and 2.45% ± 4.12% of this time licking the ipsilateral hindlimb. In contrast, Dcc^{Phox2a} mice dedicated 84.27% ± 8.9% of their licking time to the injected limb, and 0%, 9.43% ± 5.74% and 6.28% ± 4.69% to the other limbs, respectively. 10.3% decrease in licking injection site as well as a 10.5% increase in licking the ipsilateral and contralateral forepaws suggesting the impaired nociceptive topognosis in Dcc^{Phox2a} mice ($p= 0.02$ and $p= 0.01$, respectively; Fig 1F, H).

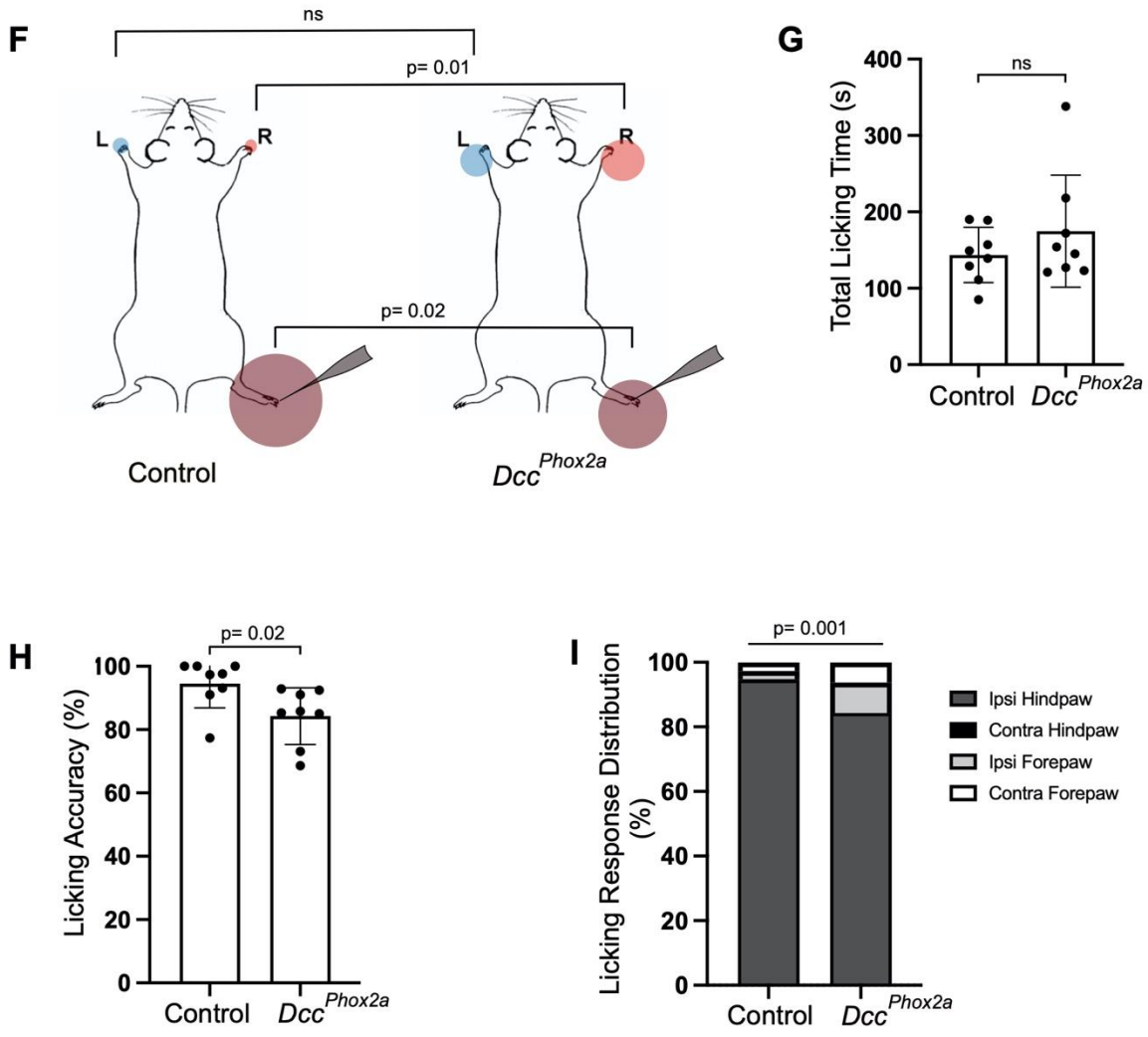

Figure 1.

F- Graphical representation of the average percentage of time spent licking each paw. Normalised by the time spent licking each paw to the total licking time: circle area is proportional to the licking time (control ipsilateral hindpaw, 94.55% ± 7.71%; control ipsilateral forepaw, 2.45% ± 4.12%; control contralateral forepaw, 2.67% ± 3.62%; *Dcc*^{Phox2a} ipsilateral hindpaw, 84.27% ± 8.95%; *Dcc*^{Phox2a} ipsilateral forepaw,

9.43% ± 5.74%; *Dcc*^{Phox2a} contralateral forepaw, 6.28% ± 4.69%). n = 8 control and n = 8 *Dcc*^{Phox2a} mice. Unpaired Student's t-test; p= 0.01 and p= 0.02, significant.

G, H - Quantification of total licking time in seconds ((G): control, 143.62 ± 36.16; *Dcc*^{Phox2a}, 174.75 ± 73.37), expressed as a fraction of the time licking the injection site (accuracy) ((H): control, 94.555 ± 7.71%; *Dcc*^{Phox2a}, 84.27% ± 8.95%). n = 8 control and n = 8 *Dcc*^{Phox2a} mice. Unpaired Student's t-test; p= 0.02 (H), significant; ns, non-significant. Data are represented as mean ± SD.

I- Licking response localisation as a percentage of total time following capsaicin injection into one of the hindpaws (control ipsilateral hindpaw, 94.55% ± 7.71%; control contralateral hindpaw, 0.26% ± 0.74%; control ipsilateral forepaw, 2.45% ± 4.12%; control contralateral forepaw, 2.67% ± 3.62%; *Dcc*^{Phox2a} ipsilateral hindpaw, 84.27% ± 8.95%; *Dcc*^{Phox2a} contralateral hindpaw, 0; *Dcc*^{Phox2a} ipsilateral forepaw, 9.43% ± 5.74%; *Dcc*^{Phox2a} contralateral forepaw, 6.28% ± 4.69%). n = 8 control and n = 8 *Dcc*^{Phox2a} mice. Mixed ANOVA, one within and one between subject factor; p= 0.001, significant. Data are represented as mean ± SD.

Dcc f/Ko ^{Phox2a} mice as an alternative strategy to knockout *Dcc* in Phox2a neurons were also tested for pain localisation accuracy. Consistent with *Dcc*^{Phox2a} result, *Dcc f/Ko* ^{Phox2a} showed reduced nociceptive topognosis accuracy and increased rostral limb licking followed by hindlimb noxious stimulus (p= 0.02 and p= 0.03; Fig 1J, K). Surprisingly, heterozygote controls that include one *Dcc* null allele show the same effect as *Dcc f/Ko* ^{Phox2a} and *Dcc*^{Phox2} groups raising the possibility that *Dcc*^{Ko} allele could induce topognosis deficit in both mutant and control groups as the result of *Dcc* haploinsufficiency (p= 0.03; Fig 1J, K). Based on this result I terminated using *Dcc f/Ko*^{Phox2a} line because the effect might not be Phox2a specific.

Since forepaws are heavily involved in grooming behaviour, I measure grooming behaviour vs forepaw licking separately to avoid grooming behaviour being confused with post-noxious stimulus licking behaviour. Grooming behaviour is performed with closed fist wiping/licking followed up by body wiping/licking, whereas nocifensive forepaw licking is not followed by body grooming and mice lick directly the forepaw open palm. Measuring the grooming time in control and *Dcc*^{phox2a} mice showed that control mice exhibit grooming behaviour 30% ± 13.56% of the total licking/grooming time, also in *Dcc*^{Phox2a} mice, 31.13% ± 21.14% of the total licking/grooming time was spent on grooming behaviour (n=8, p= 0.9; Fig 1L). These results along with forepaw licking analysis show that while the grooming behaviour did not change significantly in the mutant, nocifensive licking behaviour has been increased in *Dcc*^{Phox2a} mice. The inability of *Dcc*^{Phox2a} in localizing pain along the rostral-caudal axis raises the possibility of disruption of the somatosensory map in supraspinal targets.

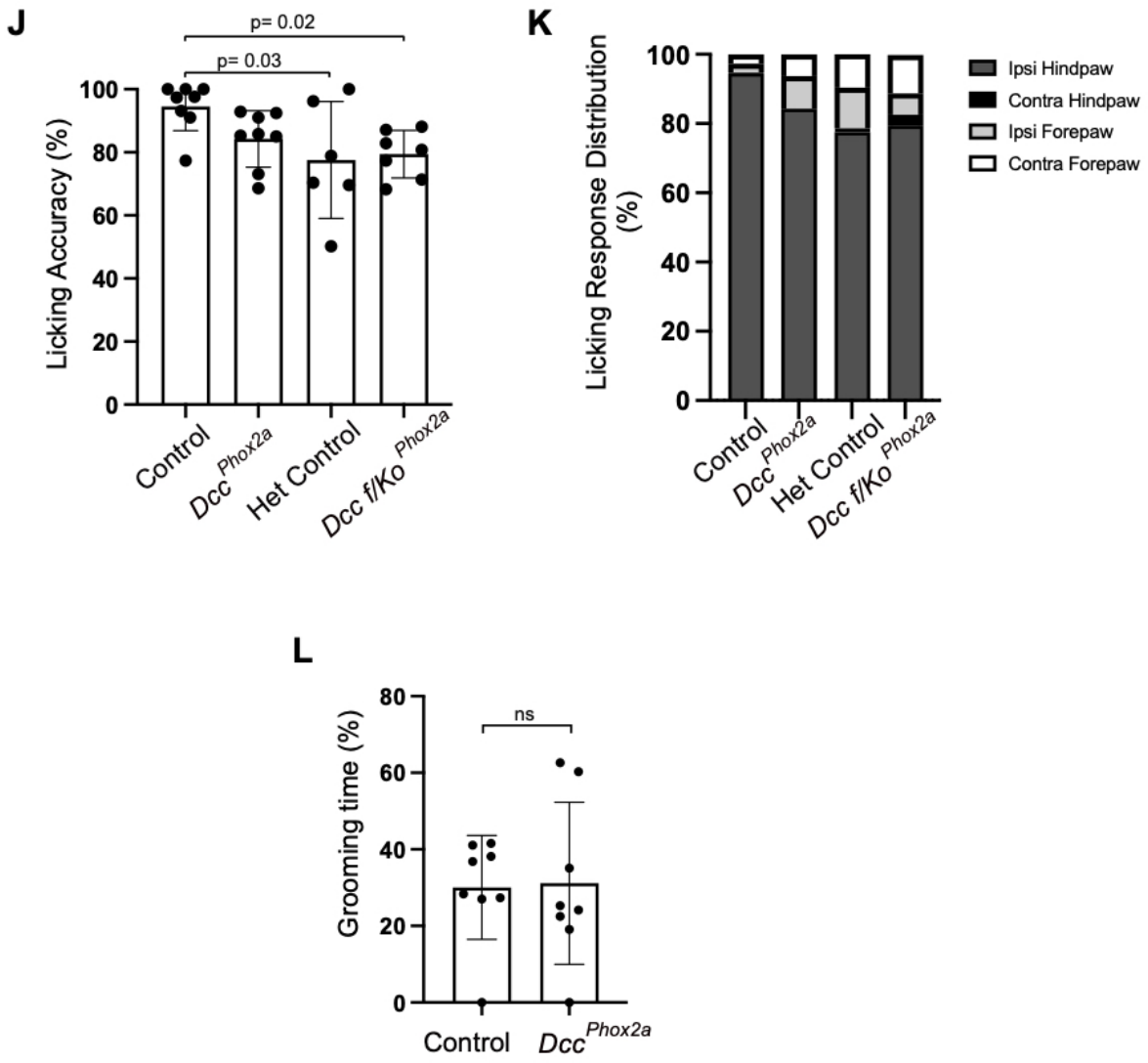

Figure1.

J - Quantification of the time licking the injection site (accuracy) as a percentage of total 4 limbs licking time: Control and *Dcc*^{Phox2a}: same as panel H, Het control, 77.55% ± 18.53%; *Dcc f/Ko*^{Phox2a}, 79.42% ± 7.53%). n = 6 Het control and n = 7 *Dcc f/Ko*^{Phox2a} mice. Unpaired Student's t-test; Control vs Het control: p= 0.03, control vs *Dcc f/Ko*^{Phox2a}: p= 0.02, significant. Data are represented as mean ± SD.

K- Licking response localisation as a percentage of total time following capsaicin injection into one of the hindpaws (Control and *Dcc*^{Phox2a}: same as panel I, Het control ipsilateral hindpaw, 77.55% ± 18.53%; Het control contralateral hindpaw, 1.06% ± 2.61%; Het control ipsilateral forepaw, 11.71% ± 11.15%; Het control contralateral forepaw, 9.66% ± 16.6%; *Dcc f/Ko*^{Phox2a} ipsilateral hindpaw, 79.42% ± 7.53%; *Dcc f/Ko*^{Phox2a} contralateral hindpaw, 3.11% ± 4.64%; *Dcc f/Ko*^{Phox2a} ipsilateral forepaw, 6.2% ± 8.85%; *Dcc f/Ko*^{Phox2a} contralateral forepaw, 11.08% ± 9.6%). n = 6 Het control and n = 7 *Dcc f/Ko*^{Phox2a} mice.

L - Quantification of the Grooming time as a percentage of the total 4 limbs licking/grooming time. Control, 30.05% ± 13.56%%; *Dcc*^{Phox2a}, 31.13%% ± 21.14%). n = 8 control and n = 8 *Dcc*^{Phox2a} mice. Unpaired Student's t-test; p= 0.9, ns, non-significant. Data are represented as mean ± SD.

3.2 Dissociation of aversive and discriminatory components of a noxious stimulus in *Dcc*^{Phox2a} mice

Dcc ablation in Phox2a neurons affects the topognostic component of the nocifensive response. However, the duration of licking behaviour post noxious stimuli is unchanged in *Dcc*^{Phox2a} and control groups suggesting a similar perception of the emotive component of pain. To investigate the motivational component of pain in *Dcc*^{Phox2a} mice, here I assessed whether this effect is specific to the discriminatory aspect of pain, or the aversive aspect of pain is also impaired by *Dcc* misfunction. The parabrachial nucleus (PB) is one of the classical targets related to the aversive response to pain (Bernard et al., 1996; Chiang *et al.*, 2019; Karthik et al., 2022). Therefore, I monitored the neuronal activity by quantifying capsaicin evoked c-Fos expression in PB neurons (Fig 3A). Counting the number of c-Fos expressing neurons 90 minutes after inducing thermal noxious stimulus showed the normal level of c-Fos activity in mutants (Fig

3A'). Although capsaicin injection induces a significant increase in the number of c-Fos expressing neurons in the control group compared to unstimulated controls, the number of c-Fos expressing neurons in control and *Dcc*^{Phox2a} groups does not show a significant difference (Fig 3A').

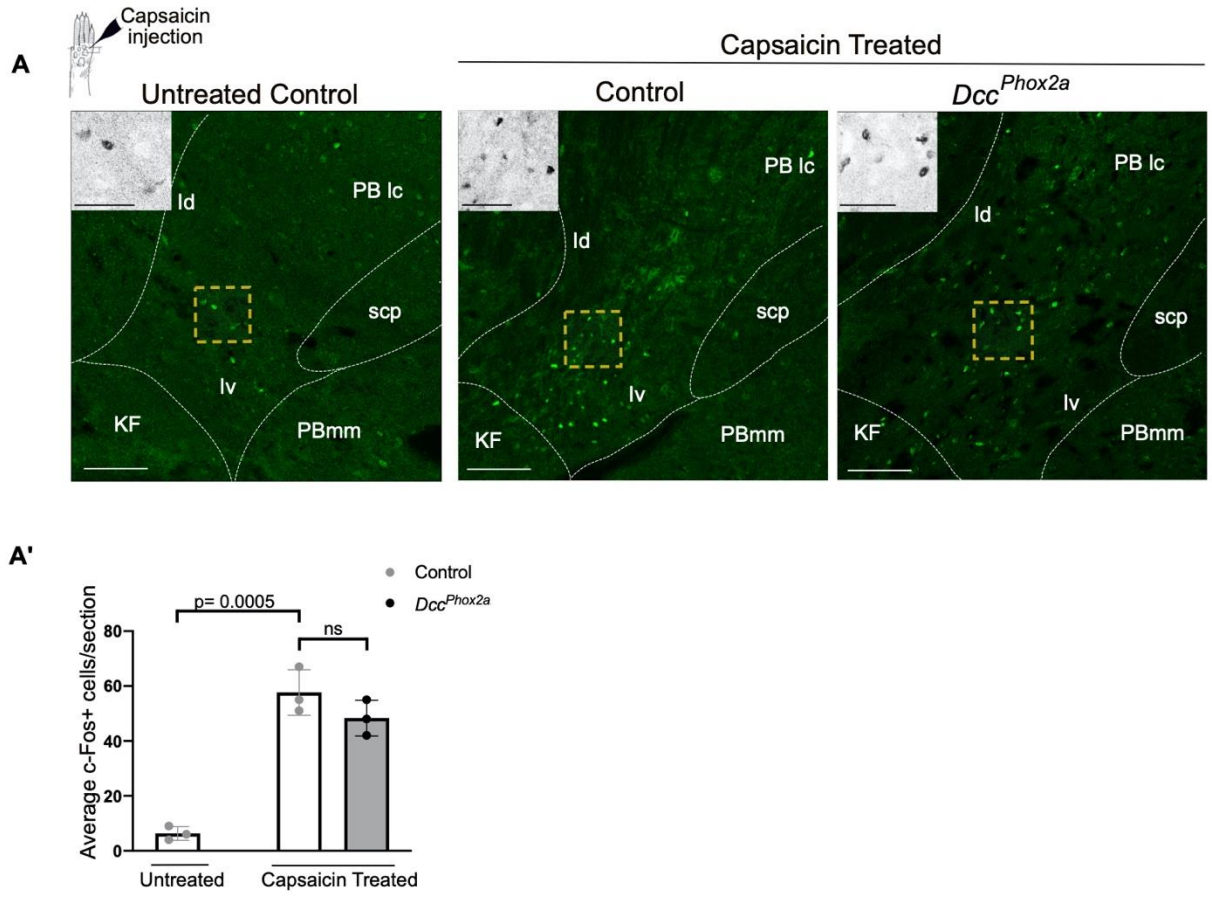

Figure 2. Normal aversive pain circuit in *Dcc*^{Phox2a} model

A and A'- c-Fos expression in the parabrachial nucleus (PB) after 1.5µg/20µL Capsaicin injection in the plantar hindpaw. The average number of c-Fos + cells in a 25 µm section of the PB nucleus. n = 3 mice per group (untreated control, 6.33 ± 2.51; capsaicin treated control, 57.66 ± 8.32; capsaicin treated *Dcc*^{Phox2a},

48.33 ± 6.5). Unpaired Student's t-test in (A'); p= 0.0005, significant; ns, non-significant. Data are represented as mean ± SD. Scale bars: 100 μm in (A) and 25 μm in (inset).

Besides PB, there are several other nuclei in the brain with a suggested role in processing the motivational component of pain. To determine the general impact of *Dcc* loss in AS neurons on the function of the motivational component of pain, I performed a behavioural assay called conditioned place aversion (CPA) test to measure the aversive dimension of pain in Dcc^{Phox2a} mice. CPA test was performed using a modified three-chamber standard paradigm which contains two translucent chambers with different visual cues connected with a small central neutral chamber. On the first and second day of the test, mice were free to explore two translucent rooms and the time spent in each chamber was measured on the second day. Mice were kept in one of the chambers (conditioning chamber) and had one of their hind paws injected with capsaicin on days three and four. On the day of testing, mice were free to move throughout the apparatus, and the length of time spent in each chamber was noted and compared using the common CPA scoring protocol.

This investigation showed that both Dcc^{Phox2a} and control mice stayed away from the conditioning chamber similarly (p= 0.006 and p= 0.007, respectively; Fig 2C, D, E). The sensitization to the noxious stimuli persisted in both groups and the mutant avoid the aversive condition as much as the control group. Thus, it appears that in the absence of DCC in Phox2a neurons defective nocifensive behaviour is specific to discriminatory but not aversive aspects of pain.

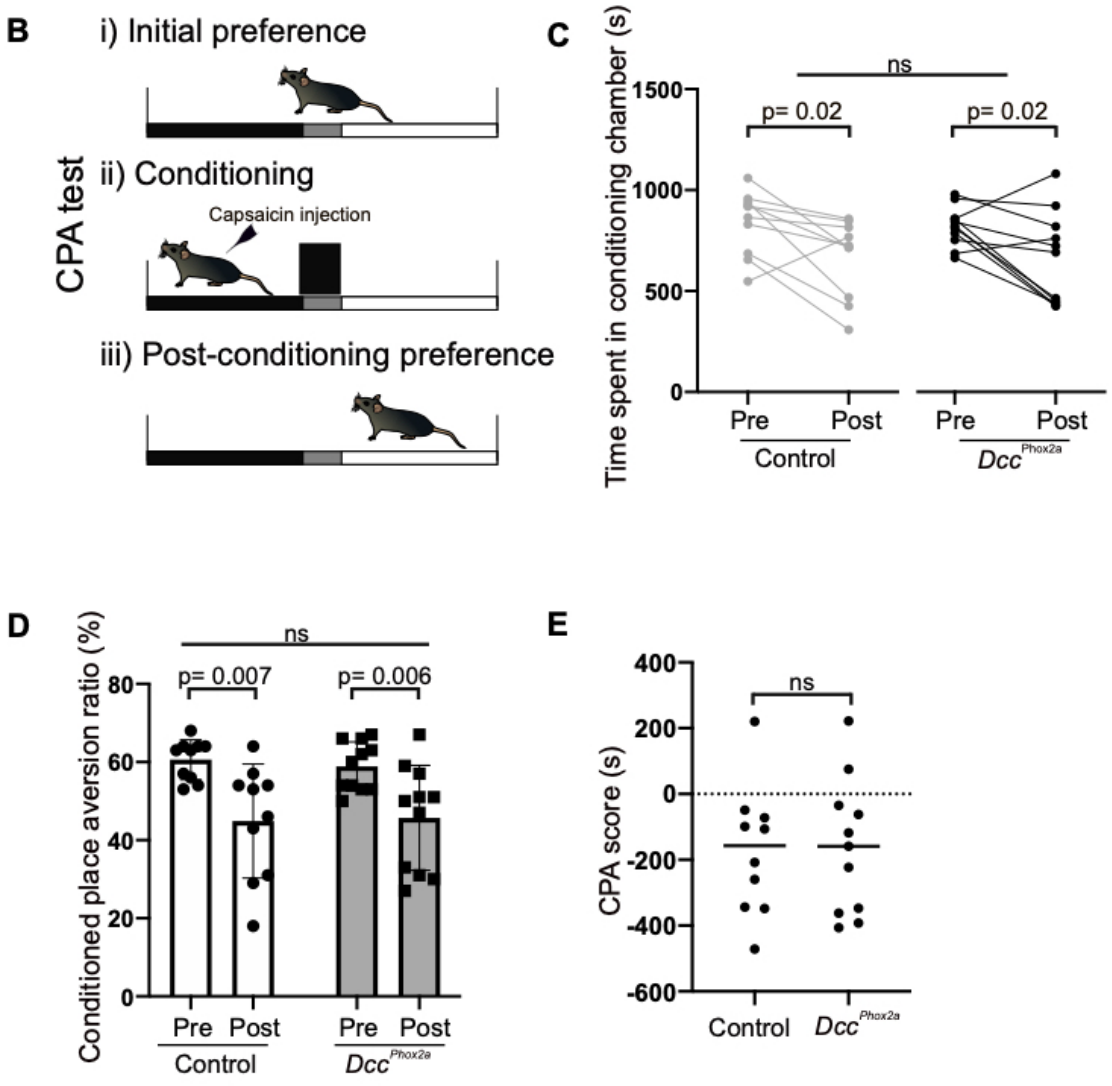
B
i) Initial preference
CPA test
ii) Conditioning
Capsaicin injection
iii) Post-conditioning preference
C
Time spent in conditioning chamber (s)
ns
p= 0.02
p= 0.02
1500
1000
500
0
Pre
Post
Pre
Post
Control
Dcc Phox2a
D
Conditioned place aversion ratio (%)
ns
p= 0.007
p= 0.006
80
60
40
20
0
Pre
Post
Pre
Post
Control
Dcc Phox2a
E
CPA score (s)
ns
400
200
0
-200
-400
-600
Control
Dcc Phox2a

Figure 2.

B- Conditioned place aversion (CPA) test: one side of the two-sided chamber was paired with thermal noxious stimuli by Capsaicin injection. The relative percentage of time spent in the Capsaicin-paired chamber before (pre) and after (post) conditioning phase was quantified in control and *Dcc*^{Phox2a} groups.

C- Time spent in Capsaicin-paired chamber before (pre) and after (post) conditioning phase. n = 10 control and n = 11 *Dcc*^{Phox2a} mice (control pre, 838.2s ± 159.34s; control post, 664.5s ± 193.22s; *Dcc*^{Phox2a} pre, 818.18s ± 97.39s; *Dcc*^{Phox2a} post, 653.9s ± 228.7s). Paired Student's t-test were used to compare the pre-post condition in each group; p= 0.02, significant. Mixed ANOVA, one within and one between subject factor; ns, non-significant.

D- Conditioned place aversion ratio as the fraction of time spent in the capsaicin-paired chamber before (pre) and after (post) conditioning phase. n = 10 control and n = 11 *Dcc*^{Phox2a} mice (control pre, 60.6% ± 5.12%; control post, 44.9% ± 14.59%; *Dcc*^{Phox2a} pre, 58.9% ± 6.25%; *Dcc*^{Phox2a} post, 45.72% ± 13.44%). Paired Student's t-test to compare the pre-post condition in each group; p= 0.007 and 0.006, significant. Mixed ANOVA; ns, non-significant.

E- CPA score: Subtraction of time spent in capsaicin-paired chamber post conditioning from before conditioning. n = 10 control and n = 11 *Dcc*^{Phox2a} mice (control, -173.7s; *Dcc*^{Phox2a}, -164.27s). Unpaired student's t-test; ns, non-significant.

3.3 Increased ipsilateral innervation of the thalamus by AS neurons in *Dcc*^{Phox2a} mice

Previous studies on the role of *Dcc* in development of somatosensory circuit anatomy suggested a contralateral to ipsilateral innervation shift in lumbar spinothalamic (ST) neurons in spinal cord-specific *Dcc* knockout model (*Dcc*^{SpC}). However, the identity of spinal projection neurons (SPNs) whose miswiring leads to the topognosis deficits remains unknown (da Silva *et al.*, 2018a). Here, I sought to use *Dcc*^{Phox2a} model to examine how *Dcc* ablation in Phox2a AS neurons might change the laterality of ST neurons at both cervical and lumbar level (Fig 3A, B). A fluorescent-conjugated Cholera Toxin B retrograde tracer was injected unilaterally into the ventral posterolateral thalamus (VPL) and neurons located in AS^{Sup} and AS^{Deep} were labelled retrogradely within the spinal cord. The number of AS^{Sup} and AS^{Deep} neurons were counted on the contralateral and ipsilateral sides of the spinal cord at cervical and lumbar levels (Fig 3A, B).

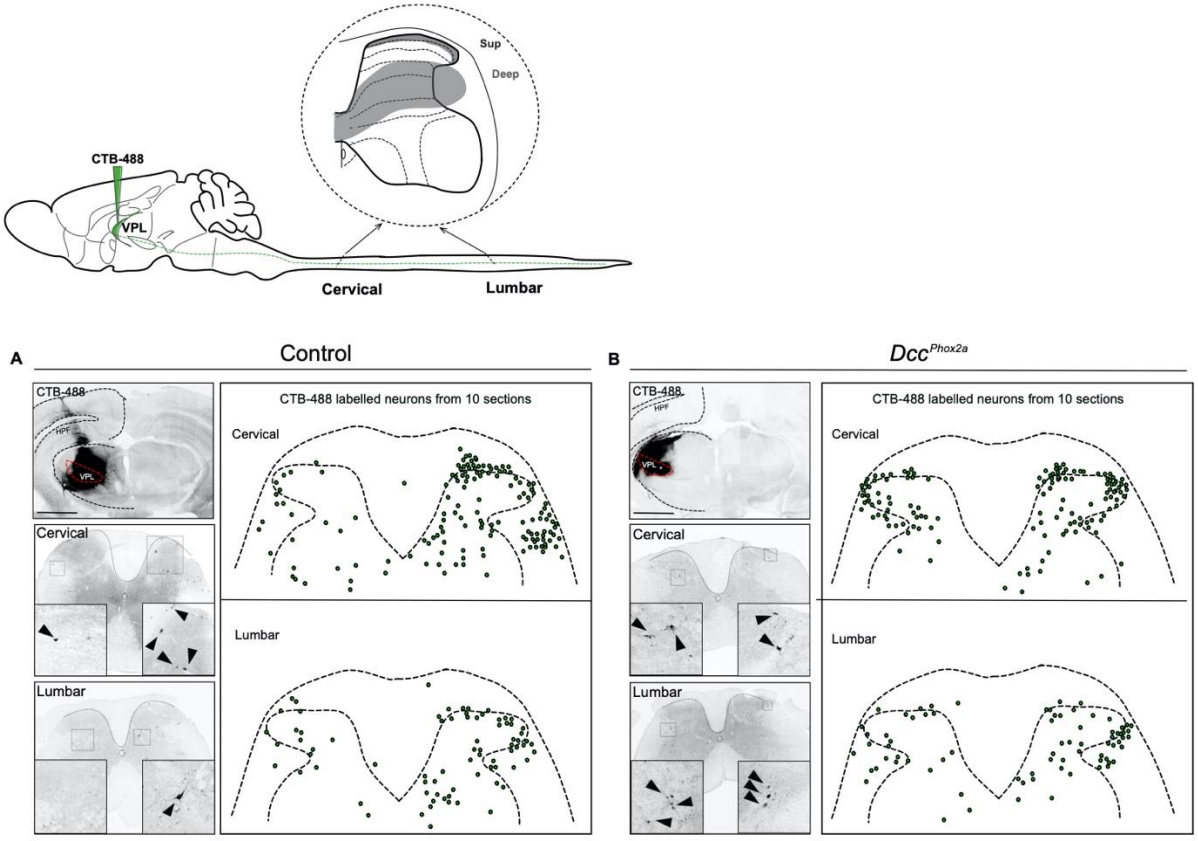

Figure 3. Increased ipsilateral innervation of the thalamus by AS neurons in *Dcc*^{Phox2a} mice

A and B- CTb-488 injection in adult control and *Dcc*^{Phox2a} VPL thalamus. Diagram illustrating the CTb-488 retrograde labeled neurons in 10 non-sequential 25 µm sections of the cervical and lumbar spinal cord of one representative mouse. Scale bars: 1.44 mm in VPL sections (A and B)

Retrograde tracer thalamic injections labelled the same number of ipsilateral and contralateral neurons in the lumbar cords of the control and *Dcc*^{Phox2a} groups, but *Dcc*^{Phox2a} mice had an increased number of ipsilateral neurons at the cervical level. (Fig 3C, 3C'). Also, normalizing for efficiency of tracer labelling, the ratio of ipsilateral to contralateral spinothalamic neurons was increased in cervical but not lumbar spinal cord of *Dcc*^{Phox2a} mice (p= 0.005; Fig 3D, D'). This is consistent with the behaviour phenotype with altered laterality of nocifensive response at the forepaw level but not the hind paws.

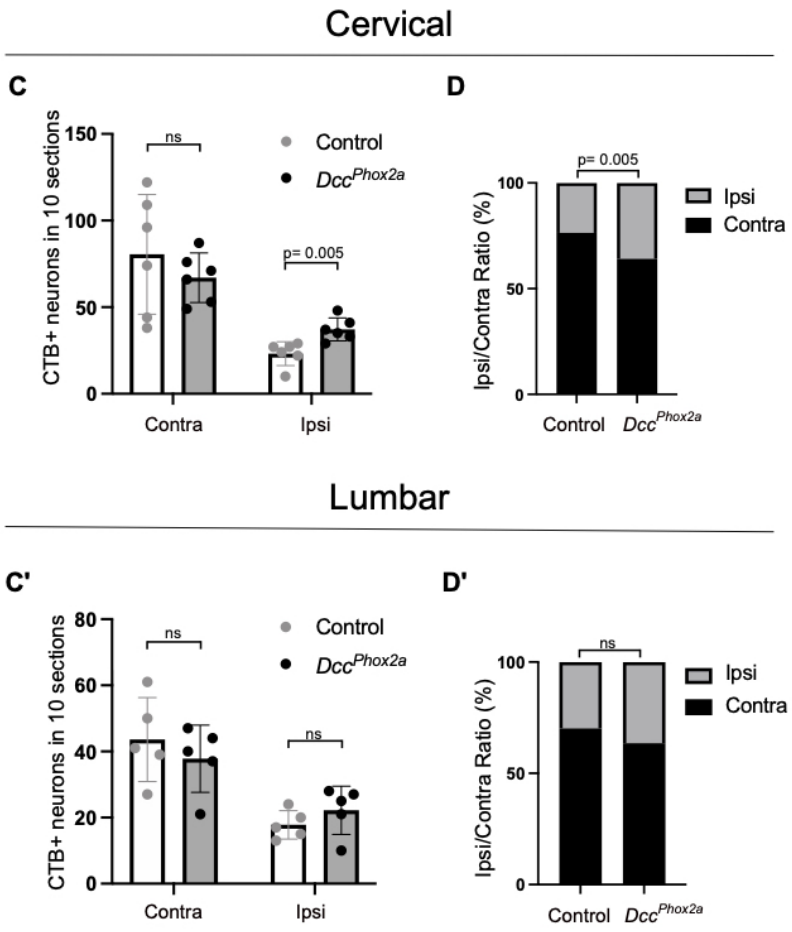

Figure 3.

C and C'- Quantification of retrograde-labeled contralateral and ipsilateral Spinothalamic neurons. Total number of the neurons in 10 sections (25 μm) at cervical and lumbar spinal cord of the control and *Dcc*^{Phox2a} groups. n = 6 cervical and n = 5 lumbar groups ((C): control contra, 80.5 ± 34.51; control ipsi, 23.16 ± 6.91; *Dcc*^{Phox2a} contra, 67 ± 14.26; *Dcc*^{Phox2a} ipsi, 37.16 ± 6.64) ((C'): control contra, 43.6 ± 12.72; control ipsi, 17.8 ± 4.32; *Dcc*^{Phox2a} contra, 37.8 ± 10.13; *Dcc*^{Phox2a} ipsi, 22.2 ± 7.32). Unpaired Student's t-test; p= 0.005, significant; ns, non-significant. Data are represented as mean ± SD.

D and D'- Percentage of ipsilateral versus contralateral thalamic projection neurons at cervical and lumbar spinal cord of the control and *Dcc*^{Phox2a} groups. n = 6 cervical and n = 5 lumbar groups ((D): control contra, 76.37% ± 8.06%; control ipsi, 23.62% ± 8.06%; *Dcc*^{Phox2a} contra, 64.13% ± 2.34%; *Dcc*^{Phox2a} ipsi, 35.86% ± 2.34%) ((D'): control contra, 70.2% ± 9.75%; control ipsi, 29.79% ± 9.75%; *Dcc*^{Phox2a} contra, 63.52% ± 3.16%; *Dcc*^{Phox2a} ipsi, 36.47% ± 3.16%). Unpaired student's t-test; p= 0.005, significant; ns, non-significant. Data are represented as mean ± SD.

Spinothalamic neurons are found in AS^{Sup} and AS^{Deep} of the spinal cord (Davidson et al., 2010). AS^{Sup} neurons encodes distinct sensory modalities with somatotopic organisation, as well as a smaller receptive field, suggest that they are involved in processing the discriminatory component of pain, whereas deeper neurons in the dorsal horn (AS^{Deep}) with a broader dynamic range appear to be involved in processing the motivational component of pain. This division leads us to check whether laterality changes are specific to one of these subregions. I counted the ST back labelled neurons at AS^{Sup} and AS^{Deep} at both cervical and lumbar levels.

Although the lumbar spinal cord, ipsilateral/contralateral ratio is not changed in Dcc^{Phox2a}, I quantified lamina-specific labelled cells to make sure the phenotype of each region is not masked by the other sub-population. Again, at the lumbar level, I could not find a significant change in the laterality of neither AS^{Sup} nor AS^{Deep} cells (Fig 3E', F'). At the cervical level, a significant increase in AS^{Sup} ipsilateral projecting neurons has been observed while the mild ipsilateral shift in the deep lamina is not significant (Fig 3E, F). This result suggests that lamina I neurons are the main sub-population that is affected by ablation of *Dcc* in the Phox2a projection neurons and do not decussate normally during development. So, the Superficial lamina I cells could be a potential population that controls the localization of the noxious stimuli.

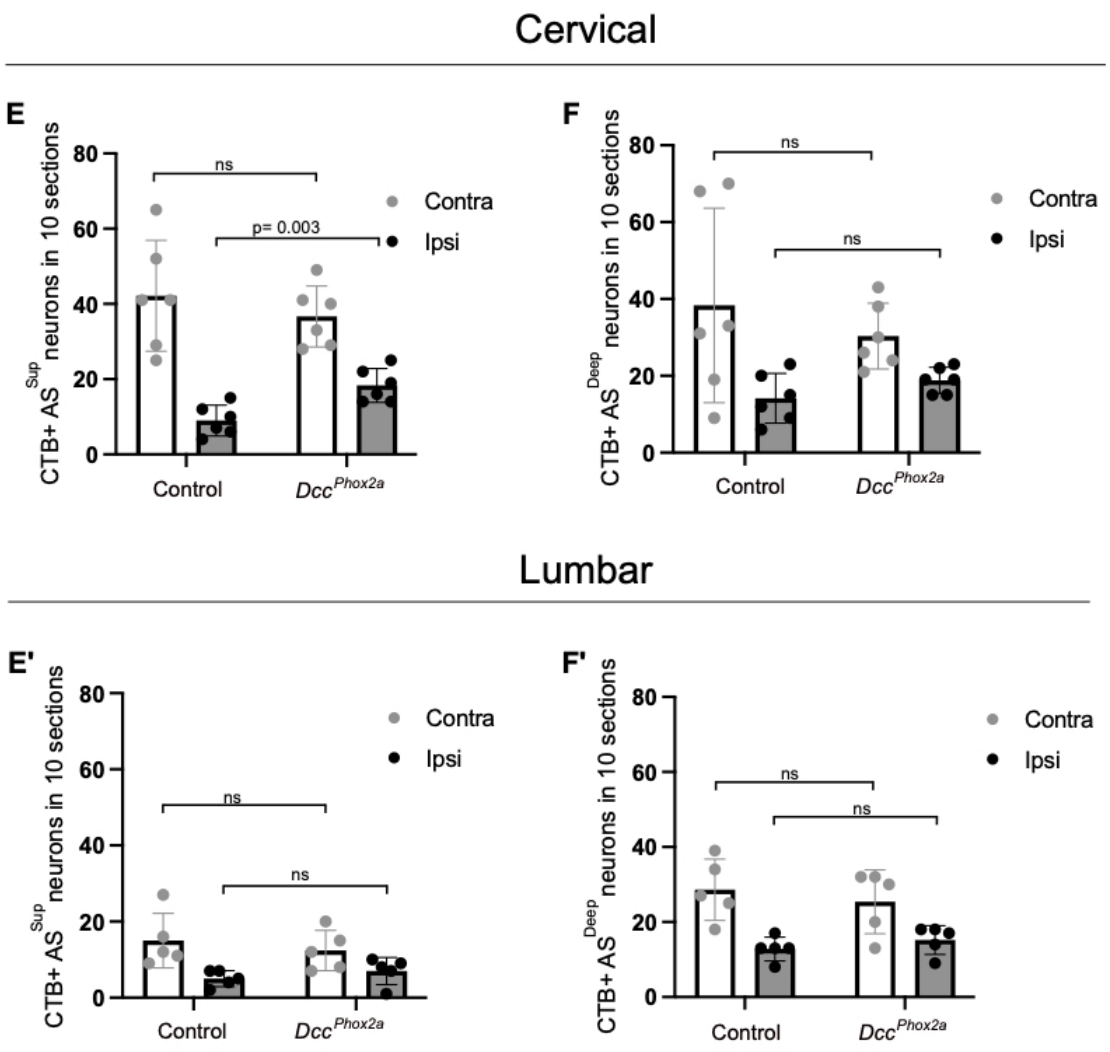
Cervical
E
CTB+ AS Sup neurons in 10 sections
80
60
40
20
0
ns
p= 0.003
Contra
Ipsi
Control
Dcc Phox2a
F
CTB+ AS Deep neurons in 10 sections
ns
ns
Contra
Ipsi
Control
Dcc Phox2a
Lumbar
E'
CTB+ AS Sup neurons in 10 sections
ns
ns
Contra
Ipsi
Control
Dcc Phox2a
F'
CTB+ AS Deep neurons in 10 sections
ns
ns
Contra
Ipsi
Control
Dcc Phox2a

Figure 3.

E and E'- Number of CTb-488 tracer labeled neurons in 10 sections (25 μm) of the cervical and lumbar AS^{Sup} neurons of control and Dcc^{Phox2a} mice. n = 6 cervical and n = 5 lumbar groups. ((E): control contra, 42.16 ± 14.75; control ipsi, 9 ± 4.09; Dcc^{Phox2a} contra, 36.66 ± 8.11; Dcc^{Phox2a} ipsi, 18.33 ± 4.5) ((E'): control contra, 15 ± 7.17; control ipsi, 5 ± 2.12; Dcc^{Phox2a} contra, 12.4 ± 5.32; Dcc^{Phox2a} ipsi, 7 ± 3.53). Unpaired student's t-test; p= 0.003, significant; ns, non-significant. Data are represented as mean ± SD.

F and F'- Number of CTb-488 tracer labeled neurons in 10 sections (25 μm) of cervical and lumbar AS^{Deep} neurons of the control and Dcc^{Phox2a} mice. n = 6 cervical and n = 5 lumbar groups ((F): control contra, 38.33 ± 25.29; control ipsi, 14.16 ± 6.49; Dcc^{Phox2a} contra, 30.33 ± 8.54; Dcc^{Phox2a} ipsi, 18.83 ± 3.37) ((F'): control contra, 28.6 ± 8.14; control ipsi, 12.8 ± 3.19; Dcc^{Phox2a} contra, 25.4 ± 8.53; Dcc^{Phox2a} ipsi, 15.2 ± 3.83). Unpaired Student's t-test; ns, non-significant. Data are represented as mean ± SD.

3.4 Impaired organization of spinothalamic innervation in *Dcc*^{Phox2a} mice

Deficient nociceptive topognosis in *Dcc*^{Phox2a} mice prompts the question of what anatomical changes caused this impaired nocifensive behaviour. Defective topognosis in rostra- caudal axis of the body might be due to an impaired topographic map in the brain. To investigate how *Dcc* loss would change the somatotopic order of spinal projections in their brain targets, I examined the organization of PN axon termini in PB, PAG and the thalamus, as three main targets of pain relaying AS projection neurons. Adeno associate viruses (AAV) carrying m-Cherry or GFP protein fused to synaptophysin (Syn) were used to specifically deliver these fluorescent proteins to synaptic vesicles and labelling axonal termini (Oh et al., 2014). Unilateral injection of mCherry-Syn and GFP-Syn encodes AAVs were performed in the cervical and lumbar spinal cord of adult *Dcc*^{Phox2a} and control mice. Four weeks after the injection, the spinal cord and the brain tissue were harvested and cryosectioned into 25 μm sections. Inspection of infection sites showed that the dorsal horn, including superficial laminae containing AS^{Sup} neurons, was consistently and unilaterally labelled (Fig 4A).

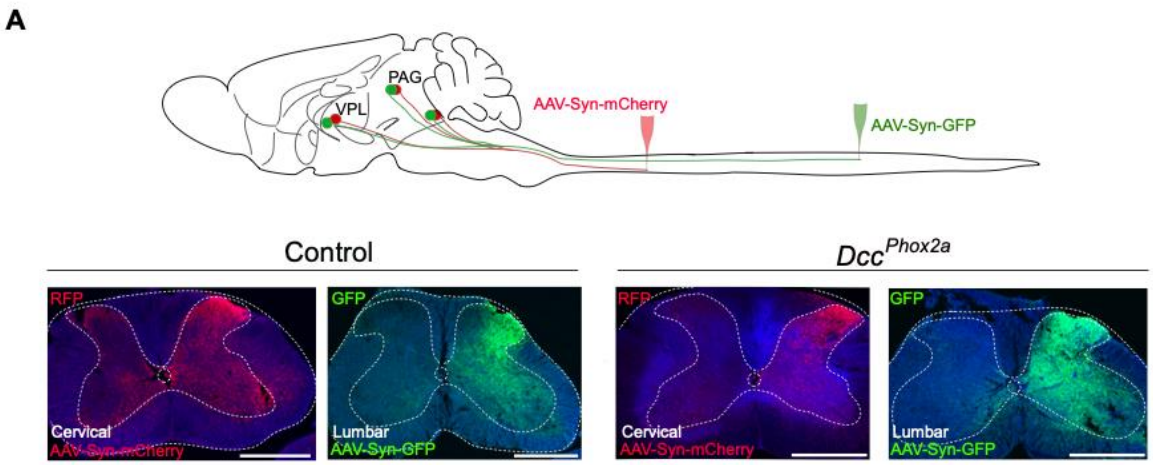

Figure 4. Impaired organisation of spinothalamic innervation in *Dcc*^{Phox2a} mice

A- Schematic of unilateral injection of AAV2/8-Syn-mCherry and AAV2/8-Syn-GFP in the cervical and lumbar spinal cord, respectively. mCherry and GFP expression was detected with anti-RFP and anti-GFP antibodies, respectively. Scale bars: 500 μm.

Comparing lumbar versus cervical virus infection revealed a more robust infection in the lumbar cord compared to the cervical which could be due to the more surgical feasibility in the lumbar cord. Also, this effect could be due to the higher efficiency of GFP-Syn than mCherry reporter. In the PB, PAG, and thalamus, GFP and mCherry-labeled AS axons were revealed with a morphology that contained varicosities attributed to the termini of spinofugal axons. (Fig 4B, C, D) (Cliffer et al., 1991).

In the three brain structures of control mice, a small percentage of mCherry+ and GFP+ puncta overlapped. This could be due to the proximity of the lumbar and cervical axonal termini or the

effect of cervical AAV injections infecting some lumbar axons ascending through the surrounding white matter. The rate of co-labelling of axonal termini with mCherry and GFP was the same in the PB, PAG, and thalamus of control mice (6.67% 1.79%, 7.6 2.88%, and 7.62% 0.6%, respectively; non-significant; Fig 4F), indicating that the signal overlap is probably the result of co-infection artifacts.

Lumbar and cervical AS axons were typically mixed and not segregated to a specific target zone or biased in their distribution along rostrocaudal or mediolateral axes in the lateral division of the PB and PAG of both groups of mice. (Fig 4B, C). In the PB and PAG of Dcc^{Phox2a}, the rate of mCherry and GFP co-labelling of axonal termini was 8.01% ± 1.89% and 6.37% ± 4.04%, respectively. This rate did not differ substantially from control animals (p=0.4 and p=0.7, respectively; see Fig 4F). All these findings point to the absence of somatotopically organized lumbar and cervical termini in the PB and PAG, supporting a recent finding in the PB based on a comparable AAV anterograde labelling (Choi *et al.*, 2020).

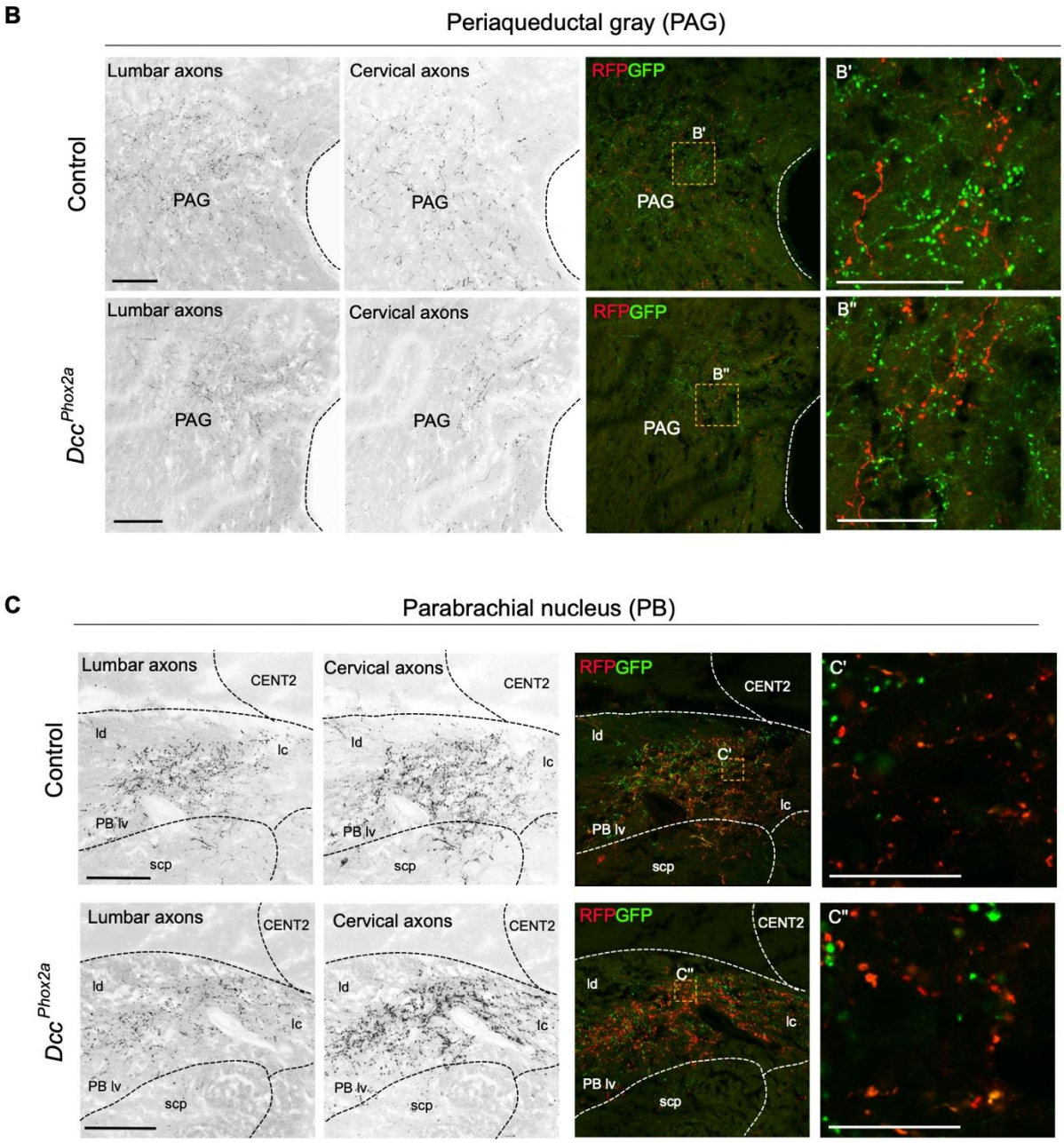
B
Periaqueductal gray (PAG)
Control
Dcc Phox2a
Lumbar axons
Cervical axons
RFPGFP
PAG
B'
B''
C
Parabrachial nucleus (PB)
CENT2
ld
lc
PB lv
scp
C'
C''

B, B’ and B’’- mCherry + and GFP + axon terminals from, respectively, cervical and lumbar spinal cord in the periaqueductal gray (PAG) nucleus. n = 3 control and n = 3 Dcc^{Phox2a} mice. Scale bars: 100 μm in (B) and 50 μm in (B’ and B”).

C, C’ and C”- mCherry+ and GFP+ axon termini from, respectively, cervical and lumbar AS axons in the parabrachial nucleus (PB). n = 3 control and n = 3 Dcc^{Phox2a} mice. Scale bars: 100 μm in (C), 20x objective; 25 μm in (C’ and C”), 63x objective.

Next, the lumbar and cervical AS axon innervation of the ventrobasal (VB) thalamus were examined, where electrophysiological characterization of neuronal receptive fields and other studies revealed a somatotopic organization in the VPL, which had previously been linked to nociception (Francis *et al.*, 2008).

In fact, lumbar AS axons encompassed a region that was ventrolateral to that inhabited by cervical axons in the caudal VPL of three control mice. However, in rostral VPL, most of the axons are from lumbar cord in similar ventrolateral locations and cervical axons rarely are traced in more rostral areas (Fig 4D). In the posterior limiting nucleus of the thalamus (PO), another thalamus area important in nociception with potential somatotopic organization, I again detected AS axons, although labelled axons were sparse and found in few sections so it was insufficient for a comprehensive investigation (Diamond et al., 1992; Frangeul et al., 2014) (data not shown).

The somatotopic order of the cervical and lumbar AS axon termini was disrupted in Dcc^{Phox2a} mice, according to a qualitative mapping of the VPL territory occupied by those axon termini. Cervical axons in control animals terminated along the whole rostrocaudal extent of the VPL, and the area they covered only sporadically included lumbar axons in more rostral parts of the

VPL (Fig 4D, e.g.: Bregma -1.07). Although cervical and lumbar termini territories were reliably segregated in control animals, lumbar axons have been detected within the territory occupied by cervical axons in the more caudal portions of the VPL in *Dcc*^{Phox2a} mice (Fig 4D, e.g.: bregma -2.18 mm, -1.81 mm etc.).

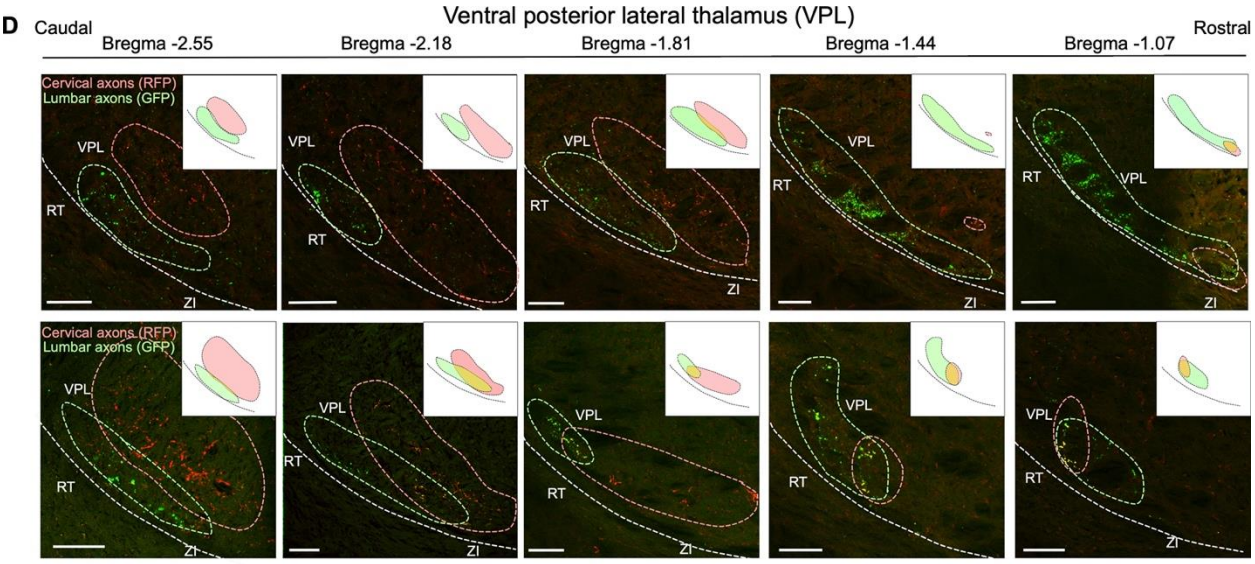

Figure 4.

D- Five sequential sections from caudal to rostral VPL thalamus (-2.55 mm to -1.07 mm to bregma) in representative control and *Dcc*^{Phox2a} animals. mCherry+ (red) and GFP+ (green) AS axon terminals (puncta) represent the axon termini of the cervical and lumbar projection neurons, respectively. Scale bars: 100 μm.

Superimposed the cervical and lumbar axon territories from multiple caudal and rostral VPL sections in three mice per genotype, showed this disordered arrangement more obviously: while

in controls these territories were mostly mutually exclusive, in *Dcc*^{Phox2a} mice there were many instances of cervical and lumbar axon territory overlap (Fig 4E, yellow shading).

A disrupted AS afferent organization was also found when cervical and lumbar axon termini overlap and the VPL areas they spanned were quantified. The frequency of co-segregation of the cervical and lumbar mCherry axon terminal signals inside the VPL of control mice was comparable to that of *Dcc*^{Phox2a}, control PB, and PAG (7.62% ± 0.6%; see above), but it increased to 9.8% ± 0.84% in the VPL of *Dcc*^{Phox2a} mice (p=0.02; Fig 4F).

Additionally, even though there was no discernible difference between the total quantity of axon terminal signal in the VPL of control and *Dcc*^{Phox2a} mice, the ratio of cervical to lumbar axon terminal signal increased in the *Dcc*^{Phox2a} VPL in favour of cervical axons (p=0.03; Fig. 4G, H).

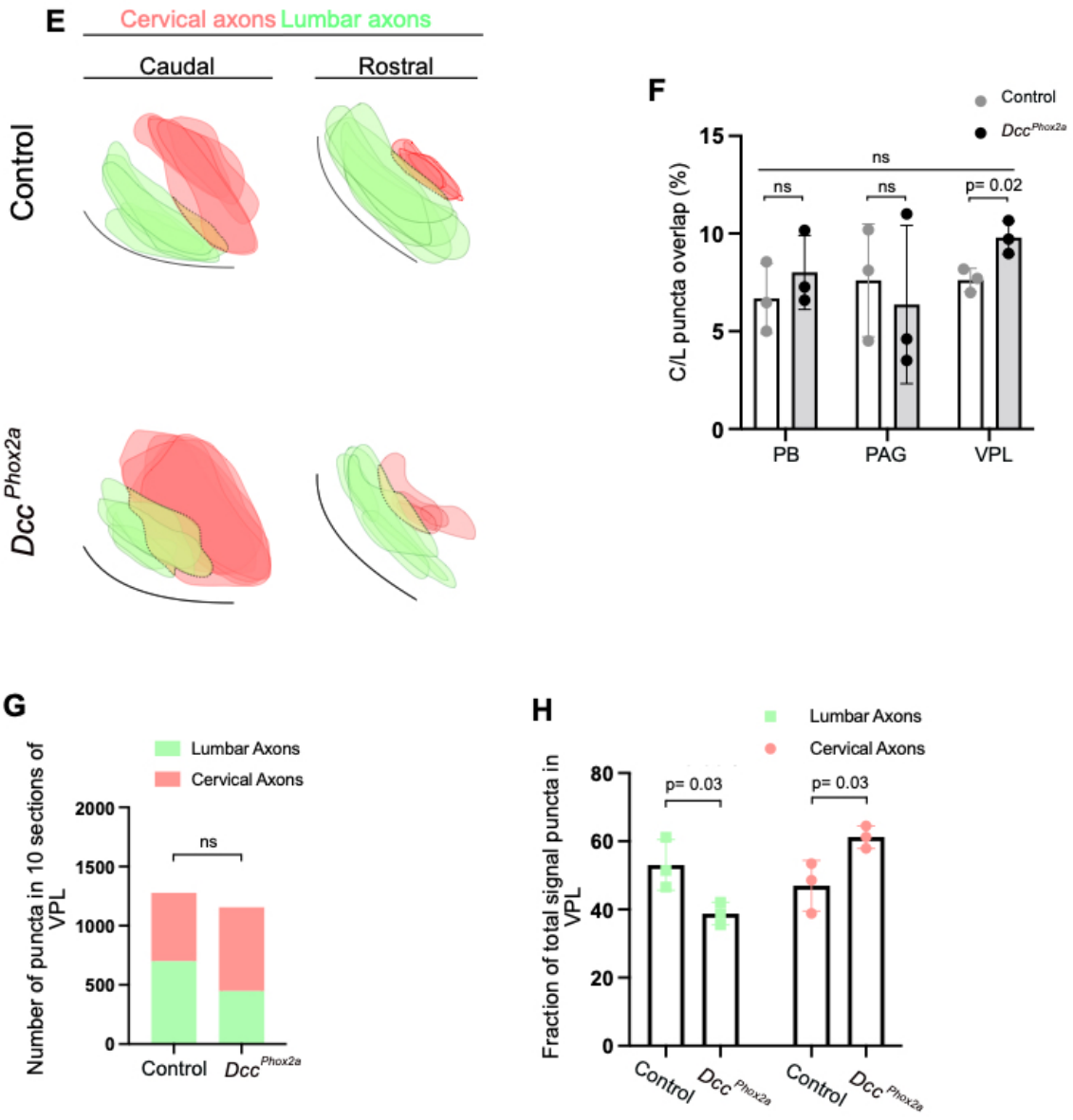

Figure 4.

E- Diagram of VPL areas innervated by cervical and lumbar AS neurons labelled with GFP and mCherry-expressing AAVs. The stacked outlines represent the innervation area of cervical/lumbar PNs averaged from 3 mice at five different levels relative to bregma, separated into rostral and caudal regions. Red

outlines represent areas of cervical AS axon spread, green outlines represent the areas of lumbar AS axon spread, while yellow represents the overlap between the lumbar and cervical AS areas. In control mice the overlap is limited while greater overlap is detected in *Dcc*^{Phox2a} mice (quantified in panel I).

F- Fraction of axon terminal puncta co-labelled with GFP and mCherry, in three brain nuclei: PB, PAG and VPL thalamus. n = 3 control and n = 3 *Dcc*^{Phox2a} mice (control PB, 6.67% ± 1.78%; control PAG, 7.6% ± 2.88%; control VPL, 7.61% ± 0.6%; *Dcc*^{Phox2a} PB, 8.01% ± 1.89%; *Dcc*^{Phox2a} PAG, 6.37% ± 4.04%; *Dcc*^{Phox2a} VPL, 9.79% ± 0.84%). Between subjects ANOVA was performed to compare three brain nuclei vs genotype; ns, non-significant. Unpaired Student's t-test was performed to separately compare the control vs *Dcc*^{Phox2a} mice in each nucleus; p= 0.02, significant; ns, non-significant. Data are represented as mean ± SD.

G- Total number of axon terminal signal puncta in the VPL, originating from lumbar (GFP+) and cervical (mCherry+) AS neurons. n = 3 control and n = 3 *Dcc*^{Phox2a} mice (control cervical axons, 578 ± 99.74; control lumbar axons, 699.66 ± 339.12; *Dcc*^{Phox2a} cervical axons, 707 ± 41.24; *Dcc*^{Phox2a} lumbar, 448 ± 36.75). Unpaired Student's t-test; ns, non-significant. Data are represented as mean ± SD.

H- Proportion of cervical versus lumbar AS axon termini puncta, as a fraction of all AS termini puncta in the VPL. n = 3 control and n = 3 *Dcc*^{Phox2a} mice (control cervical axons, 46.94% ± 7.45%; control lumbar axons, 53.05% ± 7.45%; *Dcc*^{Phox2a} cervical axons, 61.2% ± 3.31%; *Dcc*^{Phox2a} lumbar, 38.79% ± 3.31%). Unpaired Student's t-test; p= 0.03, significant. Data are represented as mean ± SD.

Measuring the overlap between the regions occupied by the lumbar and cervical axons in Fig. 4E, demonstrated that *Dcc*^{Phox2a} mutants had much higher overlap than controls (Fig. 4I). Finally, using the cervical and lumbar termini of three control mice as a proxy for the location of the VPL neurons post-synaptic to them, I compared the territory covered by *Dcc*^{Phox2a} cervical and lumbar axons to the VPL territory covered by control cervical and lumbar termini (Fig. 4J). This analysis showed that consistent with the reported number of cervical termini puncta, the *Dcc*^{Phox2a} cervical axon territory (stippled black outline) was greater than the control areas and extended into the control VPL regions subserved by lumbar axons (Fig. 4H). Similar to this, I showed that *Dcc*^{Phox2a} cervical axon territory (black outline) extended into the control VPL regions that are normally occupied by lumbar axons.

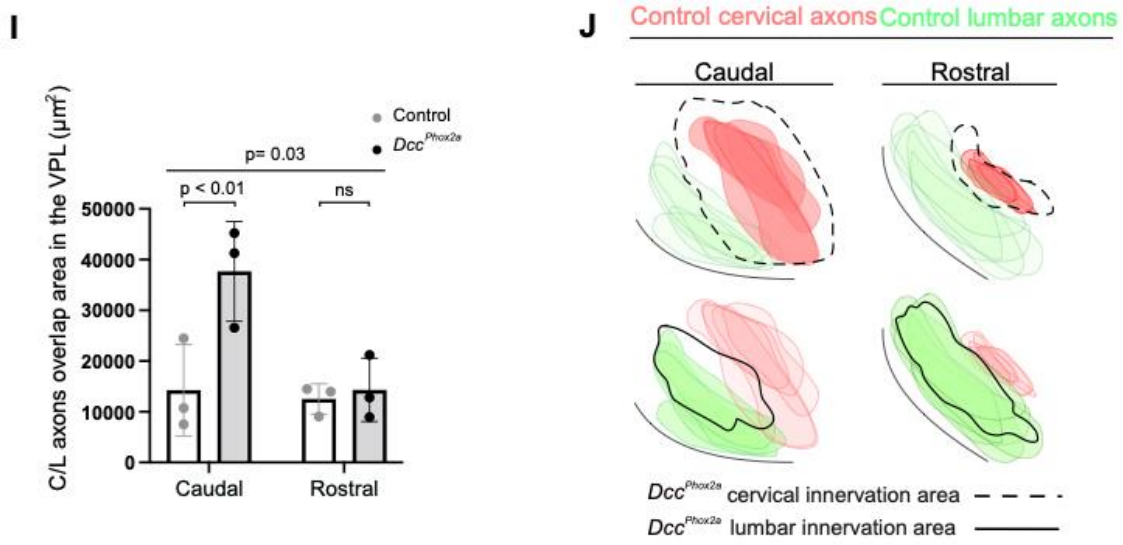

Figure 4.

I- Overlap of cervical and lumbar axon terminals innervation area (μm^2) measured in 5 sequential sections of caudal and 5 sequential sections of rostral VPL in each animal. n = 3 control and n = 3 Dcc^{Phox2a} mice (control caudal VPL, 14252 μm^2 ± 9013.99 μm^2; control rostral VPL, 12502.325 μm^2 ± 2998.46 μm^2; Dcc^{Phox2a} caudal VPL, 37684 μm^2 ± 9846.02 μm^2; Dcc^{Phox2a} rostral VPL, 14304.18 μm^2 ± 6262.310 μm^2). Between subject ANOVA with Bonferroni post-hoc analysis; p= 0.03 and p < 0.01, significant; ns, non-significant. Data are represented as mean ± SD.

J- Diagram of altered innervation area of Dcc^{Phox2a} VPL cervical/lumbar map. Normal cervical and lumbar axons innervation areas from control mice, are shown as red and green ovals, respectively. The area innervated by cervical AS axons in Dcc^{Phox2a} mutants is bound by a stippled line and Dcc^{Phox2a} lumbar PNs innervation is bound by a solid line.

Together, these findings show that Dcc^{Phox2a} disturbs the normal arrangement of AS axons in the VPL, causing more instances of cervical and lumbar axon co-segregation, as well as instances in which lumbar axons were discovered in the region of the VPL normally innervated by cervical axons and vice versa. This suggests that in Dcc^{Phox2a} mutants, VPL neurons ordinarily supplied by cervical axons may receive lumbar projections.

3.5 Timeline of embryonic AS neuron innervation of brain targets

Although many studies show the developmental timepoint of projection neurons in the spinal cord, we still do not know when the spinal cord-brain connection is completed by reaching PN axons to their brain targets. To uncover the mechanism behind anatomical and behavioural phenotypes in Dcc^{Phox2a} mice, I assessed the development of innervation of brain targets by AS neurons. The innervation development was investigated by chasing the Phox2a AS neurons from E14.5 to P2 stages. To do this, I used a Cre-FlpO recombinase-dependent tdTomato reporter ($R26^{FSF\text{-}LSL\text{-}tdT}$ or *Ai65;* (Madisen et al., 2015)), express specifically in spinal Phox2a neurons. Supra spinal expression of Phox2a was circumvented by intersecting the $Phox2a^{Cre}$ with spinal cord-specific $Cdx2^{FlpO}$ driver and double stop (Cre-FlpO) tdTomato reporter. Generating $Phox2a^{Cre}; Cdx2^{FlpO}; R26^{FSF\text{-}LSL\text{-}tdT/+}$ mice allowed us to determine the arrival timeline of Phox2a AS axons in the developing thalamus as well as PB and PAG (Fig. 5A).

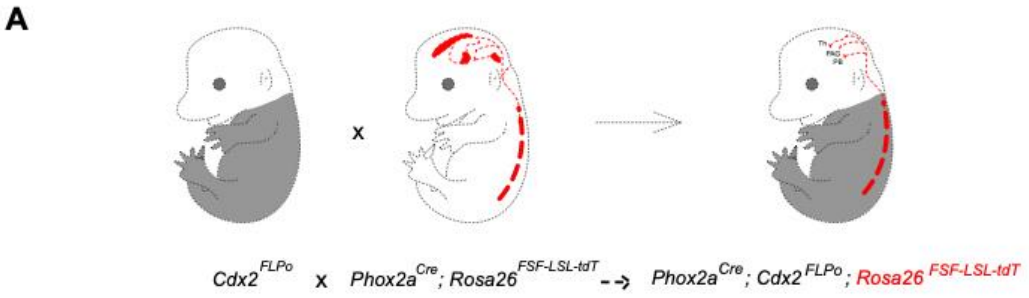

Figure 5. Development of Phox2a PNs projections from spinal cord to different brain targets

A- Visualizing the *Phox2a*^{Cre} spinal specific axons by intersecting the *Phox2a*^{Cre} with spinal cord-specific *Cdx2*^{FlpO} driver and the Cre-FlpO recombinase-dependent tdTomato reporter (*R26*$^{FSF\text{-}LSL}$-*tdT* or *Ai65*). This strategy has been used to specifically label spinal phox2a axons in the brain and trace them without labelling local axons in brain.

According to the prosomeric model of thalamic development, the ventrobasal (VB) thalamus, which houses the VPL and other AS neuron destinations, develops from a region of the thalamus with an embryonic expression of Sox2 transcription factor (Vue *et al.*, 2007). The expression of the transcription factor Pax6 allows for the identification of a nearby ventral region known as the prethalamus, which is excluded from the thalamus and separated from the thalamus by the zona limitans intrathalamica (ZLI) (Nakagawa and O'Leary, 2001; Quintana-Urzainqui et al., 2020; Walther and Gruss, 1991).

P2 newborns and embryos aged E14.5 to E16.5 were harvested to determine the onset of Phox2a PN axon arrival in the developing ventrobasal thalamus and other nociceptive areas. At E14.5, there are no spinal Phox2a tdTomato expressing axons in the thalamic area of the midbrain (Fig. 5A). The first tdTomato axons entered the Sox2-expressing thalamic domain's lateral side at E15.5. This pattern grew more medially inside the Sox2 domain between E15.5 and E16.5. The distribution of tdTomato-expressing axons in the P2 thalamus resembled the adult pattern and comprised distinct PO and VPL areas (Fig. 5B).

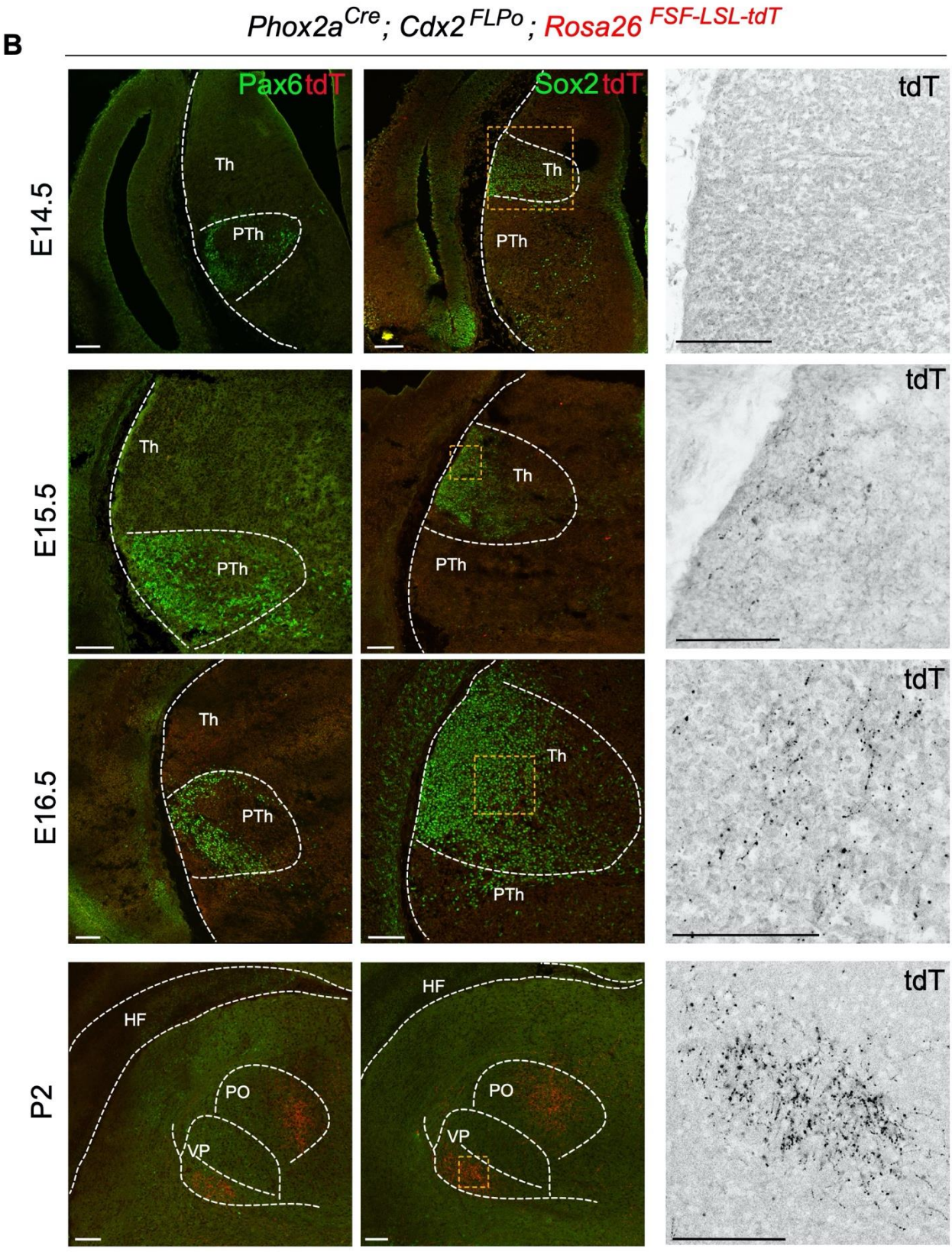
B
Phox2a Cre ; Cdx2 FLPo ; Rosa26 FSF-LSL-tdT
E14.5
E15.5
E16.5
P2
Pax6 tdT
Sox2 tdT
tdT
Th
PTh
HF
PO
VP

Figure 5.

B- Phox2a + PN axons arrival in the thalamus at E14.5, E15.5, E16.5 and P2. Sox2a and Pax6 have been used as Thalamus (Th) and prethalamus (PTh) markers, respectively. TdT signal was boosted by tdT antibody. n = 3 control and n = 3 Dcc^{Phox2a} embryos. Scale bars: 100 μm.

I utilized an anti-tdTomato or anti-RFP antibody to localize endogenous tdTomato expression in growing Phox2a AS axon termini because it was too faint to be detected via its original fluorescence. The TdTomato (tdT) antibody was used to increase the signal from the LS-tdT reporter. However, I discovered that the tdT antibody, which is a goat antibody that can be used with our Sox2 and Pax6 markers, is not powerful enough to show all of the axons in the brain. Therefore, RFP antibody was used to boost the axon signals in the brain. RFP antibody result was consistent with the tdT signal, but it provided a clearer picture of the number of axons innervating the thalamus. (Fig 5C)

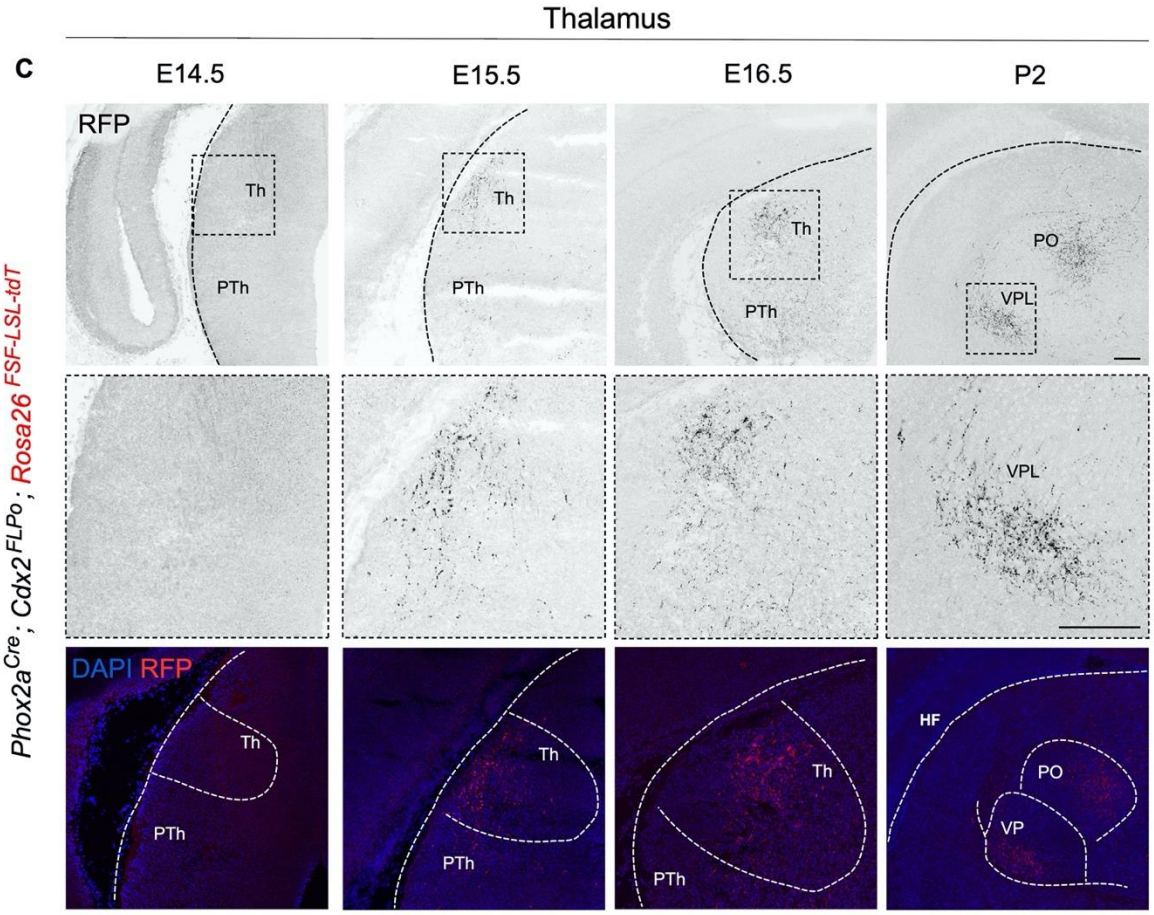

Figure 5.

C- Phox2a + PN axons arrival in the thalamus at E14.5, E15.5, E16.5 and P2. TdT signal was boosted by RFP antibody. n = 3 control and n = 3 Dcc^{Phox2a} embryos. Scale bars: 100 µm.

Looking at the parabrachial nucleus, revealed that the first projection neurons reach the PB at almost the same time as they reach the thalamus around E15.5. No axon innervation has been detected at neither rostral nor caudal PB at E14.5. Additional innervation to both rostral and caudal PB has been detected at E16.5 and P2. Assessing the proximity of Phox2a expressing PN

axons to the Phox2a expressing neurons in the PB showed that Phox2a axons are not directly connected to these supraspinal Phox2a neurons (Card et al., 2010). In contrast, Spinal-PAG connection seems to be established one day earlier at E14.5 when the first axons appear in the PAG, and these axons are in proximity of Phox2a neurons in the PAG (Fig 5D).

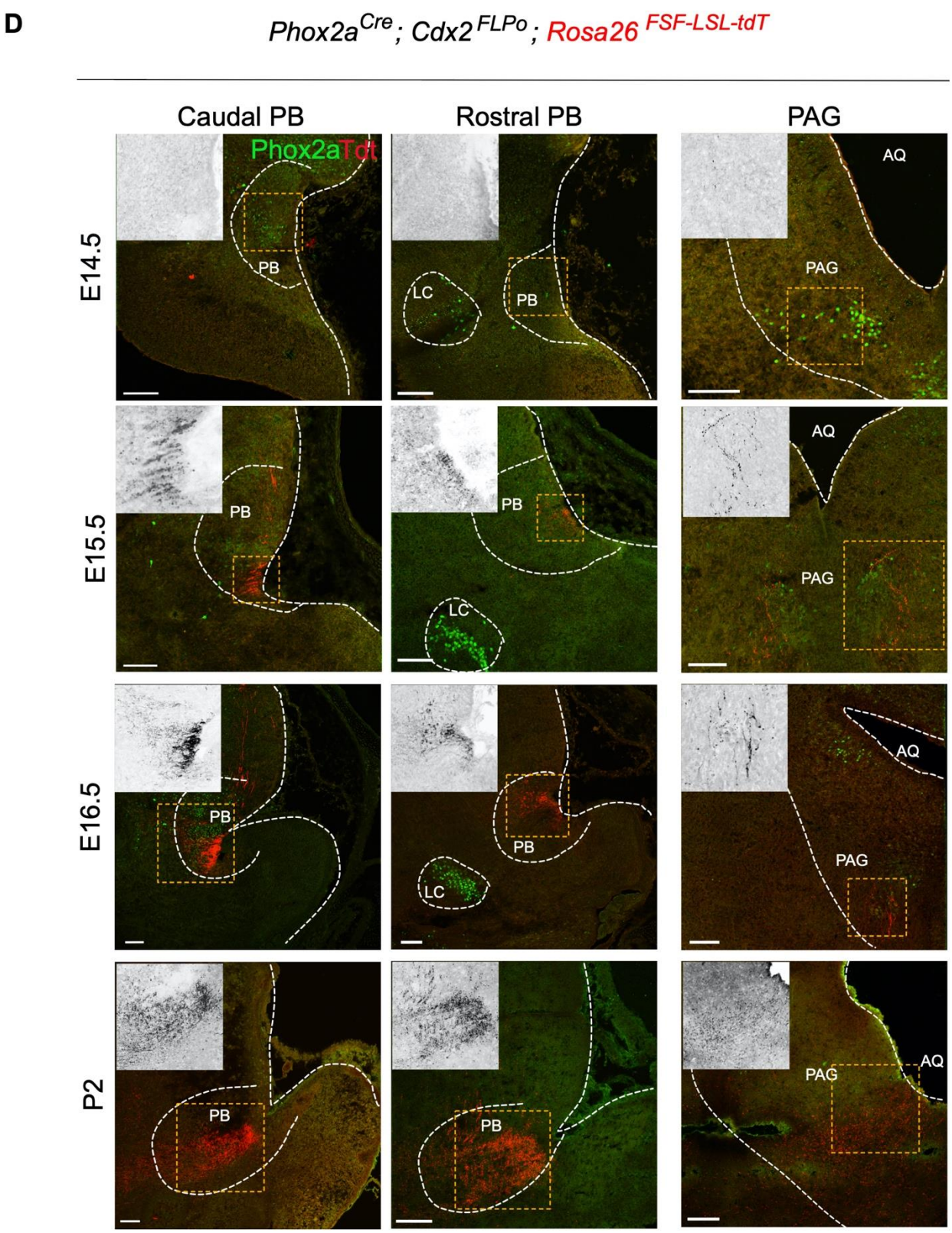
D
Phox2a^Cre ; Cdx2^FLPo ; Rosa26^FSF-LSL-tdT
Caudal PB
Rostral PB
PAG
E14.5
E15.5
E16.5
P2
Phox2aTdt
PB
LC
AQ
PAG

D- Phox2a+ AS tdT+ axons arrival to the caudal and rostral PB as well as PAG at E14.5, E15.5, E16.5 and P2. Phox2a expression has been shown in proximity of spinal Phox2a axons. Also, Phox2a expression in the locus coeruleus (LC) as an anatomical landmark has been shown in rostral PB. TdT signal was boosted by tdT antibody. n = 3 control and n = 3 Dcc^{Phox2a} embryos. Scale bars: 100 µm.

Together, this first genetic anterograde investigation of AS axonal development identifies the innervation of brain targets during the early stages of molecular differentiation and neurogenesis.

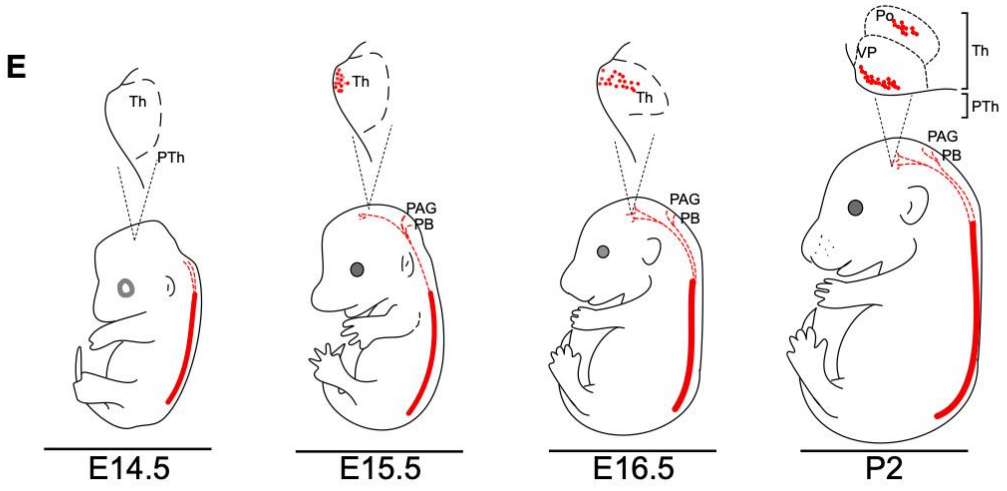

Figure 5.

E- Diagram summarizing the pattern of Phox2a spinothalamic axons in E14.5, E15.5, E16.5 and P2.

3.6 Expression of netrin-1 in the embryonic thalamus coincides with the arrival of AS axons

Lateral to the medial acquisition of the spinal axon terminals in the thalamus between E15.5 and E16.5 raises the question of which axon guidance pathway is involved in this axon positioning. Disordered AS axon innervation of the VPL as well as the defective rostrocaudal localization of painful stimuli, raised the possibility that DCC signalling is not only involved in spinal cord midline crossing of AS neurons, but also directing their innervation of the thalamus.

I thus investigated DCC ligand netrin-1 expression in the thalamus at E15,5 the time that AS axons innervate the thalamus. Similar to the previous section of this study, I used Sox2 expression to mark the developing thalamic area separated from the prethalamus. Netrin-1 protein has been detected at E15.5 developing thalamus when the Phox2a AS axons reach the thalamus (Fig 6A) (Powell et al., 2008). Moreover, *Ntn1* expression has been assessed at the mRNA level by using $Ntn1^{Bgeo}$ transgenic model which expresses B-gal in *Ntn1* expressing neurons (Fig 6C) (Skarnes *et al.*, 1995). Also, I repeat this experiment with *Ntn1 in situ* which confirmed the *Ntn1* expression in the dorsal thalamus (Fig 6C). Looking at the dorsal thalamus, netrin1 expression is stronger on the medial side, and given the lateral to medial replacement of axons at E15.5-E16.5, netrin-1 may be involved in axon termini final positioning by attracting first arrived axons toward the medial side while delayed arriving axons remain laterally.

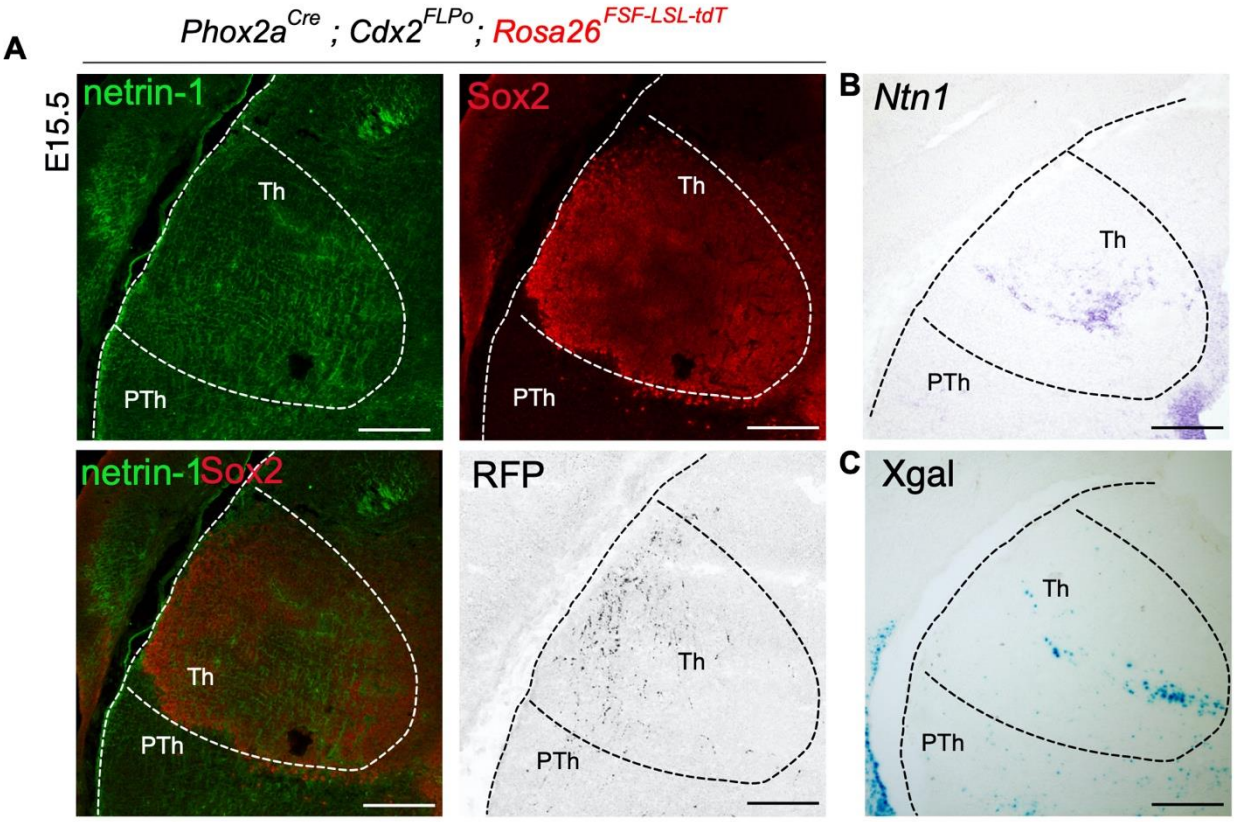

Figure 6. Role of netrin-1 - Dcc signaling in shaping the somatotopic order within embryonic thalamus

A- Netrin-1 immunofluorescence in an E15.5 *Phox2a*^{Cre}*; Cdx2*^{FlpO}*; R26*$^{FSF\text{-}LSL\text{-}tdT/+}$ embryonic thalamus in proximity to Phox2a AS RFP+ axons. Sox2 protein has been used as an embryonic thalamic marker. Coronal sections, 25 µm thick, were used to assess the distribution of netrin-1 protein and Phox2a AS RFP + axons in the neighbouring sections. n = 3 control and n = 3 *Dcc*^{Phox2a} embryos. Scale bars: 100 µm.

B- *In situ* hybridization detection of *Ntn1* mRNA in E15.5 thalamus. n = 3 control and n = 3 *Dcc*^{Phox2a} embryos. Scale bar: 100 µm.

C- X-gal staining in *Ntn1*^{Bgeo} mice reveals *Ntn1* expression in the thalamus of E15.5 embryos. n = 3 control and n = 3 *Dcc*^{Phox2a} embryos. Scale bar: 100 μm.

I looked at the distribution of DCC protein in tdTomato expressing AS axons in *Phox2a*^{Cre}*; Cdx2*^{FlpO}*; R26*$^{FSF\text{-}LSL\text{-}tdT/+}$ E15.5 embryos to see if it was expressed at the time of target innervation. First, I identified tdTomato-expressing axons in the anterolateral tract, dorso-lateral aspect of the cervical spinal white matter, which is the site of many AS axons ascending towards their brain targets on the side contralateral to the location of AS neuron somata in rodents (Albe-Fessard et al., 1985; Hodge and Apkarian, 1990). The fact that many of the axons located in the anterolateral tract co-expressed DCC protein indicates that AS axons continue to express DCC after commissural crossing (Fig. 6D). Additionally, at E15.5, I found DCC expression in the thalamus, some of which coincided with tdTomato, suggesting that although some DCC expression is endogenous to thalamic precursors, it is also present in afferent Phox2a AS axons (Fig. 6E, E').

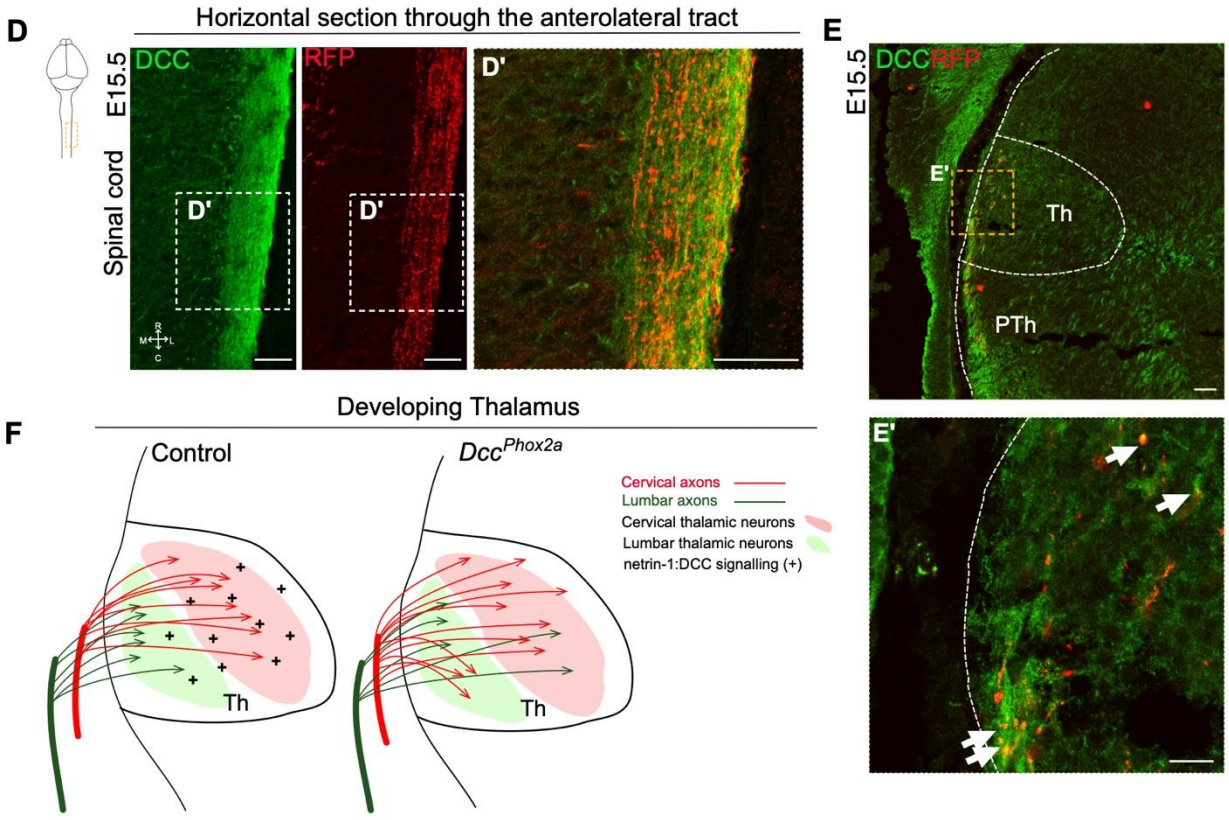

Figure 6.

D and D'- A horizontal section through the anterolateral tract showing Phox2a AS axons (RFP +) expressing DCC at E15.5. n = 3 control and n = 3 *Dcc*^{Phox2a} embryos. Scale bar: 100 µm.

E and E'- Phox2a AS axons (RFP +) express DCC in the developing thalamus at E15.5. Arrow heads: co-localization of DCC and RFP. n = 3 control and n = 3 *Dcc*^{Phox2a} embryos. Scale bar: 100 µm.

F- Model of cervical and lumbar AS axon organization within the developing thalamus and how the lack of netrin-1:DCC signalling might change the map in *Dcc*^{Phox2a} mice.

Expressing of the DCC in the AS axons as well as netrin-1 expression in the axons target suggests a possible netrin-1: DCC signalling which defines the final somatotopic organization within the thalamic area (Fig 6F).

Chapter 4: Discussion

In this study, I investigated the role of the DCC axon guidance receptor in the development of the pain somatosensory circuit. DCC expression has been demonstrated in pain-relaying Phox2a AS neurons during critical developmental stages and persists until these neurons reach their target in the brain. In Dcc^{phox2a} mice, the absence of DCC expression in Phox2a AS neurons affects not only the laterality of axon innervation to the thalamic target but also the nocifensive discriminatory behaviour. The inability to localize pain in the body is thought to be caused by disorganized axon termini within the thalamus. While previous research has suggested that netrin-1:DCC signalling controls midline crossing around E11.5, I demonstrated that DCC expression is still present days after midline decussation, implying DCC's second role in guiding spinal projection neurons. Looking at the embryonic thalamus, which is one of the main nuclei involved in pain processing, reveals the expression of netrin-1 cue, which may interact with DCC receptors on arriving axons. This study was conducted using three main approaches: anatomical studies, nocifensive behaviour assessment, and development studies. In this section, I will go through the implications of these experiments, as well as the limitations of experimental design and the relationship between this work and current knowledge in the field.

4.1 The nocifensive behaviours of Dcc^{Phox2a} mice

According to behavioural analysis, Dcc expression in Phox2a neurons is required for normal pain localization (nociceptive topognosis) (Fig1). While DCC axon guidance function is required for the discriminatory aspect of nocifensive behaviour, mice lacking DCC in their AS neurons do not experience changes in aversive component of pain. I used two knockout strategies to create the genetic mouse model. First, I used Dcc^{KO} mice to generate $Phox2a^{Cre}$; $Dcc^{flox/Ko}$ mice as a

model of *Dcc* ablation in Phox2a neurons. The logic behind this approach is that the Cre could be able to excise one *flox* allele more efficiently than two *flox* allele. However, when the pain localization assay was performed, I noticed that not only the mutants but also the heterozygote control mice, with one copy of the null *Dcc* allele, were inaccurate in localizing pain. We cannot attribute this phenotype to any pathway because the *Dcc* null allele is not specific to AS neurons. This finding suggests that missing one *Dcc* allele causes *Dcc* haploinsufficiency. The second approach involved using two Dcc^{f} alleles and this analysis revealed that $Phox2a^{Cre}$ can efficiently excise both Dcc^{f} alleles to generate a Phox2a-specific *Dcc* ablated model.

Dcc knockout in the caudal spinal cord has previously been shown to affect the laterality of pain localization (da Silva *et al.*, 2018a). Da Silva et al used $Hoxb8^{Cre}$ driver to knock out Dcc^{f} allele. Mice with silenced *Dcc* could not be able to locate pain laterality accurately and a painful stimulus in the right hindpaw caused the licking response in both left and right hind paws. This study did not specify which population of projection neurons are involved in changing the nociceptive topognosis as all the neurons in the caudal spinal cord including interneurons and non-nociceptive circuits are targeted by $Hoxb8^{Cre}$ driver. Other than that, *Dcc* ablation is restricted to the caudal spinal cord as the *Hoxb8* gene is not expressed in the upper cervical spinal cord (Witschi et al., 2010). By contrast, using $Phox2a^{Cre}$ enables us to knockout *Dcc* in a specific population of pain-related ASs in the spinal cord without affecting interneurons and other circuits. Also, Phox2a is expressed in both the cervical and lumbar spinal cord which lets us look at changes in pain localization at the rostrocaudal axis as well as the laterality changes (Roome *et al.*, 2020a). Missing the *Dcc* knockout at upper cervical level in $Hoxb8^{Cre};Dcc^{ko}$ (Dcc^{SpC}) model could explain why Da Silva et al did not observe a significant pain localizing shift from hindlimbs to forelimb as I observed with Dcc^{Phox2a} model.

4.1.1 Assessing grooming vs forepaw licking behaviour

One complication with interpreting the licking behaviour data is how to distinguish grooming from forepaw licking. Grooming is an innate behaviour with sequential order and cephalocaudal progression within this possess both forepaws are involved in wiping and licking begins at the face and continuing to the body and tail (Kalueff and Tuohimaa, 2004). My observation reveals that there are differences in forepaw licking during grooming versus forepaw licking in response to pain. First, forepaw licking in the grooming behaviour is followed by licking the body and tail due to the cephalocaudal progression nature of grooming behaviour. But in pain licking behaviour, licking the forepaws is not followed by other grooming-like behaviour. Second, mice tend to fist the forepaws in grooming while after painful stimuli, mice unfold the forepaws and lick the palm of the hand. I assessed the time that control mice spent on grooming, and as the grooming time in the control group does not show a difference compared to the mutants, I concluded that the forepaw licking alteration in mutants is independent of the grooming behaviour.

4.2 Anatomical changes in Dcc^{Phox2a} mice nociceptive circuit

In this study, *Dcc* was knocked out in *Phox2a* expressing neurons in the lamina I (AS^{Sup}) and lamina V/ LSN (AS^{Deep}) spinal cord. Phox2a is expressed during development and ablation of this transcription factor in the spinal cord causing decreased pain response in mice (Roome *et al.*,

2020a). Besides functional studies that show the role of Phox2a AS neurons in relaying pain information, the location of these neurons within the spinal cord is also consistent with their suggested role in the pain circuit. Lamina I and V/ LSN in the spinal cord are two known regions that comprise nociceptive neurons (Craig, 2004; Wercberger and Basbaum, 2019). A subset of projection neurons located in lamina I and V send their axons to pain-related brain targets via anterolateral tract. Phox2a has been used as a subset-specific marker of projection neurons in the anterolateral tract. Although using *Phox2a* gives the specificity to study a distinct population of pain-relaying projection neurons, one shortcoming of this experimental design is that *Phox2a* is also expressed in some brain regions including locus coeruleus (LC). Despite this caveat, I expect that the *Phox2a* expression in the brain is not interfering with our pain localization assay since there is no study that shows LC or other Phox2a expressing brain areas have a defined somatotopic order.

4.2.1 Assess laterality changes in ASs by retrograde tracing in Dcc^{Phox2a} mice

Contralateral innervation of projection neurons is considered the first level of somatotopy. The majority of sensory inputs to the thalamus come from the contralateral side of the spinal cord, whereas PB and PAG spinal inputs come from both sides and do not have a specific laterality (Choi *et al.*, 2020; Mouton and Holstege, 2000). Assessing the innervation laterality as a subclass of somatotopic order provides a better perspective on how DCC will change the wiring of somatosensation.

There are studies showing DCC might play a non-cell-autonomous role in guiding the spinal cord cell body positioning (Laumonnerie et al., 2015; Welniarz et al., 2017). This leads us to examine the entire spinothalamic circuit changes in the Dcc^{Phox2a} model, as the laterality change may affect not only the neurons expressing it but also the neurons adjacent to them.

I demonstrated that there is an increase in the total number of ipsilateral projections in Dcc^{Phox2a} mice cervical spinal cord. The same observation at lumbar level has been reported by da Silva et al (da Silva *et al.*, 2018a). Given that the number of contralateral projecting ST neurons is not decreased significantly in the knockout model, this increased number of labelling could happen due to bilateral innervation.

Compared to Da Silva et al phenotype (da Silva *et al.*, 2018a), Knocking out *Dcc* in *Phox2a* expressing neurons results in a milder laterality impairment phenotype that is observed at the cervical but not the lumbar spinal cord. The difference between lumbar and cervical cord could reflect a rostracaudal bias in the onset of $Phox2a^{Cre}$ expression with respect to midline crossing. Previous research indicates that $Phox2a^{Cre}$ is expressed in 50% of AS^{Sup} neurons, which, combined with their scarcity at lumbar levels (Davidson et al., 2010), suggests that subtle laterality changes in Phox2a AS neurons may not be revealed at the level of the entire AS^{Sup} population in the lumbar spinal cord. Given that only 10% of AS^{Deep} neurons express $Phox2a^{Cre}$ and that the majority of these neurons have ipsilateral anatomy, Dcc^{Phox2a} could have a minor effect on the laterality of AS^{Deep} neurons.

Another explanation is that fewer lumbar axons are normally labelled from the VPL. Homunculus representation of different parts of the body causes more innervation from the body area such as hand fingers which need to have a more precise map in the body to perform fine

tasks. Biased representation of the upper versus lower body, as well as technical difficulties in labelling lumbar projection neurons retrogradely, result in a lower number of projection neurons at the lumbar level, reducing the power of statistical tests to detect the effect.

Lamina I projection neurons with somatotopic organization, small receptive fields, and different modalities are suitable candidates for relaying somatotopy and location information, whereas deep lamina projection neurons with less stimulus specificity and poor organization suggest their involvement in non-discriminatory pain, such as emotive component of pain. (Price and Dubner, 1977).

A detailed analysis of retrogradely labelled ST neurons based on their cell body position in the spinal cord reveals that in Dcc^{Phox2a}, a shift in ST axons laterality occurs in AS^{Sup} neurons but not in AS^{Deep} neurons, including lamina V/LSN. This is consistent with our previous research, which found that while cell body migration in lamina I Phox2a neurons is dependent on netrin-1: DCC signalling, deep lamina Phox2a neurons mostly respond to reelin to migrate. (Roome *et al.*, 2022).

4.2.2 Classification of the projection neurons

One major challenge in the field is to classify projection neurons based on the message they are relaying. Pain is a complex multidimensional experience with discriminatory and affective aspects. Differentiating the affective and discriminatory aspects of pain leads to new therapeutic strategies for treating pain without losing sight of its critical cautionary aspect. Recently identified PNs markers such as *Gpr83* and *Tacr1* labelled adult neurons which mainly innervate

the PB but not VPL (Choi *et al.*, 2020). On the other hand, this study has used *Robo3* as a marker of commissures and it has been shown that commissural projection neurons innervate VPL (Choi *et al.*, 2020). Together, this result suggests that *Tacr1* and *Gpr83* PNs are not among commissural neurons innervating the thalamus and probably are not involved in somatotopy. This is consistent with their PB innervation pattern which has no defined somatotopic order. In contrast to Gpr83 and Tacr1 PNs, a subset of Phox2a PNs innervate the VPL. As a result, Choi et al's commissural PNs model may be Phox2a positive. Other than Phox2a, Tac1 is expressed in a subset of spinothalamic neurons. Phox2a and Tac1 are not colocalized in the projection neurons and are therefore considered complementary populations (Huang *et al.*, 2019; Roome *et al.*, 2020a). *Tac1* ablation suppresses licking behaviour after mustard oil injection. But licking behaviour persists after capsaicin injection in *Tac1* ablated mice. This effect is suggesting a complementary pathway to *Tac1* which I believe could be Phox2a AS neurons. Although each of the introduced genetic markers is trying to specify a population with distinct properties, still there are overlaps between the properties and populations that these markers are covering.

4.2.3 somatotopic order in the brain

Cervical and Lumbar AS axon termini did not demonstrate any spatial segregation within PB and PAG. In agreement, Choi et al reported no somatotopic order within PB (Choi *et al.*, 2020). On the other hand, clear segregation between lumbar and cervical axon termini was observed within VPL. This somatotopic organization is consistent with electrophysiology data suggesting somatotopic order within the VPL (Francis *et al.*, 2008). Given the VPL input to the SI cortex, which has a specific somatotopic organization I think that pain localization information is

gathered in the VPL and then transmit to the cortex for further processing. Access to a specific spinothalamic marker is required to study the somatotopic organization of sensory information in the VPL. The significance of Phox2a as a spinothalamic neuron marker is clear here, as this developmental marker could be used to assess the development of spinothalamic neurons as well as the role of axon guidance molecules in shaping this circuit.

Pain localizing assay supports the hypothesis that *Dcc* knockout in Phox2a AS neurons causes defective topognosis at the rostral-caudal axis of the body. To study such an effect, I sought to look at the AS axon termini innervation within the known pain-related brain nuclei. Among PB, PAG and VPL thalamus, there is a somatotopic order in the spinothalamic axon's innervation to the VPL thalamus. So, the inability to localize pain in the rostral-caudal axis of the body may be due to a defective distribution of AS afferents in the VPL, which reflects a DCC function in thalamic innervation.

Consistent with previous findings, I observed that anterolateral tract cervical axons innervate the medial side of the VPL while the lumbar axons end up on the lateral side. This order is preserved from the anterolateral tract as the cervical axons located medially and lumbar stay laterally within the tract. This specific pattern of innervation provides a precise arrangement for cervical and lumbar axons within VPL that spatially separate cervical and lumbar axon termini.

The spatial segregation of cervical and lumbar axon termini is not limited to the mediolateral axis. But it also exists at the rostral-caudal axis. Cervical axons are concentrated at caudal VPL while lumbar axons locate more rostrally in the VPL. It should be noted that however the number of cervical axons theoretically should be more than lumbar projection neurons due to homunculus representation within the brain, here in this experiment, I observed more lumbar

axons in the VPL. I assume that the technical difficulty that makes the cervical cord less accessible, makes the AAV injection less efficient at the cervical level compared to the lumbar cord.

The ratio of cervical vs lumbar innervation of VPL is impaired in Dcc^{Phox2a} model. This phenotype could be explained by the increased ipsilateral innervation at the cervical level of the spinal cord. The retrograde data showed an increased number of ipsilateral projections at the cervical level. If the more ipsilateral innervation is due to the bilateral innervation of these axons, that could explain why the cervical axon termini are increasing in mutant mice.

Also, the ipsilateral innervation could be different in some properties compared to the contralateral innervation (Renier et al., 2017). Ipsilateral axon termini might occupy more space therefore less lumbar have the chance to innervate the thalamic area. This hypothesis is based on the fact that the cervical spinal cord develops earlier than the lumbar cord (Nornes and Carry, 1978; Nornes and Das, 1974). Also, in another nervous system circuit, it has been shown that the birthdate of neurons within the cortex determines their position in the circuit (Mercer Lindsay *et al.*, 2021; Shen et al., 2006). Earlier development and proximity to the brain let cervical projection neurons reach their brain target prior to their lumbar neighbours, therefore, I assume that cervical axons take the initiative to shape the somatotopic map within the VPL. This possibility is also raised by Renier et al who showed that the competition between ipsilateral and contralateral axons defines the whisker maps within the VPM thalamus. Ipsilateral innervation in mutants arrives faster at the VPM due to the shorter path, therefore they could occupy the VPM domain which is normally innervated by the larger barreloids (Renier *et al.*, 2017). This pattern

appears to be repeated by the spinothalamic circuit, implying that there is consistency in the rules followed by different neuronal circuits during development.

An increase in the number of cervical axon termini within VPL is accompanied by the expansion of the cervical occupied region in the VPL. Given the critical arrival time of the AS axons to the VPL at E15.5, these ascending inputs could play a crucial role in the maturation and refinement of developing thalamic neurons, including thalamocortical neurons.

The rostrocaudal axis pain localization errors observed in Dcc^{Phox2a} mutants are consistent with lumbar AS axons terminating in VPL regions normally served by cervical axons, resulting in cervical VPL neurons being activated by lumbar stimuli. Therefore, the overall increased overlap between lumbar and cervical axon termini territory as well as specific innervation of lumbar axon termini to the area of thalamus normally occupied by cervical axons could explain the nociceptive topognosis phenotype.

4.3 The Development of the spinal cord- brain long-range connectivity

In this study, Phox2a AS neuron's arrival time to PB, PAG and thalamus brain nucleus were evaluated. I provided evidence that spinal-brain connectivity is established earlier than previously thought. An extensive series of experiments were undertaken at different embryonic stages, and it reveals that the first spinothalamic and spinoparabrachial axons reach the targets as early as E15.5 whereas Davidson et al showed this innervation is in place at E17- E18 but did not look at earlier stages (Davidson *et al.*, 2010). Understanding the timing of spinal somatosensory inputs is crucial as it gives us information about the thalamus organization during development.

Thalamus development occurred between E10 to E16 embryonic days (Molnar *et al.*, 2012). This finding shows that spinothalamic axons reach the thalamus when the organization of the thalamic neurons is yet to be established, therefore this input could be crucial in shaping the final organization of the neurons within the thalamus.

The convergent connection model of nervous system development suggests that shared molecular identity dictates the neuronal connectivity and neurons with shared molecular expression, either transiently or permanently, during development will wire together (Kania, 2021). This model is supported by a study that showed *Atoh1(Math1*) is expressed in all the proprioceptive neurons at different levels of the somatosensory system (Bermingham et al., 2001). Also, *Tacr1* is a recently identified marker of projection neurons expressed in both spinal afferents and recipient neurons within the PB (Barik *et al.*, 2021). I tested the Phox2a ASs model to see how compatible it is with the convergent connection model. In contrast to the convergent connection model, Phox2a AS neurons do not project to Phox2a expressing neurons within the PB. Phox2a neurons are adrenergic and supposed to be involved in keeping homeostasis. To investigate any connection between nociceptive PNs and hemostatic Phox2a neurons in the PB, we demonstrated the area Phox2a PNs innervating is close but not colocalized with Phox2a PB neurons. Therefore, our data show that, unlike Atoh1 and Tacr1, Phox2a is not present at all levels of the nociceptive circuit.

4.3.1 Thalamocortical axons require netrin-1 to guide the axons through their target

Consistent with previous studies, I showed a lateral to the medial organization of the spinothalamic neurons at the VPL. This spatial segregation should be guided through a specific axon guidance pathway.

The importance of DCC and its ligand, netrin-1, in wiring and axonal pathfinding is highlighted when studying various nervous system circuits during development. (Pourchet et al., 2021; Powell *et al.*, 2008). Olfactory bulb-sensory axons require DCC for the map formation and netrin1:DCC signalling inhibition results in aberrant innervation of sensory axons within the olfactory bulb (Lakhina et al., 2012). Also, thalamocortical axons require a netrin gradient on their way to the cortex to settle in their designated domain (Pourchet *et al.*, 2021; Powell *et al.*, 2008). This evidence led us to look at netrin-1/DCC expression within the spinothalamic circuit as a possible signalling pathway involved in shaping the spinal cord-thalamus connection.

Dcc is known for its role in guiding spinal commissures in ventral midline crossing. Although the midline crossing occurs at E11.5, interestingly DCC expression is preserved in Phox2a AS axons located in the anterolateral tract at E15.5 (Fig 6D). This observation suggests the second role of DCC in guiding anterolateral neurons besides spinal decussation.

Furthermore, netrin-1is present in the ST axons that target the developing dorsal thalamus. Examining netrin-1 protein and mRNA expression reveals the presence of netrin-1 cues on the medial side of the E15.5 dorsal thalamus. Given the expression of the DCC in the Phox2a spinothalamic axon termini and netrin-1 ligand at the same region and same time, it seems likely that netrin-1: DCC signalling is involved in shaping the mediolateral organization of the ST axons within the thalamus. Early born cervical axons may arrive first on the lateral side of the

dorsal thalamus, where the first axons have been shown at E15.5, then these first axons which still express DCC are attracting the medial dorsal thalamus where the netrin-1 protein and message are more concentrated. These attractions organize the cervical neurons, and the following late arriving lumbar axons will remain on the lateral side as the medial thalamus is already occupied.

In contrast to the normal hypothetic model of Dcc/netrin-1 guided somatotopy within VPL, in Dcc^{Phox2a} mice when *Dcc* is missing in Cervical spinal PNs, medial netrin-1 expression is ineffective and cervical axons randomly occupy more space through the thalamus. It causes less space for lumbar axons which have yet to arrive at the VP. Therefore, there is less chance for lumbar axons to end up in their target.

Chapter 5: Conclusion and future direction

In this study, *Dcc*'s role has been investigated in the development of somatosensory circuit by using Phox2a projection neurons to represent the anterolateral system. This study has been performed at anatomical and behavioural level which shows that *Dcc* absence in AS neurons not only affect the normal discriminatory nocifensive behaviour but also induce rewiring at different levels of somatosensory circuit anatomy. Disorganized AS axon termini within Dcc^{Phox2a} VPL as a somatotopically organized pain-related nucleus in the brain links a specific population of anterolateral system projection neurons to specific aspects of nociception, such as its discriminatory dimension. Due to the obligate role of PNs in relaying noxious stimuli to the brain, this work could lead us to new therapeutic approaches to treating chronic pain: a genetic dissociation of ascending pain pathways that transmit the location and intensity of a painful stimulus from those that transmit its emotional aspect could provide insights into new therapeutic approaches to the treatment of chronic pain. Understanding how pain sensation develops would also provide insights into neurodevelopmental defects of the somatosensory system, such as autism spectrum disorders.

Appendix:

Table1: Resources and reagents used:

Reagent or resource	Source/reference	Identifier
Mice (MGI notation)		
Dcc^{flox}	Krimpenfort *et al.*, 2012	MGI: 3665466
Phox2a^{Cre}	Roome *et al.,* 2021	RRID: N/A
Ai14 *(B6;129S6-Gt (ROSA)26Sortm14(CAG- The Jackson Laboratory tdTomato) Hze/J)*	The Jackson Laboratory	Cat#: JAX:007908 RRID: IMSR_JAX:007908
Cdx2^{FlpO} *(Tg(CDX2-flpo)#Gld)*	Dr. Martyn Goulding (Salk Institute, San Diego, United States)	Cat#: MGI: 5911680 RRID: N/A
Ai65 *(B6;129S-Gt ROSA)26Sortm65.1(CAG- The Jackson Laboratory tdTomato) Hze/J)*	The Jackson Laboratory	Cat#: JAX:021875 RRID: IMSR_JAX:021875
Ntn1^{Bgeo}	Skarnes *et al.*, 1995	RRID: N/A
129S1/SvImJ	The Jackson Laboratory	JAX:002448 RRID: IMSR_JAX:002448
B6C3F1/J	The Jackson Laboratory	Cat#: JAX: 100010 RRID: IMSR_JAX: 100010
Primary antibodies		
Goat anti-mouse DCC (1:500)	R&D Systems	Cat#: AF844 RRID: AB_2089765
Rabbit anti-Phox2a (1:10,000 from frozen stock)	Jean-François Brunet (École normale superieure, Paris, France)	RRID: AB_2315159

	(Tiveron *et al.,* 1996)	
Rabbit anti-RFP (red fluorescent protein) (1:1000)	Rockland	Cat#: 600-401-379 RRID: AB_2209751
Goat anti-tdT (red fluorescent protein) (1:300)	SICGEN	Cat#: AB8181-200 RRID: AB_2722750
Rabbit anti-GFP (1:1000)	Life Technologies	Cat#: A-11122 AB_221569
Goat anti-netrin-1 (1: 200)	R&D Systems	Cat#: AF1109, RRID: AB_2298775
Rabbit anti-c-Fos (1: 500)	Cell Signalling Technology	Cat#: 2250S RRID: AB_2247211
Rabbit anti-Pax6 (1: 500)	Millipore	Cat#: AB2237, RRID: AB_1587367
Rabbit anti-Sox2 (1: 200)	Abcam	Cat#: 97959 RRID: AB_2341193
Secondary antibodies		
Alexa 488 Donkey anti-Rabbit (1:500)	Jackson ImmunoResearch Laboratories	Cat#: 711-545-152 Lot#: 141848 RRID: AB_2313584
Alexa 488 Donkey anti-Goat (1:500)	Jackson ImmunoResearch Laboratories	Cat#: 705-545-147 Lot#: 136089 RRID: AB_2336933
Cy3 Donkey anti-Rabbit (1:500)	Jackson ImmunoResearch Laboratories	Cat#: 711-165-152 Lot#: 138270 RRID: AB_2307443
Cy3 Donkey anti-Goat (1:500)	Jackson ImmunoResearch Laboratories	Cat#: 705-165-147 Lot#: 134527 RRID: AB_2307351
Cy5 Donkey anti-Rabbit (1:500)	Jackson ImmunoResearch Laboratories	Cat#: 711-175-152 Lot#: 138336 RRID: AB_2340607
Cy5 Donkey anti-Goat (1:500)	Jackson ImmunoResearch Laboratories	Cat#: 705-175-147 Lot#: 134531 RRID: AB_2340415
Chemicals		

(*E*)-Capsaicin	TOCRIS	Cat#: 0462 Lot#: 7A/218361 RRID: N/A
4',6-diamidino-2-phenylindole (DAPI)	Thermo Fisher Scientific	Cat#: D1306 RRID: N/A
Alexa 488-conjugated Choleratoxin B	Thermo Fisher Scientific	Cat#: C22841 Lot#: 2038245 RRID: N/A
Xgal	Millipore Sigma	Cat#: 7240-90-6 RRID: N/A
Mowiol	Millipore Sigma	Cat#: 81381 RRID: N/A

Abbreviation:

AAV	Adeno-associated virus
AS	anterolateral system
BAC	bacterial artificial chromosome
bHLH	basic helix-loop-helix
C-LTMRs	C low threshold mechanoreceptors
CGRP	calcitonin gene related peptide
cKO	conditional knock out
CNS	central nervous system
CPA	conditioned place avoidance
CPSP	post stroke thalamic syndrome
CVLM	caudal ventrolateral medulla
Dcc	Deleted in colorectal cancer
dI	dorsal interneuron classes (e.g. dI5)
dLG	dorsal lateral geniculate
DREZ	dorsal root entry zone
DRG	dorsal root ganglion/ganglia
dTh	dorsal thalamus
Flp/FlpO	Flippase / Flippase (codonoptimized)
HD	homeodomain
HGPPS	horizontal gaze palsy with progressive scoliosis
IASP	International Association for the Study of Pain

Ig	immunoglobulin-like domain
LC	locus coeruleus
LSN	lateral spinal nucleus
MMD	Mirror movement disorder
MNTB	Medial nucleus of trapezoid body
NK1R	neurokinin 1 receptor
NTS	nucleus of solitary tract
PAG	periaqueductal gray
PB	parabrachial nucleus
PBcl	central-lateral parabrachial nucleus
PBdl	dorsal-lateral parabrachial nucleus
PBdm	dorsal-medial parabrachial nucleus
PBel	external-lateral parabrachial nucleus
PBil	internal-lateral parabrachial nucleus
PCP	non-canonical planar cell polarity
Pf	Parafascicular thalamus
Phox2a	Paired-like homeobox 2a
PN	projection neuron
PO	Posterior nucleus of the thalamus
Pth	Prethalamus
RGC	retinal ganglionic cell
Robo3	roundabout guidance receptor 3
RVM	rostral ventromedial medulla

S1	Primary somatosensory cortex
Shh	Sonic hedgehog
SP	substance-P (neuropeptide)
SPB	Spinoparabrachial
ST	spinothalamic
Tac1	preprotachykinin 1
tdT	tdTomato
TFs	transcription factors
Th	Thalamus
TRP	Transient receptor potential
VB	ventrobasal complex
VP	ventral posterior thalamus
VPI	ventral posterior inferior thalamus
VPL	ventroposterolateral thalamus
vTH	ventral thalamus
VZ	ventricular zone

References:

Abdul Aziz, A.A., Finn, D.P., Mason, R., and Chapman, V. (2005). Comparison of responses of ventral posterolateral and posterior complex thalamic neurons in naive rats and rats with hindpaw inflammation: mu-opioid receptor mediated inhibitions. Neuropharmacology *48*, 607-616. 10.1016/j.neuropharm.2004.11.002.

Abraira, V.E., and Ginty, D.D. (2013). The sensory neurons of touch. Neuron *79*, 618-639. 10.1016/j.neuron.2013.07.051.

Abraira, V.E., Kuehn, E.D., Chirila, A.M., Springel, M.W., Toliver, A.A., Zimmerman, A.L., Orefice, L.L., Boyle, K.A., Bai, L., Song, B.J., et al. (2017). The Cellular and Synaptic Architecture of the Mechanosensory Dorsal Horn. Cell *168*, 295-310 e219. 10.1016/j.cell.2016.12.010.

Abu-Amero, K.K., al Dhalaan, H., al Zayed, Z., Hellani, A., and Bosley, T.M. (2009). Five new consanguineous families with horizontal gaze palsy and progressive scoliosis and novel ROBO3 mutations. J Neurol Sci *276*, 22-26. 10.1016/j.jns.2008.08.026.

Akopians, A.L., Babayan, A.H., Beffert, U., Herz, J., Basbaum, A.I., and Phelps, P.E. (2008). Contribution of the Reelin signaling pathways to nociceptive processing. Eur J Neurosci *27*, 523-537. 10.1111/j.1460-9568.2008.06056.x.

Al-Khater, K.M., Kerr, R., and Todd, A.J. (2008). A quantitative study of spinothalamic neurons in laminae I, III, and IV in lumbar and cervical segments of the rat spinal cord. J Comp Neurol *511*, 1-18. 10.1002/cne.21811.

Al-Khater, K.M., and Todd, A.J. (2009). Collateral projections of neurons in laminae I, III, and IV of rat spinal cord to thalamus, periaqueductal gray matter, and lateral parabrachial area. J Comp Neurol *515*, 629-646. 10.1002/cne.22081.

Albe-Fessard, D., Berkley, K.J., Kruger, L., Ralston, H.J., 3rd, and Willis, W.D., Jr. (1985). Diencephalic mechanisms of pain sensation. Brain Res *356*, 217-296. 10.1016/0165-0173(85)90013-x.

Alsulaiman, W.A.A., Quillet, R., Bell, A.M., Dickie, A.C., Polgar, E., Boyle, K.A., Watanabe, M., Roome, R.B., Kania, A., Todd, A.J., and Gutierrez-Mecinas, M. (2021). Characterisation of lamina I anterolateral system neurons that express Cre in a Phox2a-Cre mouse line. Sci Rep *11*, 17912. 10.1038/s41598-021-97105-w.

Andersen, G., Vestergaard, K., Ingeman-Nielsen, M., and Jensen, T.S. (1995). Incidence of central post-stroke pain. Pain *61*, 187-193. 10.1016/0304-3959(94)00144-4.

Avraham, O., Hadas, Y., Vald, L., Zisman, S., Schejter, A., Visel, A., and Klar, A. (2009). Transcriptional control of axonal guidance and sorting in dorsal interneurons by the Lim-HD proteins Lhx9 and Lhx1. Neural Dev *4*, 21. 10.1186/1749-8104-4-21.

Barik, A., Sathyamurthy, A., Thompson, J., Seltzer, M., Levine, A., and Chesler, A. (2021). A spinoparabrachial circuit defined by Tacr1 expression drives pain. Elife *10*. 10.7554/eLife.61135.

Barik, A., Thompson, J.H., Seltzer, M., Ghitani, N., and Chesler, A.T. (2018). A Brainstem-Spinal Circuit Controlling Nocifensive Behavior. Neuron *100*, 1491-1503 e1493. 10.1016/j.neuron.2018.10.037.

Basbaum, A.I., Bautista, D.M., Scherrer, G., and Julius, D. (2009). Cellular and molecular mechanisms of pain. Cell *139*, 267-284. 10.1016/j.cell.2009.09.028.

Berkley, K.J., Guilbaud, G., Benoist, J.M., and Gautron, M. (1993). Responses of neurons in and near the thalamic ventrobasal complex of the rat to stimulation of uterus, cervix, vagina, colon, and skin. J Neurophysiol *69*, 557-568. 10.1152/jn.1993.69.2.557.

Bermingham, N.A., Hassan, B.A., Wang, V.Y., Fernandez, M., Banfi, S., Bellen, H.J., Fritzsch, B., and Zoghbi, H.Y. (2001). Proprioceptor pathway development is dependent on Math1. Neuron *30*, 411-422. 10.1016/s0896-6273(01)00305-1.

Bernard, J.F., Bester, H., and Besson, J.M. (1996). Involvement of the spino-parabrachio -amygdaloid and -hypothalamic pathways in the autonomic and affective emotional aspects of pain. Prog Brain Res *107*, 243-255. 10.1016/s0079-6123(08)61868-3.

Bernard, J.F., Huang, G.F., and Besson, J.M. (1994). The parabrachial area: electrophysiological evidence for an involvement in visceral nociceptive processes. J Neurophysiol *71*, 1646-1660. 10.1152/jn.1994.71.5.1646.

Bittencourt, A.S., Nakamura-Palacios, E.M., Mauad, H., Tufik, S., and Schenberg, L.C. (2005). Organization of electrically and chemically evoked defensive behaviors within the deeper collicular layers as compared to the periaqueductal gray matter of the rat. Neuroscience *133*, 873-892. 10.1016/j.neuroscience.2005.03.012.

Blanchard, D.C., Blanchard, R.J., Lee, M.C., and Williams, G. (1981). Taming in the wild Norway rat following lesions in the basal ganglia. Physiol Behav *27*, 995-1000. 10.1016/0031-9384(81)90360-7.

Bordi, F., and Quartaroli, M. (2000). Modulation of nociceptive transmission by NMDA/glycine site receptor in the ventroposterolateral nucleus of the thalamus. Pain *84*, 213-224. 10.1016/s0304-3959(99)00205-5.

Borowska, J., Jones, C.T., Zhang, H., Blacklaws, J., Goulding, M., and Zhang, Y. (2013). Functional subpopulations of V3 interneurons in the mature mouse spinal cord. J Neurosci *33*, 18553-18565. 10.1523/JNEUROSCI.2005-13.2013.

Borst, J.G., and Soria van Hoeve, J. (2012). The calyx of Held synapse: from model synapse to auditory relay. Annu Rev Physiol *74*, 199-224. 10.1146/annurev-physiol-020911-153236.

Briscoe, J., Pierani, A., Jessell, T.M., and Ericson, J. (2000). A homeodomain protein code specifies progenitor cell identity and neuronal fate in the ventral neural tube. Cell *101*, 435-445. 10.1016/s0092-8674(00)80853-3.

Card, J.P., Lois, J., and Sved, A.F. (2010). Distribution and phenotype of Phox2a-containing neurons in the adult sprague-dawley rat. J Comp Neurol *518*, 2202-2220. 10.1002/cne.22327.

Chaplan, S.R., Bach, F.W., Pogrel, J.W., Chung, J.M., and Yaksh, T.L. (1994). Quantitative assessment of tactile allodynia in the rat paw. J Neurosci Methods *53*, 55-63. 10.1016/0165-0270(94)90144-9.

Chedotal, A. (2011). Further tales of the midline. Curr Opin Neurobiol *21*, 68-75. 10.1016/j.conb.2010.07.008.

Chedotal, A. (2014). Development and plasticity of commissural circuits: from locomotion to brain repair. Trends Neurosci *37*, 551-562. 10.1016/j.tins.2014.08.009.

Chedotal, A. (2019). Roles of axon guidance molecules in neuronal wiring in the developing spinal cord. Nat Rev Neurosci *20*, 380-396. 10.1038/s41583-019-0168-7.

Chen, S., Zhou, H., Guo, S., Zhang, J., Qu, Y., Feng, Z., Xu, K., and Zheng, X. (2015). Optogenetics Based Rat-Robot Control: Optical Stimulation Encodes "Stop" and "Escape" Commands. Ann Biomed Eng *43*, 1851-1864. 10.1007/s10439-014-1235-x.

Chen, Z., Gore, B.B., Long, H., Ma, L., and Tessier-Lavigne, M. (2008). Alternative splicing of the Robo3 axon guidance receptor governs the midline switch from attraction to repulsion. Neuron *58*, 325-332. 10.1016/j.neuron.2008.02.016.

Cheng, L., Arata, A., Mizuguchi, R., Qian, Y., Karunaratne, A., Gray, P.A., Arata, S., Shirasawa, S., Bouchard, M., Luo, P., et al. (2004). Tlx3 and Tlx1 are post-mitotic selector genes determining glutamatergic over GABAergic cell fates. Nat Neurosci *7*, 510-517. 10.1038/nn1221.

Chesnutt, C., Burrus, L.W., Brown, A.M., and Niswander, L. (2004). Coordinate regulation of neural tube patterning and proliferation by TGFbeta and WNT activity. Dev Biol *274*, 334-347. 10.1016/j.ydbio.2004.07.019.

Chiang, M.C., Bowen, A., Schier, L.A., Tupone, D., Uddin, O., and Heinricher, M.M. (2019). Parabrachial Complex: A Hub for Pain and Aversion. J Neurosci *39*, 8225-8230. 10.1523/JNEUROSCI.1162-19.2019.

Cho, H.H., Cargnin, F., Kim, Y., Lee, B., Kwon, R.J., Nam, H., Shen, R., Barnes, A.P., Lee, J.W., Lee, S., and Lee, S.K. (2014). Isl1 directly controls a cholinergic neuronal identity in the developing forebrain and spinal cord by forming cell type-specific complexes. PLoS Genet *10*, e1004280. 10.1371/journal.pgen.1004280.

Choi, S., Hachisuka, J., Brett, M.A., Magee, A.R., Omori, Y., Iqbal, N.U., Zhang, D., DeLisle, M.M., Wolfson, R.L., Bai, L., et al. (2020). Parallel ascending spinal pathways for affective touch and pain. Nature *587*, 258-263. 10.1038/s41586-020-2860-1.

Cliffer, K.D., Burstein, R., and Giesler, G.J., Jr. (1991). Distributions of spinothalamic, spinohypothalamic, and spinotelencephalic fibers revealed by anterograde transport of PHA-L in rats. J Neurosci *11*, 852-868.

Corder, G., Castro, D.C., Bruchas, M.R., and Scherrer, G. (2018). Endogenous and Exogenous Opioids in Pain. Annu Rev Neurosci *41*, 453-473. 10.1146/annurev-neuro-080317-061522.

Craig, A.D. (1995). Distribution of brainstem projections from spinal lamina I neurons in the cat and the monkey. J Comp Neurol *361*, 225-248. 10.1002/cne.903610204.

Craig, A.D. (2004). Lamina I, but not lamina V, spinothalamic neurons exhibit responses that correspond with burning pain. J Neurophysiol *92*, 2604-2609. 10.1152/jn.00385.2004.

Cunningham, C.L., Gremel, C.M., and Groblewski, P.A. (2006). Drug-induced conditioned place preference and aversion in mice. Nat Protoc *1*, 1662-1670. 10.1038/nprot.2006.279.

da Silva, R.V., Johannssen, H.C., Wyss, M.T., Roome, R.B., Bourojeni, F.B., Stifani, N., Marsh, A.P.L., Ryan, M.M., Lockhart, P.J., Leventer, R.J., et al. (2018a). DCC Is Required for the Development of Nociceptive Topognosis in Mice and Humans. Cell Rep *22*, 1105-1114. 10.1016/j.celrep.2018.01.004.

Da Silva, R.V., Johannssen, H.C., Wyss, M.T., Roome, R.B., Bourojeni, F.B., Stifani, N., Marsh, A.P.L., Ryan, M.M., Lockhart, P.J., Leventer, R.J., et al. (2018b). DCC Is Required for the Development of Nociceptive Topognosis in Mice and Humans. Cell Reports *22*, 1105-1114. 10.1016/j.celrep.2018.01.004.

Davidson, S., Truong, H., and Giesler, G.J., Jr. (2010). Quantitative analysis of spinothalamic tract neurons in adult and developing mouse. J Comp Neurol *518*, 3193-3204. 10.1002/cne.22392.

DAVISON, C., and SCHICK, W. (1935). SPONTANEOUS PAIN AND OTHER SUBJECTIVE SENSORY DISTURBANCES: A CLINICOPATHOLOGIC STUDY. Archives of Neurology & Psychiatry *34*, 1204-1237. 10.1001/archneurpsyc.1935.02250240073007.

Denes, A.S., Jekely, G., Steinmetz, P.R., Raible, F., Snyman, H., Prud'homme, B., Ferrier, D.E., Balavoine, G., and Arendt, D. (2007). Molecular architecture of annelid nerve cord supports common origin of nervous system centralization in bilateria. Cell *129*, 277-288. 10.1016/j.cell.2007.02.040.

Dessaud, E., Yang, L.L., Hill, K., Cox, B., Ulloa, F., Ribeiro, A., Mynett, A., Novitch, B.G., and Briscoe, J. (2007). Interpretation of the sonic hedgehog morphogen gradient by a temporal adaptation mechanism. Nature *450*, 717-720. 10.1038/nature06347.

Diamond, M.E., Armstrong-James, M., and Ebner, F.F. (1992). Somatic sensory responses in the rostral sector of the posterior group (POm) and in the ventral posterior medial nucleus (VPM) of the rat thalamus. J Comp Neurol *318*, 462-476. 10.1002/cne.903180410.

Djarmati-Westenberger, A., Bruggemann, N., Espay, A.J., Bhatia, K.P., and Klein, C. (2011). A novel DCC mutation and genetic heterogeneity in congenital mirror movements. Neurology *77*, 1580. 10.1212/WNL.0b013e318230b140.

Ducuing, H., Gardette, T., Pignata, A., Tauszig-Delamasure, S., and Castellani, V. (2019). Commissural axon navigation in the spinal cord: A repertoire of repulsive forces is in command. Semin Cell Dev Biol *85*, 3-12. 10.1016/j.semcdb.2017.12.010.

Dum, R.P., Levinthal, D.J., and Strick, P.L. (2009). The spinothalamic system targets motor and sensory areas in the cerebral cortex of monkeys. J Neurosci *29*, 14223-14235. 10.1523/JNEUROSCI.3398-09.2009.

Engle, E.C. (2010). Human genetic disorders of axon guidance. Cold Spring Harb Perspect Biol *2*, a001784. 10.1101/cshperspect.a001784.

Fazeli, A., Dickinson, S.L., Hermiston, M.L., Tighe, R.V., Steen, R.G., Small, C.G., Stoeckli, E.T., Keino-Masu, K., Masu, M., Rayburn, H., et al. (1997). Phenotype of mice lacking functional Deleted in colorectal cancer (Dcc) gene. Nature *386*, 796-804. 10.1038/386796a0.

Finci, L., Zhang, Y., Meijers, R., and Wang, J.H. (2015). Signaling mechanism of the netrin-1 receptor DCC in axon guidance. Prog Biophys Mol Biol *118*, 153-160. 10.1016/j.pbiomolbio.2015.04.001.

Finger, J.H., Bronson, R.T., Harris, B., Johnson, K., Przyborski, S.A., and Ackerman, S.L. (2002). The netrin 1 receptors Unc5h3 and Dcc are necessary at multiple choice points for the guidance of corticospinal tract axons. J Neurosci *22*, 10346-10356.

Francis, J.T., Xu, S., and Chapin, J.K. (2008). Proprioceptive and cutaneous representations in the rat ventral posterolateral thalamus. J Neurophysiol *99*, 2291-2304. 10.1152/jn.01206.2007.

Frangeul, L., Porrero, C., Garcia-Amado, M., Maimone, B., Maniglier, M., Clasca, F., and Jabaudon, D. (2014). Specific activation of the paralemniscal pathway during nociception. Eur J Neurosci *39*, 1455-1464. 10.1111/ejn.12524.

Friocourt, F., and Chedotal, A. (2017). The Robo3 receptor, a key player in the development, evolution, and function of commissural systems. Dev Neurobiol *77*, 876-890. 10.1002/dneu.22478.

Fulwiler, C.E., and Saper, C.B. (1984). Subnuclear organization of the efferent connections of the parabrachial nucleus in the rat. Brain Res *319*, 229-259. 10.1016/0165-0173(84)90012-2.

Gallea, C., Popa, T., Billot, S., Meneret, A., Depienne, C., and Roze, E. (2011). Congenital mirror movements: a clue to understanding bimanual motor control. J Neurol *258*, 1911-1919. 10.1007/s00415-011-6107-9.

Gauriau, C., and Bernard, J.F. (2002). Pain pathways and parabrachial circuits in the rat. Exp Physiol *87*, 251-258. 10.1113/eph8702357.

Gauriau, C., and Bernard, J.F. (2004). A comparative reappraisal of projections from the superficial laminae of the dorsal horn in the rat: the forebrain. J Comp Neurol *468*, 24-56. 10.1002/cne.10873.
Geiger, B.M., Frank, L.E., Caldera-Siu, A.D., and Pothos, E.N. (2008). Survivable stereotaxic surgery in rodents. J Vis Exp. 10.3791/880.

Gentry, C., Stoakley, N., Andersson, D.A., and Bevan, S. (2010). The roles of iPLA2, TRPM8 and TRPA1 in chemically induced cold hypersensitivity. Mol Pain *6*, 4. 10.1186/1744-8069-6-4.

Gezelius, H., and Lopez-Bendito, G. (2017). Thalamic neuronal specification and early circuit formation. Dev Neurobiol *77*, 830-843. 10.1002/dneu.22460.

Godement, P., Salaun, J., and Imbert, M. (1984). Prenatal and postnatal development of retinogeniculate and retinocollicular projections in the mouse. J Comp Neurol *230*, 552-575. 10.1002/cne.902300406.

Goulding, M. (2009). Circuits controlling vertebrate locomotion: moving in a new direction. Nat Rev Neurosci *10*, 507-518. 10.1038/nrn2608.

Grant, E., Hoerder-Suabedissen, A., and Molnar, Z. (2012). Development of the corticothalamic projections. Front Neurosci *6*, 53. 10.3389/fnins.2012.00053.

Gritsch, S., Bali, K.K., Kuner, R., and Vardeh, D. (2016). Functional characterization of a mouse model for central post-stroke pain. Mol Pain *12*. 10.1177/1744806916629049.

Guilbaud, G., Berkley, K.J., Benoist, J.M., and Gautron, M. (1993). Responses of neurons in thalamic ventrobasal complex of rats to graded distension of uterus and vagina and to uterine suprafusion with bradykinin and prostaglandin F2 alpha. Brain Res *614*, 285-290. 10.1016/0006-8993(93)91046-u.

Guilbaud, G., Peschanski, M., Gautron, M., and Binder, D. (1980). Neurones responding to noxious stimulation in VB complex and caudal adjacent regions in the thalamus of the rat. Pain *8*, 303-318. 10.1016/0304-3959(80)90076-7.

Guo, S., Brush, J., Teraoka, H., Goddard, A., Wilson, S.W., Mullins, M.C., and Rosenthal, A. (1999). Development of noradrenergic neurons in the zebrafish hindbrain requires BMP, FGF8, and the homeodomain protein soulless/Phox2a. Neuron *24*, 555-566. 10.1016/s0896-6273(00)81112-5.

Gutierrez-Mecinas, M., Bell, A.M., Marin, A., Taylor, R., Boyle, K.A., Furuta, T., Watanabe, M., Polgar, E., and Todd, A.J. (2017). Preprotachykinin A is expressed by a distinct population of excitatory neurons in the mouse superficial spinal dorsal horn including cells that respond to noxious and pruritic stimuli. Pain *158*, 440-456. 10.1097/j.pain.0000000000000778.

Han, J.S., Adwanikar, H., Li, Z., Ji, G., and Neugebauer, V. (2010). Facilitation of synaptic transmission and pain responses by CGRP in the amygdala of normal rats. Mol Pain *6*, 10. 10.1186/1744-8069-6-10.

Hargreaves, K., Dubner, R., Brown, F., Flores, C., and Joris, J. (1988). A new and sensitive method for measuring thermal nociception in cutaneous hyperalgesia. Pain *32*, 77-88.

Hernandez-Enriquez, B., Wu, Z., Martinez, E., Olsen, O., Kaprielian, Z., Maness, P.F., Yoshida, Y., Tessier-Lavigne, M., and Tran, T.S. (2015). Floor plate-derived neuropilin-2 functions as a secreted semaphorin sink to facilitate commissural axon midline crossing. Genes Dev *29*, 2617-2632. 10.1101/gad.268086.115.

Hodge, C.J., Jr., and Apkarian, A.V. (1990). The spinothalamic tract. Crit Rev Neurobiol *5*, 363-397.

Horn, K.E., Glasgow, S.D., Gobert, D., Bull, S.-J., Luk, T., Girgis, J., Tremblay, M.-E., McEachern, D., Bouchard, J.-F., and Haber, M. (2013). DCC expression by neurons regulates synaptic plasticity in the adult brain. Cell reports *3*, 173-185.

Horng, S., Kreiman, G., Ellsworth, C., Page, D., Blank, M., Millen, K., and Sur, M. (2009). Differential gene expression in the developing lateral geniculate nucleus and medial geniculate nucleus reveals novel roles for Zic4 and Foxp2 in visual and auditory pathway development. J Neurosci *29*, 13672-13683. 10.1523/JNEUROSCI.2127-09.2009.

Huang, T., Lin, S.H., Malewicz, N.M., Zhang, Y., Zhang, Y., Goulding, M., LaMotte, R.H., and Ma, Q. (2019). Identifying the pathways required for coping behaviours associated with sustained pain. Nature *565*, 86-90. 10.1038/s41586-018-0793-8.

Hunt, S.P., Pini, A., and Evan, G. (1987). Induction of c-fos-like protein in spinal cord neurons following sensory stimulation. Nature *328*, 632-634. 10.1038/328632a0.

Jasmin, L., Burkey, A.R., Card, J.P., and Basbaum, A.I. (1997). Transneuronal labeling of a nociceptive pathway, the spino-(trigemino-)parabrachio-amygdaloid, in the rat. J Neurosci *17*, 3751-3765.

Jaworski, A., Long, H., and Tessier-Lavigne, M. (2010). Collaborative and specialized functions of Robo1 and Robo2 in spinal commissural axon guidance. J Neurosci *30*, 9445-9453. 10.1523/JNEUROSCI.6290-09.2010.

Jen, J.C., Chan, W.M., Bosley, T.M., Wan, J., Carr, J.R., Rub, U., Shattuck, D., Salamon, G., Kudo, L.C., Ou, J., et al. (2004). Mutations in a human ROBO gene disrupt hindbrain axon pathway crossing and morphogenesis. Science *304*, 1509-1513. 10.1126/science.1096437.

Jeong, Y., Dolson, D.K., Waclaw, R.R., Matise, M.P., Sussel, L., Campbell, K., Kaestner, K.H., and Epstein, D.J. (2011). Spatial and temporal requirements for sonic hedgehog in the regulation of thalamic interneuron identity. Development *138*, 531-541. 10.1242/dev.058917.

Jessell, T.M. (2000). Neuronal specification in the spinal cord: inductive signals and transcriptional codes. Nat Rev Genet *1*, 20-29. 10.1038/35049541.

Jones, E.G., and Rubenstein, J.L. (2004). Expression of regulatory genes during differentiation of thalamic nuclei in mouse and monkey. J Comp Neurol *477*, 55-80. 10.1002/cne.20234.

Kaas, J.H. (1983). What, if anything, is SI? Organization of first somatosensory area of cortex. Physiol Rev *63*, 206-231. 10.1152/physrev.1983.63.1.206.

Kadison, S.R., and Kaprielian, Z. (2004). Diversity of contralateral commissural projections in the embryonic rodent spinal cord. J Comp Neurol *472*, 411-422. 10.1002/cne.20086.

Kadison, S.R., Murakami, F., Matise, M.P., and Kaprielian, Z. (2006). The role of floor plate contact in the elaboration of contralateral commissural projections within the embryonic mouse spinal cord. Dev Biol *296*, 499-513. 10.1016/j.ydbio.2006.06.022.

Kalueff, A.V., and Tuohimaa, P. (2004). Grooming analysis algorithm for neurobehavioural stress research. Brain Res Brain Res Protoc *13*, 151-158. 10.1016/j.brainresprot.2004.04.002.

Kania, A. (2021). Sensational developments in somatosensory development? Curr Opin Neurobiol *66*, 212-223. 10.1016/j.conb.2020.12.011.

Karthik, S., Huang, D., Delgado, Y., Laing, J.J., Peltekian, L., Iverson, G.N., Grady, F., Miller, R.L., McCann, C.M., Fritzsch, B., et al. (2022). Molecular ontology of the parabrachial nucleus. J Comp Neurol. 10.1002/cne.25307.

Kenshalo, D.R., and Willis, W.D. (1991). The Role of the Cerebral Cortex in Pain Sensation. In Normal and Altered States of Function, A. Peters, and E.G. Jones, eds. (Springer US), pp. 153-212. 10.1007/978-1-4615-6622-9_5.

Kiehn, O. (2011). Development and functional organization of spinal locomotor circuits. Curr Opin Neurobiol *21*, 100-109. 10.1016/j.conb.2010.09.004.

Kim, J.H., Greenspan, J.D., Coghill, R.C., Ohara, S., and Lenz, F.A. (2007). Lesions limited to the human thalamic principal somatosensory nucleus (ventral caudal) are associated with loss of cold sensations and central pain. J Neurosci *27*, 4995-5004. 10.1523/JNEUROSCI.0716-07.2007.

Koch, S.C., Acton, D., and Goulding, M. (2018). Spinal Circuits for Touch, Pain, and Itch. Annu Rev Physiol *80*, 189-217. 10.1146/annurev-physiol-022516-034303.

Kohro, Y., Sakaguchi, E., Tashima, R., Tozaki-Saitoh, H., Okano, H., Inoue, K., and Tsuda, M. (2015). A new minimally-invasive method for microinjection into the mouse spinal dorsal horn. Scientific reports *5*, 14306.

Krimpenfort, P., Song, J.Y., Proost, N., Zevenhoven, J., Jonkers, J., and Berns, A. (2012). Deleted in colorectal carcinoma suppresses metastasis in p53-deficient mammary tumours. Nature *482*, 538-541. 10.1038/nature10790.

Kuhlenbeck, H. (1973). The Central Nervous System of Vertebrates, Vol. 3/II (Karger Publishers).
Kuner, R., and Kuner, T. (2021). Cellular Circuits in the Brain and Their Modulation in Acute and Chronic Pain. Physiol Rev *101*, 213-258. 10.1152/physrev.00040.2019.

Kutejova, E., Sasai, N., Shah, A., Gouti, M., and Briscoe, J. (2016). Neural Progenitors Adopt Specific Identities by Directly Repressing All Alternative Progenitor Transcriptional Programs. Dev Cell *36*, 639-653. 10.1016/j.devcel.2016.02.013.

Lai, H.C., Seal, R.P., and Johnson, J.E. (2016). Making sense out of spinal cord somatosensory development. Development *143*, 3434-3448. 10.1242/dev.139592.

Lakhina, V., Marcaccio, C.L., Shao, X., Lush, M.E., Jain, R.A., Fujimoto, E., Bonkowsky, J.L., Granato, M., and Raper, J.A. (2012). Netrin/DCC signaling guides olfactory sensory axons to their correct location in the olfactory bulb. J Neurosci *32*, 4440-4456. 10.1523/JNEUROSCI.4442-11.2012.

Laumonnerie, C., Da Silva, R.V., Kania, A., and Wilson, S.I. (2014). Netrin 1 and Dcc signalling are required for confinement of central axons within the central nervous system. Development *141*, 594-603. 10.1242/dev.099606.

Laumonnerie, C., Tong, Y.G., Alstermark, H., and Wilson, S.I. (2015). Commissural axonal corridors instruct neuronal migration in the mouse spinal cord. Nat Commun *6*, 7028. 10.1038/ncomms8028.

Lein, E.S., Hawrylycz, M.J., Ao, N., Ayres, M., Bensinger, A., Bernard, A., Boe, A.F., Boguski, M.S., Brockway, K.S., Byrnes, E.J., et al. (2007). Genome-wide atlas of gene expression in the adult mouse brain. Nature *445*, 168-176. 10.1038/nature05453.

Liang, D.-Y., Zheng, M., Sun, Y., Sahbaie, P., Low, S.A., Peltz, G., Scherrer, G., Flores, C., and Clark, J.D. (2014). The Netrin-1 receptor DCC is a regulator of maladaptive responses to chronic morphine administration. BMC genomics *15*, 345.

Liem, K.F., Jr., Tremml, G., and Jessell, T.M. (1997). A role for the roof plate and its resident TGFbeta-related proteins in neuronal patterning in the dorsal spinal cord. Cell *91*, 127-138. 10.1016/s0092-8674(01)80015-5.

Lin, L., Lesnick, T.G., Maraganore, D.M., and Isacson, O. (2009). Axon guidance and synaptic maintenance: preclinical markers for neurodegenerative disease and therapeutics. Trends Neurosci *32*, 142-149. 10.1016/j.tins.2008.11.006.

Long, H., Sabatier, C., Ma, L., Plump, A., Yuan, W., Ornitz, D.M., Tamada, A., Murakami, F., Goodman, C.S., and Tessier-Lavigne, M. (2004). Conserved roles for Slit and Robo proteins in midline commissural axon guidance. Neuron *42*, 213-223. 10.1016/s0896-6273(04)00179-5.

Lund, R.D. (1965). Uncrossed Visual Pathways of Hooded and Albino Rats. Science *149*, 1506-1507. 10.1126/science.149.3691.1506.

Lyuksyutova, A.I., Lu, C.C., Milanesio, N., King, L.A., Guo, N., Wang, Y., Nathans, J., Tessier-Lavigne, M., and Zou, Y. (2003). Anterior-posterior guidance of commissural axons by Wnt-frizzled signaling. Science *302*, 1984-1988. 10.1126/science.1089610.

Madisen, L., Garner, A.R., Shimaoka, D., Chuong, A.S., Klapoetke, N.C., Li, L., van der Bourg, A., Niino, Y., Egolf, L., Monetti, C., et al. (2015). Transgenic mice for intersectional targeting of neural sensors and effectors with high specificity and performance. Neuron *85*, 942-958. 10.1016/j.neuron.2015.02.022.

Madisen, L., Zwingman, T.A., Sunkin, S.M., Oh, S.W., Zariwala, H.A., Gu, H., Ng, L.L., Palmiter, R.D., Hawrylycz, M.J., Jones, A.R., et al. (2010). A robust and high-throughput Cre reporting and characterization system for the whole mouse brain. Nat Neurosci *13*, 133-140. 10.1038/nn.2467.

Mantyh, P.W., Rogers, S.D., Honore, P., Allen, B.J., Ghilardi, J.R., Li, J., Daughters, R.S., Lappi, D.A., Wiley, R.G., and Simone, D.A. (1997). Inhibition of hyperalgesia by ablation of lamina I spinal neurons expressing the substance P receptor. Science *278*, 275-279. 10.1126/science.278.5336.275.

Mercer Lindsay, N., Chen, C., Gilam, G., Mackey, S., and Scherrer, G. (2021). Brain circuits for pain and its treatment. Sci Transl Med *13*, eabj7360. 10.1126/scitranslmed.abj7360.

Michalski, N., Babai, N., Renier, N., Perkel, D.J., Chedotal, A., and Schneggenburger, R. (2013). Robo3-driven axon midline crossing conditions functional maturation of a large commissural synapse. Neuron *78*, 855-868. 10.1016/j.neuron.2013.04.006.

Miesegaes, G.R., Klisch, T.J., Thaller, C., Ahmad, K.A., Atkinson, R.C., and Zoghbi, H.Y. (2009). Identification and subclassification of new Atoh1 derived cell populations during mouse spinal cord development. Dev Biol *327*, 339-351. 10.1016/j.ydbio.2008.12.016.

Mirza, R., Kivrak, B.G., and Erzurumlu, R.S. (2013). Cooperative slit and netrin signaling in contralateralization of the mouse trigeminothalamic pathway. J Comp Neurol *521*, 312-325. 10.1002/cne.23188.

Mogil, J.S., Graham, A.C., Ritchie, J., Hughes, S.F., Austin, J.-S., Schorscher-Petcu, A., Langford, D.J., and Bennett, G.J. (2010). Hypolocomotion, asymmetrically directed behaviors (licking, lifting, flinching, and shaking) and dynamic weight bearing (gait) changes are not measures of neuropathic pain in mice. Molecular pain *6*, 34.

Molnar, Z., Garel, S., Lopez-Bendito, G., Maness, P., and Price, D.J. (2012). Mechanisms controlling the guidance of thalamocortical axons through the embryonic forebrain. Eur J Neurosci *35*, 1573-1585. 10.1111/j.1460-9568.2012.08119.x.

Moore, S.W., Tessier-Lavigne, M., and Kennedy, T.E. (2007). Netrins and their receptors. Adv Exp Med Biol *621*, 17-31. 10.1007/978-0-387-76715-4_2.

Moreno-Bravo, J.A., Roig Puiggros, S., Blockus, H., Dominici, C., Zelina, P., Mehlen, P., and Chedotal, A. (2018). Commissural neurons transgress the CNS/PNS boundary in absence of ventricular zone-derived netrin 1. Development *145*. 10.1242/dev.159400.

Mouton, L.J., and Holstege, G. (2000). Segmental and laminar organization of the spinal neurons projecting to the periaqueductal gray (PAG) in the cat suggests the existence of at least five separate clusters of spino-PAG neurons. J Comp Neurol *428*, 389-410. 10.1002/1096-9861(20001218)428:3<389::aid-cne2>3.0.co;2-b.

Nakagawa, Y. (2019). Development of the thalamus: From early patterning to regulation of cortical functions. Wiley Interdiscip Rev Dev Biol *8*, e345. 10.1002/wdev.345.

Nakagawa, Y., and O'Leary, D.D. (2001). Combinatorial expression patterns of LIM-homeodomain and other regulatory genes parcellate developing thalamus. J Neurosci *21*, 2711-2725.

Nakagawa, Y., and Shimogori, T. (2012). Diversity of thalamic progenitor cells and postmitotic neurons. Eur J Neurosci *35*, 1554-1562. 10.1111/j.1460-9568.2012.08089.x.

Nishi, Y., Zhang, X., Jeong, J., Peterson, K.A., Vedenko, A., Bulyk, M.L., Hide, W.A., and McMahon, A.P. (2015). A direct fate exclusion mechanism by Sonic hedgehog-regulated transcriptional repressors. Development *142*, 3286-3293. 10.1242/dev.124636.

Nornes, H.O., and Carry, M. (1978). Neurogenesis in spinal cord of mouse: an autoradiographic analysis. Brain Res *159*, 1-6. 10.1016/0006-8993(78)90105-1.

Nornes, H.O., and Das, G.D. (1974). Temporal pattern of neurogenesis in spinal cord of rat. I. An autoradiographic study--time and sites of origin and migration and settling patterns of neuroblasts. Brain Res *73*, 121-138. 10.1016/0006-8993(74)91011-7.

Oh, S.W., Harris, J.A., Ng, L., Winslow, B., Cain, N., Mihalas, S., Wang, Q., Lau, C., Kuan, L., Henry, A.M., et al. (2014). A mesoscale connectome of the mouse brain. Nature *508*, 207-214. 10.1038/nature13186.

Onishi, K., and Zou, Y. (2017). Sonic Hedgehog switches on Wnt/planar cell polarity signaling in commissural axon growth cones by reducing levels of Shisa2. Elife *6*. 10.7554/eLife.25269.

Orlino, E.N., Jr., Wong, C.M., and Phelps, P.E. (2000). L1 and GAD65 are expressed on dorsal commissural axons in embryonic rat spinal cord. Brain Res Dev Brain Res *125*, 117-130. 10.1016/s0165-3806(00)00087-0.

Pain terms: a list with definitions and notes on usage. Recommended by the IASP Subcommittee on Taxonomy. (1979). Pain *6*, 249.

Peschanski, M., Guilbaud, G., Gautron, M., and Besson, J.M. (1980). Encoding of noxious heat messages in neurons of the ventrobasal thalamic complex of the rat. Brain Res *197*, 401-413. 10.1016/0006-8993(80)91125-7.

Petros, T.J., Rebsam, A., and Mason, C.A. (2008). Retinal axon growth at the optic chiasm: to cross or not to cross. Annu Rev Neurosci *31*, 295-315. 10.1146/annurev.neuro.31.060407.125609.

Pilyavskii, A.I., Maznychenko, A.V., Maisky, V.A., Kostyukov, A.I., Hellstrom, F., and Windhorst, U. (2005). Capsaicin-induced effects on c-fos expression and NADPH-diaphorase activity in the feline spinal cord. Eur J Pharmacol *521*, 70-78. 10.1016/j.ejphar.2005.08.006.

Pivetta, C., Esposito, M.S., Sigrist, M., and Arber, S. (2014). Motor-circuit communication matrix from spinal cord to brainstem neurons revealed by developmental origin. Cell *156*, 537-548. 10.1016/j.cell.2013.12.014.

Ploner, M., Freund, H.J., and Schnitzler, A. (1999). Pain affect without pain sensation in a patient with a postcentral lesion. Pain *81*, 211-214. 10.1016/s0304-3959(99)00012-3.

Polgar, E., Wright, L.L., and Todd, A.J. (2010). A quantitative study of brainstem projections from lamina I neurons in the cervical and lumbar enlargement of the rat. Brain Res *1308*, 58-67. 10.1016/j.brainres.2009.10.041.

Pourchet, O., Morel, M.P., Welniarz, Q., Sarrazin, N., Marti, F., Heck, N., Gallea, C., Doulazmi, M., Roig Puiggros, S., Moreno-Bravo, J.A., et al. (2021). Loss of floor plate Netrin-1 impairs midline crossing of corticospinal axons and leads to mirror movements. Cell Rep *34*, 108654. 10.1016/j.celrep.2020.108654.

Powell, A.W., Sassa, T., Wu, Y., Tessier-Lavigne, M., and Polleux, F. (2008). Topography of thalamic projections requires attractive and repulsive functions of Netrin-1 in the ventral telencephalon. PLoS Biol *6*, e116. 10.1371/journal.pbio.0060116.

Price, D.D., and Dubner, R. (1977). Neurons that subserve the sensory-discriminative aspects of pain. Pain *3*, 307-338. 10.1016/0304-3959(77)90063-X.

Quintana-Urzainqui, I., Hernandez-Malmierca, P., Clegg, J.M., Li, Z., Kozic, Z., and Price, D.J. (2020). The role of the diencephalon in the guidance of thalamocortical axons in mice. Development *147*. 10.1242/dev.184523.

Remple, M.S., Henry, E.C., and Catania, K.C. (2003). Organization of somatosensory cortex in the laboratory rat (Rattus norvegicus): Evidence for two lateral areas joined at the representation of the teeth. J Comp Neurol *467*, 105-118. 10.1002/cne.10909.

Renier, N., Dominici, C., Erzurumlu, R.S., Kratochwil, C.F., Rijli, F.M., Gaspar, P., and Chedotal, A. (2017). A mutant with bilateral whisker to barrel inputs unveils somatosensory mapping rules in the cerebral cortex. Elife *6*. 10.7554/eLife.23494.

Rexed, B. (1952). The cytoarchitectonic organization of the spinal cord in the cat. J Comp Neurol *96*, 414-495.

Rodriguez, E., Sakurai, K., Xu, J., Chen, Y., Toda, K., Zhao, S., Han, B.X., Ryu, D., Yin, H., Liedtke, W., and Wang, F. (2017). A craniofacial-specific monosynaptic circuit enables heightened affective pain. Nat Neurosci *20*, 1734-1743. 10.1038/s41593-017-0012-1.

Roeder, Z., Chen, Q., Davis, S., Carlson, J.D., Tupone, D., and Heinricher, M.M. (2016). Parabrachial complex links pain transmission to descending pain modulation. Pain *157*, 2697-2708. 10.1097/j.pain.0000000000000688.

Roelink, H., Porter, J.A., Chiang, C., Tanabe, Y., Chang, D.T., Beachy, P.A., and Jessell, T.M. (1995). Floor plate and motor neuron induction by different concentrations of the amino-terminal cleavage product of sonic hedgehog autoproteolysis. Cell *81*, 445-455. 10.1016/0092-8674(95)90397-6.

Roome, R.B., Bourojeni, F.B., Mona, B., Rastegar-Pouyani, S., Blain, R., Dumouchel, A., Salesse, C., Thompson, W.S., Brookbank, M., Gitton, Y., et al. (2020a). Phox2a Defines a Developmental Origin of the Anterolateral System in Mice and Humans. Cell Rep *33*, 108425. 10.1016/j.celrep.2020.108425.

Roome, R.B., Bourojeni, F.B., Mona, B., Rastegar-Pouyani, S., Blain, R., Dumouchel, A., Salesse, C., Thompson, W.S., Brookbank, M., Gitton, Y., et al. (2020b). Phox2a Defines a Developmental Origin of the Anterolateral System in Mice and Humans. Cell Reports *33*, 108425. 10.1016/j.celrep.2020.108425.

Roome, R.B., Rastegar-Pouyani, S., Ker, A., Dumouchel, A., Kmita, M., and Kania, A. (2022). Netrin1 and reelin signaling are required for the migration of anterolateral system neurons in the embryonic spinal cord. Pain *163*, e527-e539. 10.1097/j.pain.0000000000002444.

Rozen, S., and Skaletsky, H. (2000). Primer3 on the WWW for general users and for biologist programmers. Methods Mol Biol *132*, 365-386. 10.1385/1-59259-192-2:365.

Sabatier, C., Plump, A.S., Le, M., Brose, K., Tamada, A., Murakami, F., Lee, E.Y., and Tessier-Lavigne, M. (2004). The divergent Robo family protein rig-1/Robo3 is a negative regulator of slit responsiveness required for midline crossing by commissural axons. Cell *117*, 157-169. 10.1016/s0092-8674(04)00303-4.

Sakai, N., and Kaprielian, Z. (2012). Guidance of longitudinally projecting axons in the developing central nervous system. Front Mol Neurosci *5*, 59. 10.3389/fnmol.2012.00059.

Sakurada, T., Katsumata, K., Tan-No, K., Sakurada, S., and Kisara, K. (1992). The capsaicin test in mice for evaluating tachykinin antagonists in the spinal cord. Neuropharmacology *31*, 1279-1285.

Schneider, C.A., Rasband, W.S., and Eliceiri, K.W. (2012). NIH Image to ImageJ: 25 years of image analysis. Nat Methods *9*, 671-675. 10.1038/nmeth.2089.

Serafini, T., Colamarino, S.A., Leonardo, E.D., Wang, H., Beddington, R., Skarnes, W.C., and Tessier-Lavigne, M. (1996). Netrin-1 is required for commissural axon guidance in the developing vertebrate nervous system. Cell *87*, 1001-1014. 10.1016/s0092-8674(00)81795-x.

Shen, Q., Wang, Y., Dimos, J.T., Fasano, C.A., Phoenix, T.N., Lemischka, I.R., Ivanova, N.B., Stifani, S., Morrisey, E.E., and Temple, S. (2006). The timing of cortical neurogenesis is encoded within lineages of individual progenitor cells. Nat Neurosci *9*, 743-751. 10.1038/nn1694.

Silva, E., Quinones, B., Freund, N., Gonzalez, L.E., and Hernandez, L. (2001). Extracellular glutamate, aspartate and arginine increase in the ventral posterolateral thalamic nucleus during nociceptive stimulation. Brain Res *923*, 45-49. 10.1016/s0006-8993(01)03195-x.

Sivilotti, L., and Woolf, C.J. (1994). The contribution of GABAA and glycine receptors to central sensitization: disinhibition and touch-evoked allodynia in the spinal cord. J Neurophysiol *72*, 169-179. 10.1152/jn.1994.72.1.169.

Skarnes, W.C., Moss, J.E., Hurtley, S.M., and Beddington, R.S. (1995). Capturing genes encoding membrane and secreted proteins important for mouse development. Proc Natl Acad Sci U S A *92*, 6592-6596. 10.1073/pnas.92.14.6592.

Spike, R.C., Puskar, Z., Andrew, D., and Todd, A.J. (2003). A quantitative and morphological study of projection neurons in lamina I of the rat lumbar spinal cord. Eur J Neurosci *18*, 2433-2448. 10.1046/j.1460-9568.2003.02981.x.

Sprenger, T., Seifert, C.L., Valet, M., Andreou, A.P., Foerschler, A., Zimmer, C., Collins, D.L., Goadsby, P.J., Tolle, T.R., and Chakravarty, M.M. (2012). Assessing the risk of central post-stroke pain of thalamic origin by lesion mapping. Brain *135*, 2536-2545. 10.1093/brain/aws153.

Srour, M., Riviere, J.B., Pham, J.M., Dube, M.P., Girard, S., Morin, S., Dion, P.A., Asselin, G., Rochefort, D., Hince, P., et al. (2010). Mutations in DCC cause congenital mirror movements. Science *328*, 592. 10.1126/science.1186463.

Stein, E., and Tessier-Lavigne, M. (2001). Hierarchical organization of guidance receptors: silencing of netrin attraction by slit through a Robo/DCC receptor complex. Science *291*, 1928-1938. 10.1126/science.1058445.

Suter, T., DeLoughery, Z.J., and Jaworski, A. (2017). Meninges-derived cues control axon guidance. Dev Biol *430*, 1-10. 10.1016/j.ydbio.2017.08.005.

Suzuki-Hirano, A., Ogawa, M., Kataoka, A., Yoshida, A.C., Itoh, D., Ueno, M., Blackshaw, S., and Shimogori, T. (2011). Dynamic spatiotemporal gene expression in embryonic mouse thalamus. J Comp Neurol *519*, 528-543. 10.1002/cne.22531.

Szabo, N.E., da Silva, R.V., Sotocinal, S.G., Zeilhofer, H.U., Mogil, J.S., and Kania, A. (2015). Hoxb8 intersection defines a role for Lmx1b in excitatory dorsal horn neuron development, spinofugal connectivity, and nociception. J Neurosci *35*, 5233-5246. 10.1523/JNEUROSCI.4690-14.2015.
Todd, A.J. (2010). Neuronal circuitry for pain processing in the dorsal horn. Nat Rev Neurosci *11*, 823-836. 10.1038/nrn2947.

Trommsdorff, M., Gotthardt, M., Hiesberger, T., Shelton, J., Stockinger, W., Nimpf, J., Hammer, R.E., Richardson, J.A., and Herz, J. (1999). Reeler/Disabled-like disruption of neuronal migration in knockout mice lacking the VLDL receptor and ApoE receptor 2. Cell *97*, 689-701. 10.1016/s0092-8674(00)80782-5.

Tzschentke, T.M. (2014). Conditioned Place Preference and Aversion. In Encyclopedia of Psychopharmacology, pp. 1-7. 10.1007/978-3-642-27772-6_146-2.

Uddin, O., Studlack, P., Akintola, T., Raver, C., Castro, A., Masri, R., and Keller, A. (2018). Amplified parabrachial nucleus activity in a rat model of trigeminal neuropathic pain. Neurobiol Pain *3*, 22-30. 10.1016/j.ynpai.2018.02.002.

Varadarajan, S.G., Kong, J.H., Phan, K.D., Kao, T.J., Panaitof, S.C., Cardin, J., Eltzschig, H., Kania, A., Novitch, B.G., and Butler, S.J. (2017). Netrin1 Produced by Neural Progenitors, Not Floor Plate Cells, Is Required for Axon Guidance in the Spinal Cord. Neuron *94*, 790-799 e793. 10.1016/j.neuron.2017.03.007.

Villeda, S.A., Akopians, A.L., Babayan, A.H., Basbaum, A.I., and Phelps, P.E. (2006). Absence of Reelin results in altered nociception and aberrant neuronal positioning in the dorsal spinal cord. Neuroscience *139*, 1385-1396. 10.1016/j.neuroscience.2006.01.042.

Vowles, K.E., McEntee, M.L., Julnes, P.S., Frohe, T., Ney, J.P., and van der Goes, D.N. (2015). Rates of opioid misuse, abuse, and addiction in chronic pain: a systematic review and data synthesis. Pain *156*, 569-576. 10.1097/01.j.pain.0000460357.01998.f1.

Vue, T.Y., Aaker, J., Taniguchi, A., Kazemzadeh, C., Skidmore, J.M., Martin, D.M., Martin, J.F., Treier, M., and Nakagawa, Y. (2007). Characterization of progenitor domains in the developing mouse thalamus. J Comp Neurol *505*, 73-91. 10.1002/cne.21467.

Vue, T.Y., Bluske, K., Alishahi, A., Yang, L.L., Koyano-Nakagawa, N., Novitch, B., and Nakagawa, Y. (2009). Sonic hedgehog signaling controls thalamic progenitor identity and nuclei specification in mice. J Neurosci *29*, 4484-4497. 10.1523/JNEUROSCI.0656-09.2009.

Walther, C., and Gruss, P. (1991). Pax-6, a murine paired box gene, is expressed in the developing CNS. Development *113*, 1435-1449. 10.1242/dev.113.4.1435.

Welniarz, Q., Morel, M.P., Pourchet, O., Gallea, C., Lamy, J.C., Cincotta, M., Doulazmi, M., Belle, M., Meneret, A., Trouillard, O., et al. (2017). Non cell-autonomous role of DCC in the guidance of the corticospinal tract at the midline. Sci Rep *7*, 410. 10.1038/s41598-017-00514-z.

Wercberger, R., and Basbaum, A.I. (2019). Spinal cord projection neurons: a superficial, and also deep, analysis. Curr Opin Physiol *11*, 109-115. 10.1016/j.cophys.2019.10.002.

Willis, W.D., and Westlund, K.N. (1997). Neuroanatomy of the pain system and of the pathways that modulate pain. J Clin Neurophysiol *14*, 2-31. 10.1097/00004691-199701000-00002.

Wilson, S.I., Shafer, B., Lee, K.J., and Dodd, J. (2008). A molecular program for contralateral trajectory: Rig-1 control by LIM homeodomain transcription factors. Neuron *59*, 413-424. 10.1016/j.neuron.2008.07.020.

Witschi, R., Johansson, T., Morscher, G., Scheurer, L., Deschamps, J., and Zeilhofer, H.U. (2010). Hoxb8-Cre mice: A tool for brain-sparing conditional gene deletion. Genesis *48*, 596-602. 10.1002/dvg.20656.

Wolf, A.M., Lyuksyutova, A.I., Fenstermaker, A.G., Shafer, B., Lo, C.G., and Zou, Y. (2008). Phosphatidylinositol-3-kinase-atypical protein kinase C signaling is required for Wnt attraction and anterior-posterior axon guidance. J Neurosci *28*, 3456-3467. 10.1523/JNEUROSCI.0029-08.2008.

Xu, Y., Lopes, C., Wende, H., Guo, Z., Cheng, L., Birchmeier, C., and Ma, Q. (2013). Ontogeny of excitatory spinal neurons processing distinct somatic sensory modalities. J Neurosci *33*, 14738-14748. 10.1523/JNEUROSCI.5512-12.2013.

Yam, P.T., Kent, C.B., Morin, S., Farmer, W.T., Alchini, R., Lepelletier, L., Colman, D.R., Tessier-Lavigne, M., Fournier, A.E., and Charron, F. (2012). 14-3-3 proteins regulate a cell-intrinsic switch from sonic hedgehog-mediated commissural axon attraction to repulsion after midline crossing. Neuron *76*, 735-749. 10.1016/j.neuron.2012.09.017.

Yeh, L.F., Ozawa, T., and Johansen, J.P. (2021). Functional organization of the midbrain periaqueductal gray for regulating aversive memory formation. Mol Brain *14*, 136. 10.1186/s13041-021-00844-0.

Yuge, K., Kataoka, A., Yoshida, A.C., Itoh, D., Aggarwal, M., Mori, S., Blackshaw, S., and Shimogori, T. (2011). Region-specific gene expression in early postnatal mouse thalamus. J Comp Neurol *519*, 544-561. 10.1002/cne.22532.

Zhang, E.T., and Craig, A.D. (1997). Morphology and distribution of spinothalamic lamina I neurons in the monkey. J Neurosci *17*, 3274-3284.

Zhang, X., Davidson, S., and Giesler, G.J., Jr. (2006). Thermally identified subgroups of marginal zone neurons project to distinct regions of the ventral posterior lateral nucleus in rats. J Neurosci *26*, 5215-5223. 10.1523/JNEUROSCI.0701-06.2006.

Zou, Y., Stoeckli, E., Chen, H., and Tessier-Lavigne, M. (2000). Squeezing axons out of the gray matter: a role for slit and semaphorin proteins from midline and ventral spinal cord. Cell *102*, 363-375. 10.1016/s0092-8674(00)00041-6.